Retrospective Theses and Dissertations

Iowa State University Capstones, Theses and Dissertations

2003

Studies of immobilized homogeneous metal catalysts on silica supports

Keith James Stanger
Iowa State University

Follow this and additional works at: https://lib.dr.iastate.edu/rtd

⚙ Part of the Inorganic Chemistry Commons, and the Organic Chemistry Commons

Recommended Citation

Stanger, Keith James, "Studies of immobilized homogeneous metal catalysts on silica supports " (2003). *Retrospective Theses and Dissertations*. 621.
https://lib.dr.iastate.edu/rtd/621

INFORMATION TO USERS

This manuscript has been reproduced from the microfilm master. UMI films the text directly from the original or copy submitted. Thus, some thesis and dissertation copies are in typewriter face, while others may be from any type of computer printer.

The quality of this reproduction is dependent upon the quality of the copy submitted. Broken or indistinct print, colored or poor quality illustrations and photographs, print bleedthrough, substandard margins, and improper alignment can adversely affect reproduction.

In the unlikely event that the author did not send UMI a complete manuscript and there are missing pages, these will be noted. Also, if unauthorized copyright material had to be removed, a note will indicate the deletion.

Oversize materials (e.g., maps, drawings, charts) are reproduced by sectioning the original, beginning at the upper left-hand corner and continuing from left to right in equal sections with small overlaps.

NOTE TO USERS

This reproduction is the best copy available.

UMI®

Studies of immobilized homogeneous metal catalysts on silica supports

by

Keith James Stanger

A dissertation submitted to the graduate faculty

in partial fulfillment of the requirements for the degree of

DOCTOR OF PHILOSOPHY

Major: Organic Chemistry

Program of Study Committee:
Robert J. Angelici (Major Professor)
James H. Espenson
Earl G. Hammond
George A. Kraus
Richard C. Larock

Iowa State University

Ames, Iowa

2003

UMI Number: 3085947

UMI®

ii

Graduate College
Iowa State University

This is to certify that the doctoral dissertation of

Keith James Stanger

has met the dissertation requirements of Iowa State University

Major Professor

For the Major Program

TABLE OF CONTENTS

Arene Hydrogenation Using Supported Rhodium Metal Catalysts Prepared from [Rh(COD)H]$_4$, [Rh(COD)$_2$]$^+$BF$_4^-$, and [Rh(COD)Cl]$_2$ Adsorbed on SiO_2 and Pd-SiO_2

Abstract

The tethered, chiral, chelating diphosphine rhodium complex (shown below), which

catalyzes the enantioselective hydrogenation of methyl-α-acetamidocinnamate (MAC), has

the illustrated structure as established by ^{31}P NMR and IR studies. Spectral and catalytic

investigations also suggest that the mechanism of action of the tethered complex is the same

as that of the untethered complex in solution.
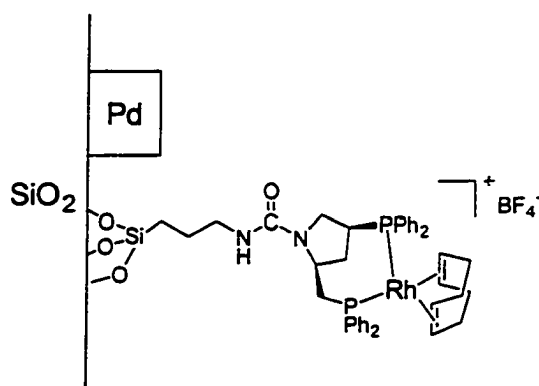
The rhodium complexes, [Rh(COD)H]$_4$, [Rh(COD)$_2$]$^+$BF$_4^-$, [Rh(COD)Cl]$_2$, and

RhCl$_3$•3H$_2$O, adsorbed on SiO$_2$ are optimally activated for toluene hydrogenation by

pretreatment with H$_2$ at 200 °C. The same complexes on Pd-SiO$_2$ are equally active without

pretreatments. The active species in all cases is rhodium metal. The catalysts were

characterized by XPS, TEM, DRIFTS, and mercury poisoning experiments.
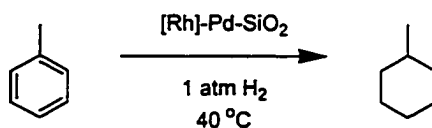
Rhodium on silica catalyzes the hydrogenation of fluorobenzene to produce

predominately fluorocyclohexane in heptane and 1,2-dichloroethane solvents. In

heptane/methanol and heptane/water solvents, hydrodefluorination to benzene and

subsequent hydrogenation to cyclohexane occurs exclusively. Benzene inhibits the

hydrodefluorination of fluorobenzene. In DCE or heptane solvents, fluorocyclohexane reacts

with hydrogen fluoride to form cyclohexene. Reaction conditions can be chosen to

selectively yield fluorocyclohexane, cyclohexene, benzene, or cyclohexane.
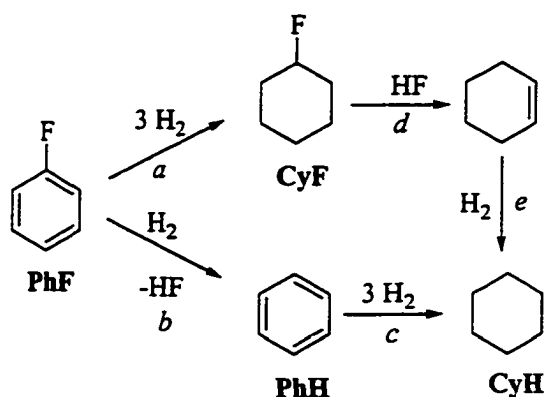
The oxorhenium(V) dithiolate catalyst [-S(CH$_2$)$_3$S-]Re(O)(Me)(PPh$_3$) was modified

by linking it to a tether that could be attached to a silica support. Spectroscopic investigation

and catalytic oxidation reactivity showed the heterogenized catalyst's structure and reactivity

to be similar to its homogeneous analog. However, the immobilized catalyst offered

additional advantages of recycleability, extended stability, and increased resistance to

deactivation.

(1)

R=H   DBT
R=Me   4,6-Me$_2$DBT

(SiO$_2$-RTA)Re(O)(Me)(PPh$_3$)
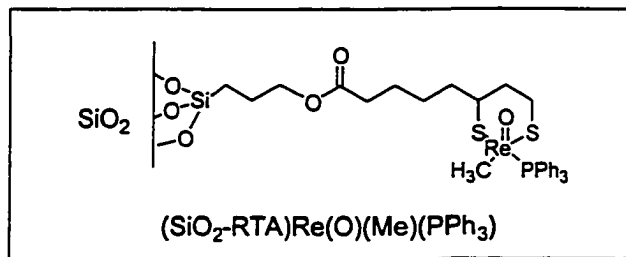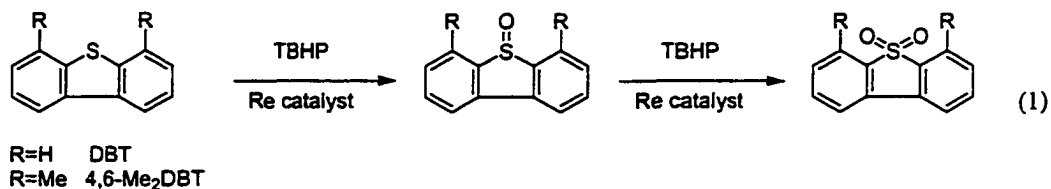
General Introduction

Dissertation Organization

This dissertation contains four papers, Chapters 2-5, in the format required for publication in the Journal of Molecular Catalysis A: Chemical describing the research I have performed at Iowa State University. The first chapter consists of an organizational overview and brief introduction to the topics covered. A general conclusion is included as Chapter 6 after the final paper. In the introduction, conclusion, as well as the papers, the literature citations, schemes, tables, equations, and figures pertain only to the chapters in which they appear.

Introduction

Homogeneous catalysts are capable of performing a wide range of chemical transformations, can be rationally modified to achieve diverse selectivity, and can be easily characterized. However, the homogeneous nature of the catalysts makes their separation and recovery after a reaction challenging. One strategy for the separation and reuse of homogeneous catalysts is to immobilize them on supports [1-5]. This immobilization affords the advantages of both homogeneous and heterogeneous catalysts. The selectivity, tunability, and ease of characterization of the homogeneous catalyst are retained as the active sites remain homogeneous single sites, similar to their solution analogs. In addition, the support allows separation and recovery of the catalyst from the reaction medium by simple filtration. Thus, the immobilization of homogeneous catalysts on solid supports gives a catalyst with the advantages of both homogeneous (selectivity, tuneability, and homogeneous sites) and heterogeneous (separation, recovery, and reuse) catalysts. Furthermore, additional benefits

due to site-isolation of the catalyst centers may occur since immobilization isolates the catalyst sites and prevents bimolecular deactivation pathways.

In previous studies of tethered catalysts in the Angelici group [6-11], it was observed that rhodium complexes tethered to silica that also contained supported palladium metal were highly active catalysts for the hydrogenation of arenes under mild conditions (1 atm, 40 °C). Both the tethered rhodium complex and supported palladium metal contributed to the high activities of the catalysts. Their activities were much greater than either the complex tethered to silica or palladium on silica separately. The specific roles of the tethered complex and supported palladium are not known, but it was suggested [6-11] that the increased activity is due to hydrogen activation by the palladium, hydrogen spillover [12] to the silica surface, and utilization of the activated hydrogen by the tethered rhodium catalyst. Another possibility is that the activity of the catalyst is due to rhodium metal on the silica, which is formed by palladium-promoted reduction of rhodium that dissociates from the tethered complex.

There is currently much interest in the synthesis of chiral organic compounds using enantioselective transition metal catalysts for the hydrogenation of prochiral olefins [1-4]. Within this methodology, the use of chiral phosphine-metal complexes represents an effective and highly studied area [1-4]. When such enantioselective catalysts are tethered on solid supports, the resulting catalysts combine the advantages of both homogeneous (selectivity, tuneability, and homogeneous sites) and heterogeneous (recovery and separation) catalysts [1-3]. Therefore, the immobilization of enantioselective homogeneous catalysts is a highly desirable goal.

One of the best examples of an immobilized enantioselective hydrogenation catalyst

is that reported by Pugin and Müller [13] and Pugin [14], who examined the enantioselective

hydrogenation of methyl-α-acetamidocinnamate, MAC, Eq. (1), using rhodium catalysts
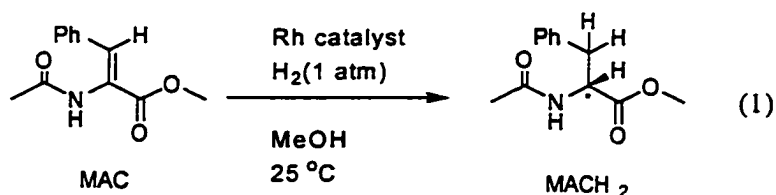
containing the chiral chelating phosphine (2S,4S)-4-(diphenylphosphino)-2-

(diphenylphosphinomethyl)pyrrolidine, PPM, Eq. (2),
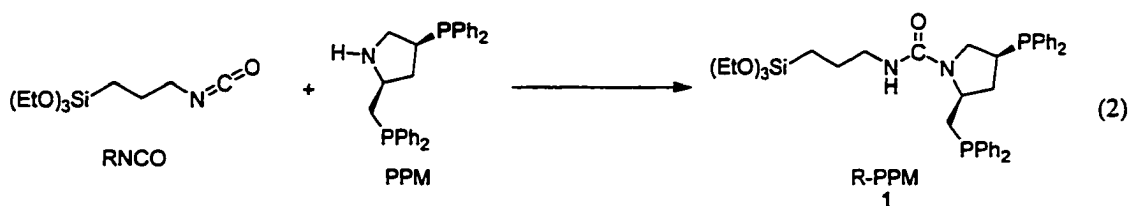
tethered on silica. The addition of $[Rh(COD)_2]^+BF_4^-$, where COD = 1,5 cyclooctadiene, to

the immobilized chiral, bidentate PPM ligand produced a very active and highly

enantioselective catalyst SiO_2-R-PPM-Rh-COD, with activities and enantioselectivities

comparable to those of the untethered $[(B-PPM)Rh(COD)]^+BF_4^-$ [B = CO_2(t-Bu)] in solution,

with turnover frequencies (TOF) of 6.25-12.5 min^{-1} and enantiomeric excesses (ee's) of 89.8-

94.5% [13].

Given the high enantioselectivity of Pugin's SiO_2-R-PPM-Rh-COD catalyst, we

sought to determine whether this catalyst in combination with supported Pd metal would

serve as an enantioselective catalyst for the hydrogenation of prochiral arenes. Prior to

performing the arene hydrogenation studies, we sought to characterize the SiO_2-R-PPM-Rh-

COD catalyst and to understand its stability, especially with respect to air oxidation. These

studies, together with initial investigations of arene hydrogenation using Pd-SiO$_2$-R-PPM-Rh-COD, consisting of SiO$_2$-R-PPM-Rh-COD and supported Pd metal, are described in this paper. These catalysts were investigated by ^{31}P NMR spectroscopy, diffuse reflectance infrared Fourier transform (DRIFT) spectroscopy, reaction studies (including measurements of rates and enantioselectivities of hydrogenation reactions), and mercury metal poisoning experiments.

In Chapter 3, we have attempted to determine whether palladium promotes the formation of rhodium metal in catalysts that are prepared by adsorbing Rh complexes on Pd-SiO$_2$. It was previously observed that rhodium complexes tethered to silica that also contained supported palladium metal were more active, for the hydrogenation of arenas, than either the complex tethered to silica or palladium on silica separately [6-11]. In the literature, there are reports of rhodium/palladium bimetallic catalysts on silica or alumina supports that are less active for arene hydrogenation than rhodium alone. Papers by del Angel *et. al.* [15] and Araya *et. al.* [16] show that supported bimetallic rhodium/palladium catalysts prepared by impregnation of RhCl$_3$ and PdCl$_2$ in aqueous solutions or bis(acetylacetonato)palladium in dichloromethane onto silica or alumina are less active for benzene hydrogenation than rhodium-only supported catalysts [15,16]. In contrast, tethered rhodium complexes and supported palladium metal are more active for arene hydrogenation than catalysts consisting of the tethered rhodium complexes only [6-11]. Therefore, we investigated conditions under which palladium increases or decreases the arene hydrogenation activity of rhodium catalysts.

Silica- and alumina-supported rhodium is known to be much more active than supported palladium as an arene hydrogenation catalyst [15-17]. The activity of the

palladium-supported catalyst is known to be structure insensitive and does not depend on the size of the palladium particles [17]. On the other hand, the activity of supported rhodium catalysts is structure sensitive and depends on particle size. Rhodium metal clusters of 10 Å or larger are needed for arene hydrogenation; smaller particles show no arene hydrogenation activity [17-20].

Considering the structure sensitive nature of supported rhodium catalysts, we also examined variations in activities of catalysts prepared from different types of rhodium complexes. Thus, the following four rhodium complexes were examined: $RhCl_3 \cdot 3H_2O$, $[Rh(COD)Cl]_2$ [21], $[Rh(COD)_2]^+BF_4^-$ [22], and $[Rh(COD)H]_4$ [23, 24]. $RhCl_3 \cdot 3H_2O$ was chosen as a Rh catalyst precursor because it is commonly used for the preparation of supported rhodium metal catalysts by the incipient wetness impregnation method. It is reduced to metallic rhodium on silica surfaces by exposure to hydrogen gas above 200 °C [25]. $[Rh(COD)Cl]_2$ is frequently used as a starting material for the synthesis of homogeneous rhodium hydrogenation catalysts [21], and was chosen for these studies as a model of surface species that may result from decomposition of rhodium halide catalysts. Also, Blum and coworkers [26] showed that a sol-gel-entrapped $[Rh(COD)Cl]_2$ becomes an active arene hydrogenation catalyst if metallic palladium is present in the sol-gel matrix. The authors suggested the activity of these catalysts arose from a synergy facilitated by the close proximity of the rhodium and palladium in the matrix. The cationic $[Rh(COD)_2]^+BF_4^-$ is frequently used to prepare homogeneous rhodium hydrogenation catalysts [22] and is a precursor for a number of tethered catalysts on silica [6-9,13]. In addition, the very similar $[Rh(COD)(PhCN)_2]^+ClO_4^-$ is reduced to metallic rhodium under hydrogenation conditions of 25 °C-100 °C in methanol, methylene chloride, or in the solid state [27]. Finally,

[Rh(COD)H]$_4$, which catalyzes the hydrogenation of toluene at room temperature (AR = 0.11 mol MeCy/mol Rh • min), is reduced to rhodium nanoclusters, with an average size of 2 nm, under the reaction conditions [24].

For the studies in Chapter 3, the RhCl$_3$•3H$_2$O catalysts were prepared by the standard impregnation method, while the other catalysts were synthesized by adsorbing the rhodium complexes onto silica (SiO$_2$) or palladium supported on silica (Pd-SiO$_2$) under conditions (refluxing toluene for 4 h) similar to those used in the synthesis of TCSM catalysts [6-11]. These catalysts were examined for their activities in toluene hydrogenation, under mild conditions of 1 atm H$_2$ and 40 °C (Eq. (3)). Sometimes the catalysts were studied without
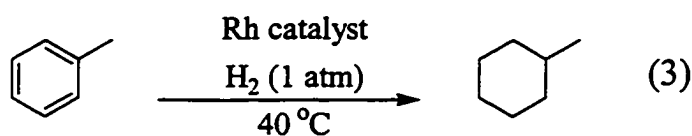
$$\text{Rh catalyst} \quad \xrightarrow[\text{40 °C}]{\text{H}_2\text{ (1 atm)}} \qquad (3)$$

pretreatment; at other times, they were pretreated with hydrogen at 40 °C for 24 h or 200 °C for 4 h. The 40 °C hydrogen pretreatment was chosen to reflect conditions that would be present under prolonged hydrogenation reaction times (Eq. (3)). The 200 °C hydrogen pretreatment was chosen to simulate conditions used in the production of Rh-SiO$_2$ from RhCl$_3$•3H$_2$O. The catalysts were also characterized by DRIFTS, TEM, and XPS.

Another reaction that is catalyzed by tethered rhodium complexes on silica containing supported palladium metal is the hydrodefluorination of fluorobenzene. It was shown previously that rhodium pyridylphosphine and bipyridyl complexes tethered to Pd-SiO$_2$ under 4 atm of hydrogen at 70 °C efficiently converted PhF to a mixture of CyH and CyF [10]. The product distribution was influenced by the solvent. In heptane, fluorocyclohexane (CyF) was the major product, but in heptane/ethanol, with added base (NaOAc being the

best), benzene (PhH) was formed initially but subsequently hydrogenated to cyclohexane

(CyH). The hydrodefluorination of fluorobenzene is noteworthy since carbon-fluorine bonds

are the strongest that carbon can form [28]. Also, although there are several examples of the

stoichiometric cleavage of C-F bonds by organometallic complexes, few complexes have

been reported that are capable of catalytic transformations of C-F bonds [29-38]. Even fewer

systems are capable of catalytic hydrodefluorination to remove fluorine from non-activated

monofluoroarenes [10,39-49]. Palladium on carbon (Pd/C), in the presence of NaOH at 82

°C, hydrodefluorinates fluorobenzene (PhF) to benzene (PhH) by hydrogen-transfer from

isopropanol [40, 41], but palladium was unable to catalyze the same reaction by hydrogen-

transfer from HCOOK in ethanol/water (1:3) or under 4 atm of H_2 at 37 °C in methanol [42].

The first example of hydrodefluorination of a monofluoroarene by hydrogen gas over a

heterogeneous metal was reported in 1920 by Swarts [43], who used Pt(black) in water to

hydrodefluorinate PhF to cyclohexane (CyH) and p-fluorobenzoic acid to

cyclohexanecarboxylic acid. Renoll utilized Swarts' conditions to hydrodefluorinate 2-

fluoro-4'-acetylbiphenyl to p-cyclohexylethylbenzene [44]. Pattison and Saunders reported

the hydrodefluorination of p-fluorophenylacetic acid to ethyl cyclohexylphenylacetate with

Raney Ni at 180-200 °C under 160-180 atm H_2 in ethanol [45]. Tashiro et.al. used Raney Ni-

Al and Raney Cu-Al alloys for the hydrodefluorination of p-fluoroacetophenone to 1-

phenylethanol at 50 °C in 10% NaOH(aq) [46]. The first reported use of rhodium metal for

the hydrodefluorination of a monofluoroarene was by Freedman et. al. [47] who converted

fluoroarylphosphonic acids to cyclohexylphosphonic acids under 4 atm of H_2 at room

temperature in 95% ethanol. Young and Grushin used [(Cy$_3$P)$_2$Rh(H)Cl$_2$] to catalytically

hydrodefluorinate 1-fluoronapthalene to naphthalene under 80 psi hydrogen at 95 °C in the

presence of 40% NaOH [48]. However, [(Cy₃P)₂Rh(H)Cl₂] was incapable of hydrodefluorinating PhF, 4-fluorotoluene, 3- or 4-fluoroanisole, or 4-fluoroaniline. Under identical conditions, metallic rhodium nanoparticles [48] catalyzed the hydrodefluorination of the C-F bond in 1-fluoronapthalene, PhF, 4-fluorotoluene, 3- or 4-fluoroanisole, and 4-fluoroaniline while catalyzing only trace amounts of hydrogenation of the resulting arenes. Blum *et. al.* reports that sol-gel encapsulated RhCl₃-Aliquat 336 catalyzes the hydrodefluorination and hydrogenation of fluorobenzene (PhF), 2- or 4-fluorotoluene, and 2-, 3-, or 4-fluoroanisole in 1,2-dichloroethane (DCE) at 80 °C under 16 atm of hydrogen to the corresponding dehalogenated, substituted cyclohexanes [49].

Our examination of supported bimetallic rhodium and palladium catalysts for arene hydrogenation, Chapters 2 and 3, prompted us to explore their hydrodefluorination capabilities. In Chapter 4, Rh-SiO₂ catalysts have been used in the hydrodefluorination of PhF to CyF, PhH, and/or CyH. The effects of solvent, pH, added base, temperature, and hydrogen pressure on product selectivity and reaction rates have been determined. Reaction selectivity can be controlled by reaction conditions. When used with the proper solvent and pH, Rh-SiO₂ catalyzes the hydrodefluorination of PhF under the mildest reported conditions (1 atm H₂ at 40°C) while still providing rates that are faster than those of other hydrodefluorination systems.

The last project described in this dissertation, Chapter 5, was motivated by the current EPA mandate for the reduction, by 2006, in total sulfur content of gasoline to 25 ppm from the current allowed level of 400 ppm [50]. This removal will need to come from refractory sulfides not currently removed by the first stages of hydrodesulfurization (HDS) [51]. Oxidative chemistry could be utilized for further sulfur reduction in oil as the oxides of

sulfides exhibit different solubility and reactivity properties [52-57]. While the oxidation of sulfides to sulfoxides and sulfones can be achieved by a variety of biological and laboratory methods [1-3, 5,57-59], the class of oxorhenium(V) dithiolate compounds stand out as highly effective and desirable oxygen atom transfer (OAT) catalysts from both kinetic as well as selectivity standpoints with many aspects of their mechanism and activities recently elucidated [52, 60-69]. Furthermore, the homogeneous oxorhenium(V) dithiolate compounds have already been shown to be very effective catalysts for *tert*-butylhydroperoxide (TBHP) oxidation of refractory sulfides, such as dibenzothiophene (DBT) and 4,6-dimethyldibenzothiophene (4,6-Me$_2$DBT) [52]. However, the utility of the catalysts would be increased if they could be more easily recycled and re-utilized after reactions. Catalyst immobilization is a viable method to achieve the best possible combination of catalyst activities, rates, and lifetimes. Thus, it was decided that the immobilization of oxorhenium(V) dithiolate catalysts be undertaken with particular emphasis on their oxidation activities for HDS relevant sulfides. The first example of a tethered oxorhenium(V) dithiolate catalyst is described in Chapter 5.

References

[1] J.D. Morrison (Ed.), Asymmetric Synthesis, Vol. 5, Chiral Catalysis, Academic Press, Orlando, 1985.

[2] D.E. Vos, I.F.J. Vankelecom, P.A. Jacobs (Eds.), Chiral Catalyst Immobilization and Recycling, Wiley-VCH, New York, 2000.

[3] E.N. Jacobsen, A. Pfaltz, H. Yamamoto (Eds.), Comprehensive Asymmetric Catalysis, Vols. 1 and 3, Springer, New York, 1999.

[4] M.J. Burk, F. Bienewald, Transition Met. Org. Synth. 2 (1998) 13.

[5] D.E. DeVos, B.F. Sels, P.A. Jacobs, Advances in Catalysis 46 (2001) 1.

[6] H. Gao, R.J. Angelici, J. Mol. Catal. A: Chem. 149 (1999) 63.

[7] H. Gao, R.J. Angelici, J. Am. Chem. Soc. 119 (1997) 6937.

[8] H. Gao, R.J. Angelici, Organometallics 18 (1999) 989.

[9] H. Gao, R.J. Angelici, New J. Chem. 23 (1999) 633.

[10] H. Yang, H. Gao, R.J. Angelici, Organometallics 18 (1999) 2285.

[11] H. Yang, H. Gao, R.J. Angelici, Organometallics 19 (2000) 622.

[12] W.C. Conner Jr., J.L. Falconer, Chem. Rev. 95 (1995) 759.

[13] B. Pugin, M. Müller, in M. Guisnet et. al. (Ed.), Stud. Surf. Sci. Cat. Part 78:

Heterogeneous Catalysis and Fine Chemicals III, Elsevier (1993) 107.

[14] B. Pugin, J. Mol. Catal. A: Chem. 107 (1996) 273.

[15] G. del Angel, B. Coq, F. Figueras, J. Catal. 95 (1985) 167.

[16] P.E. Araya, E.E. Miro, L. Cornaglia, J. Chem. Research (S) (1997) 258.

[17] G.A. del Angel, B. Coq, G. Ferrat, F. Figueras, Surface Science 156 (1985) 943.

[18] W.F. Graydon, M.D. Langan, J. Catal. 69 (1981) 180.

[19] T. Ioannide, X.E. Verykios, J. Catal. 143 (1993) 175.

[20] F. Fajardie, J.-F. Tempere, G. Djega-Mariadassou, G. Blanchard, J. Catal. 163 (1996) 77.

[21] G. Giordano, R.H. Crabtree, Inorg. Synth. 19 (1979) 218.

[22] R.R. Schrock, J.A. Osborn, J. Am. Chem. Soc. 93 (1971) 3089.

[23] M. Kulzick, R.T. Price, E.L. Muetterties, V.W. Day, Organometallics 1 (1982) 1256.

[24] Z. Duan, M.J. Hampden-Smith, A.P. Sylwester, Chem. Mater. 4 (1992) 1146.

[25] T. Ioannides, X. Veeykios, J. Catal. 140 (1993) 353.

[26] a) R. Abu-Reziq, D. Avnir, I. Miloslavski, H. Schumann, J. Blum, J. Mol. Catal. A: Chem. 185 (2002) 179.

b) R. Abu-Reziq, D. Avnir, J. Blum, J. Mol. Catal. A: Chem. 187 (2002) 277.

[27] C.S. Chin, B. Lee, J. Moon, J. Song, Y. Park, Bull. Korean Chem. Soc. 16 (1995) 528.

[28] M. Hudlicky, Chemistry of Organic Fluorine Compounds, Prentice-Hall, New York, 1992, p. 175.

[29] J.L. Kiplinger, T.G. Richmond, C.E. Osterberg, Chem. Rev. 94 (1994) 373.

[30] J. Burdeniuc, B. Jedlicka, R.H. Crabtree Chem. Ber./Recl. 130 (1997) 145.

[31] E. Murphy, R. Murugavel, H. W. Roesky, Chem. Rev. 97 (1997) 3425.

[32] T.G. Richmond, Topics in Organomet. Chem. 3 (1999) 243.

[33] R. Bosque, E. Clot, S. Fantcci, F. Maseras, O. Eisenstein, R.N. Perutz, K.B. Renkema, K.G. Caulton, J. Am. Chem. Soc. 120 (1998) 12634.

[34] N.Y. Adonin, V.F. Starichenko, Mendeleev Commun. 2 (2000) 60.

[35] D. Huang, P.R. Koren, K. Folting, E.R. Davidson, K.G. Caulton, J. Am. Chem. Soc. 122 (2000) 8916.

[36] K.M. Bradley, R.J. Lachicotte, W.D. Jones, J. Am. Chem. Soc. 123 (2001) 10973.

[37] K.M. Bradley, W.D. Jones, J. Am. Chem. Soc. 124 (2002) 8681.

[38] R.P. Huges, S. Willemsen, A. Williamson, D. Zhang, Organometallics 21 (2002) 3085.

[39] M. Hudlicky, J. Fluorine Chem. 44 (1989) 345.

[40] F.J. Urbano, J.M. Marinas, J. Mol. Catal. A: Chem 173 (2001) 329.

[41] Y. Ukisu, T. Miyadera, J. Mol. Catal. A: Chem. 125 (1997) 135.

[42] M.A. Aramendia, V. Borua, I.M. Garcia, C. Jimenez, A. Marinas, J.M. Marinas, F.J. Urbano, C. R. Acad. Sci. Paris, Serie IIC, Chimie, 3 (2000) 465.

[43] a) F. Swarts, Bull. Acad. Roy. Belg. (1920) 399; Chem. Abstr. 16 (1922) 2316.

a) F. Swarts, Bull. Acad. Roy. Belg. (1936) 122; Chem. Abstr. 30 (1936) 4154.

[44] M.W. Renoll, J. Am. Chem. Soc. 68 (1946) 1159.

[45] F.L.M Pattison, B.C. Saunders, J. Chem. Soc. (1949) 2745.

[46] M. Tashiro, H. Nakamura, K. Nakayama, Org. Prep. Proc. Int. 19 (1987) 442.

[47] L.D. Freedman, G.O. Doak, E.L. Petit, J. Am. Chem. Soc. 77 (1955) 4262.

[48] R.J. Young, V.V. Grushin, Organometallics 18 (1999) 294.

[49] J. Blum, A. Rosenfeld, F. Gelman, H. Schumann, D. Avnir, J. Mol. Catal. A: Chem. 146 (1999) 117.

[50] M. Borushko, Fed. Regist. 66 (2001) 5001.

[51] a) D.D. Whitehurst, T. Isoda, I. Mochida, Adv. Catal. 42 (1998) 345.

b) B.C. Gates, H. Topsøe, Polyhedron 16 (1997) 3213.

c) H. Topsøe; B.S. Clausen, F.E. Massoth, Hydrotreating Catalysis Science and Technology, Springer, Berlin, (1996) p. 7.

[52] Y. Wang, G. Lente, J.H. Espenson, Inorg. Chem. 41 (2002) 1272.

[53] F.M. Collins, A.R. Lucy, C. Sharp, J. Mol. Catal. A: Chem. 117 (1997) 397.

[54] K. Yatsu, H. Miki, K. Ukegaw, N. Yamamoto, (Ministry of Economy, Trade and Industry; National Industrial Research Institute, Japan). Jpn. Kokai Tokkyo Koho 2001; Patent No. JP2001/29376, p 12.

[55] S. Otsuki, T. Nonaka, W. Qian, A. Ishihara, T. Kabe, Sekiyu Gakkaishi 42 (1999) 315.

[56] K. Yazu, Y. Yamamoto, T. Furuya, K. Miki, K. Ukegawa, Energy & Fuels 15 (2001) 1535.

[57] C. Song, X. Ma, Appl. Catal. B: Environ. 41 (2003) 207.

[58] a) R. Hille, Chem. Rev. 96 (1996) 2757.

b) R.H. Holm, J.M. Berg, Acc. Chem. Res. 19 (1986) 363.

c) R.H. Holm, Chem. Rev. 87 (1987) 1401.

d) S.J. Lippard, J.M. Berg, Principles of Bioinorganic Chemistry; University Science Books: Mill Valley, CA, 1994.

[59] a) G. N. George, J. Hilton, C. Temple, R.C. Prince, K.V. Rajagopalan, J. Am. Chem. Soc. 121 (1999) 1256.

b) K.-M Sung, R.H. Holm, J. Am. Chem. Soc. 123 (2001) 1931.

c) L.J. Laughlin, C.G. Young, Inorg. Chem. 35 (1996) 1050.

d) P.D. Smith, A.J. Millar, C.G. Young, A. Ghosh, P.J. Basu, J. Am. Chem. Soc. 122 (2000) 9298.

e) P.D. Smith, D.A. Slizys, G.N. George, C.G. Young, J. Am. Chem. Soc. 122 (2000) 2946.

[60] J. Jacob, J.H. Espenson, Chem. Commun. (1999) 1003.

[61] J. Jacob, I.A. Guzei, J.H. Espenson, Inorg. Chem. 38 (1999) 1040.

[62] J. Jacob, G. Lente, I.A. Guzei, J.H. Espenson, Inorg. Chem. 38 (1999) 3762.

[63] G. Lente, J. Jacob, I.A. Guzei, J.H. Espenson, Inorg. React. Mech. (Amsterdam) 2 (2000) 169.

[64] G. Lente, I.A. Guzei, J.H. Espenson, Inorg. Chem. 39 (2000) 1311.

[65] G. Lente, X. Shan, I.A. Guzei, J.H. Espenson, Inorg. Chem. 39 (2000) 3572.

[66] G. Lente, J.H. Espenson, Inorg. Chem. 39 (2000) 4809.

[67] D.W. Lahti, J.H. Espenson, J. Am. Chem. Soc. 123 (2001) 6014.

[68] J.H. Espenson, X. Shan, Y. Wang, R. Huang, D.W. Lahti, J. Dixon, G. Lente, A. Ellern, I.A. Guzei, Inorg. Chem. 41 (2002) 2583.

[69] J. Dixon, J.H. Espenson, Inorg. Chem. 41 (2002) 4727.

^{31}P NMR and IR Characterization of Enantioselective Olefin and Arene Hydrogenation Catalysts Containing a Rhodium-Chiral Phosphine Complex Tethered on Silica

Keith J. Stanger, Jerzy W. Wiench, Marek Pruski, and Robert J. Angelici

Abstract

Rhodium complexes of the chiral chelating phosphine (2S,4S)-4-(diphenylphosphino)-2-(diphenylphosphinomethyl)pyrrolidine (X-PPM) tethered on silica (SiO_2), tethered on silica with supported palladium (Pd-SiO_2), and in solution were characterized by ^{31}P NMR and IR spectroscopies. These studies show that the (X-PPM)Rh(COD)$^+$ complex, which is highly enantioselective for the hydrogenation of the prochiral olefin methyl-α-acetamidocinnamate (MAC), retains its composition in the tethered catalysts regardless of its mode of preparation or the presence of Pd on the silica surface. These investigations also show that the chiral diphosphine ligand remains coordinated to the rhodium during the reaction. Both the tethered and solution catalysts are moderately air sensitive prior to use, giving the free phosphine oxide of X-PPM, which is no longer coordinated to the rhodium. During and after use in catalytic reactions, the tethered rhodium complexes are extremely air-sensitive, but were characterized by ^{31}P NMR and IR spectra of their carbon monoxide derivatives. Finally, the catalysts were examined for their arene hydrogenation activity. It was established that Pd in the (X-PPM)Rh(COD)$^+$/Pd-SiO_2 catalyst causes the reduction of any uncomplexed Rh to metallic species during the

hydrogenation reactions. It was these metallic Rh species that were responsible for the

toluene hydrogenation activity of these tethered $(X\text{-}PPM)Rh(COD)^+/Pd\text{-}SiO_2$ catalysts.

1. Introduction

There is currently much interest in the synthesis of chiral organic compounds using

enantioselective transition metal catalysts for the hydrogenation of prochiral olefins [1-4].

Within this methodology, the use of chiral phosphine-metal complexes represents an

effective and highly studied area [1-4]. When such enantioselective catalysts are tethered on

solid supports, the resulting catalysts combine the advantages of both homogeneous

(selectivity, tuneability, and homogeneous sites) and heterogeneous (recovery and

separation) catalysts [1-3]. Therefore, the immobilization of enantioselective homogeneous

catalysts is a highly desirable goal.

One of the best examples of an immobilized enantioselective hydrogenation catalyst

is that reported by Pugin and Müller [5] and Pugin [6], who examined the enantioselective

hydrogenation of methyl-α-acetamidocinnamate, MAC, Eq. (1), using rhodium catalysts

$$(1)$$

containing the chiral chelating phosphine (2S,4S)-4-(diphenylphosphino)-2-
(diphenylphosphinomethyl)pyrrolidine, PPM, Eq. (2),

$$(2)$$
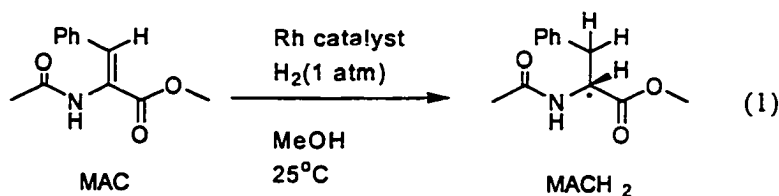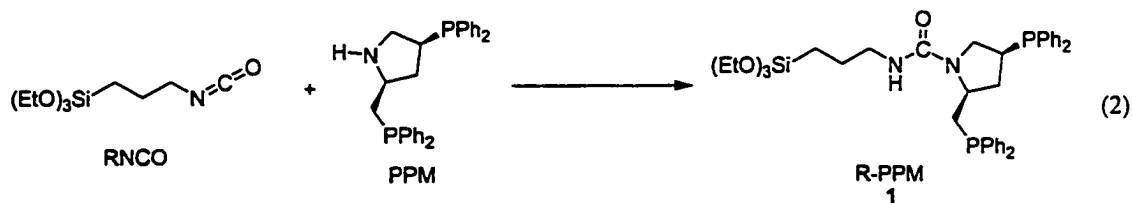
tethered on silica. The catalysts were prepared as shown in Scheme 1. The addition of

$[Rh(COD)_2]^+BF_4^-$ (4), where COD=1,5 cyclooctadiene, to the immobilized chiral, bidentate

PPM ligand produced a very active and highly enantioselective catalyst SiO_2-R-PPM-Rh-

COD (3), with activities and enantioselectivities comparable to those of the untethered [(B-

PPM)Rh(COD)]$^+BF_4^-$ (5) [B = -CO_2(t-Bu)] in solution, with turnover frequencies (TOF) of

6.25-12.5 min^{-1} and enantiomeric excesses (ee's) of 89.8-94.5% [5].

In previous studies from our group [7-11], we observed that rhodium complexes

immobilized on silica that also contained supported palladium metal were highly active

catalysts for the hydrogenation of arenes. Given the high enantioselectivity of Pugin's SiO_2-

R-PPM-Rh-COD (3) catalyst, we sought to determine whether this catalyst in combination

with supported Pd metal would serve as an enantioselective catalyst for the hydrogenation of

prochiral arenes.

Prior to performing the arene hydrogenation studies, we sought to characterize the

SiO_2-R-PPM-Rh-COD (3) catalyst and to understand its stability especially with respect to

air oxidation. These studies, together with initial investigations of arene hydrogenation using

Pd-SiO_2-R-PPM-Rh-COD (6), consisting of SiO_2-R-PPM-Rh-COD (3) and supported Pd

metal, are described in this paper. These catalysts were investigated by ^{31}P NMR

spectroscopy, diffuse reflectance infrared Fourier transform (DRIFT) spectroscopy, reaction

studies (including measurements of rates and enantioselectivities of hydrogenation reactions),

and mercury metal poisoning experiments.

2. Experimental

2.1. General considerations

The chemicals $RhCl_3 \cdot 3H_2O$ (Pressure Chemicals), $PdCl_2$ (DFG), 3-isocyanatopropyltriethoxysilane RNCO (Fluka), H_2O_2 (30 wt. %), PPM, and COD (Aldrich) were purchased from commercial sources and used as received. Silica gel Merck grade 10184 (B.E.T. surface area, 300 m^2 g^{-1}; pore size 100 Å) (Aldrich) was dried under vacuum at 150 °C for 12 h and kept under argon before use. Toluene and methylene chloride were dried prior to use by passage through an alumina column under argon [12]. Methanol was distilled from Mg/ I_2 under nitrogen [13]. The preparation of MAC followed a literature procedure [14,15] that utilized methanolysis of Z-methyl-4-benzaloxazolone [15]. Purification of MAC was achieved by repeated recrystallization from MeOH. The compound $[Rh(COD)_2]^+BF_4^-$ (4) was prepared by the general procedures reported by Schrock and Osborn [16]. The preparation of $Pd-SiO_2$ (10% Pd w/w) (7) [17,18] was described previously. All manipulations involving rhodium or phosphine were carried out under an argon atmosphere using standard Schlenk techniques.

FTIR and DRIFT spectra were obtained on a Nicolet 560 spectrophotometer. The main compartment, equipped with a TGS detector and an NaCl solution cell, was used to take solution IR spectra. An auxiliary experiment module (AEM) containing a Harrick diffuse reflectance accessory with a MCT detector was used to obtain the DRIFT spectra of solid samples. Gas chromatographic (GC) analyses were performed on a Hewlett Packard HP 6890 GC using a 25 m HP-1 capillary column and an FID (flame ionization detector). Enantiomeric excesses were determined by GC analysis of products on a Chirasil-Val capillary column (50 m x 250 μm) (Alltech) capable of separating the two enantiomers of the

hydrogenation product *N*-acetyl-phenylalanine methyl ester, MACH$_2$ (**8**). GC samples were taken from the reaction mixtures and either run as obtained or diluted with ethanol as necessary.

^{31}P NMR spectra of liquid samples were run at 161.92 MHz on a Bruker DRX 400-MHz NMR spectrometer. ^{31}P solid-state NMR spectra were carried out at the same frequency using a Chemagnetics CMX Infinity spectrometer equipped with a 3.2 mm magic angle spinning (MAS) probe. The MAS rotors were loaded in a glove bag under dry nitrogen to reduce oxidation of samples during the experiments. The relaxation measurements yielded T$_1$ values of at least 300 s for ^{31}P and 1 to 3 s for ^{1}H. Thus, cross polarization (CP) between ^{1}H and ^{31}P was applied in order to enhance the sensitivity and reduce the recycle delay between consecutive scans. The experiments used a cosine-modulated CP scheme synchronized with the rotor period [19], using a sample rotation rate of 18 kHz (unless specified otherwise), contact time of 0.5 ms, continuous wave ^{1}H decoupling at 70 kHz, pulse delay of 5 s and number of scans between 128 and 8,000. All phosphorus chemical shifts are reported using the δ scale, with positive values being downfield, and are referenced to an 85% solution of H$_3$PO$_4$ in water.

Rhodium content of the supported catalysts was determined by ICP-AES conducted by MPC Analytical Services of the Ames Laboratory. Samples for analysis were prepared by dissolving 50 mg of the supported catalyst in 5.0 ml of aqua regia at 90 °C; then 5.0 ml of 5% aqueous HF was added and the mixture was heated to the same temperature. The resulting solution was diluted to 25 ml in a volumetric flask. For the catalysts prepared by method A, the average rhodium loadings on SiO$_2$ were 79% (78.9 ± 9.4) of the rhodium added; those on Pd-SiO$_2$ were 70% (69.9 ± 10.5) of the rhodium added. For the catalysts

prepared by method **B** or by adsorbing the Rh complexes on SiO_2 or $Pd-SiO_2$, the rhodium

added to the system corresponds to the rhodium present (as no washings precede catalyst

use). The experimentally determined rhodium compositions were used in the rate (TOF)

calculations.

2.2. Preparation of rhodium complexes.

PPM-Rh-COD (**9**): A mixture of 15.0 mg (33.1 μmol) of PPM and 13.4 mg (33.0

μmol) of $[Rh(COD)_2]^+BF_4^-$ (**4**) dissolved in 1.0 ml of degassed CH_2Cl_2 or $CDCl_3$ was stirred

under argon for 15 min. The ^{31}P NMR spectrum of (**9**) in $CDCl_3$ is very similar to that

reported in the literature for the same complex with another counter anion (ClO_4^-) [20]: δ

42.4 (d of d, J_{Rh-P} = 113 Hz, J_{P-P} = 37 Hz) and 32.5 (d of d, J_{Rh-P} = 110 Hz, J_{P-P} = 37 Hz).

R-PPM (**1**): Compound **1** was prepared in a manner similar to that described in the

literature [5]. Solid PPM, 15.0 mg (33.1 μmol), dissolved in 1.0 ml of CH_2Cl_2 was treated

with 9.1 μl (37 μmol, 1.2 eq) of RNCO and stirred for 20 min. The resulting solution of R-

PPM (**1**) was used directly for complexation to rhodium or tethering to silica. The procedure

worked equally well in toluene or $CDCl_3$. Spectral data are identical to those reported in the

literature [5]. ^{31}P NMR ($CDCl_3$): δ -8.2 (s) and –22.3 (s).

R-PPM-Rh-COD (**10**): The preparation of the phosphine-rhodium complex R-PPM-

Rh-COD (**10**) was similar to that for analogous $Rh(diphosphine)(COD)^+$ complexes reported

in the literature [3,20-23]. A CH_2Cl_2 or $CDCl_3$ solution of 9.6 mg (14 μmol) of R-PPM (**1**) in

0.7 ml of solvent was added to 5.0 mg (12 μmol, 0.9 eq) of $[Rh(COD)_2]^+BF_4^-$ (**4**) and stirred

for 10 min. The resulting product **10** was isolated by removal of solvent under vacuum,

.

washing with hexanes (3 x 1 ml), and drying under vacuum. ^{31}P NMR (CDCl$_3$): δ 44.2 (d of

d, J_{Rh-P} = 146 Hz, J_{P-P} = 38 Hz) and 16.8 (d of d, J_{Rh-P} = 140 Hz, J_{P-P} = 38 Hz).

2.3. Preparation of silica-tethered complexes

SiO$_2$-R-PPM (2): Following a general procedure for tethering trialkoxysilanes to

silica surfaces [7], 23.2 mg (33.1 μmol) of R-PPM (1) was dissolved in 3.0 ml of toluene and

slurried over 0.12 g of SiO$_2$. The mixture was stirred at reflux for 12 h and then cooled to RT

and stirred overnight. The resulting solid was washed three times with 5.0 ml of toluene and

then dried under vacuum. ^{31}P CPMAS NMR (Fig. 1a): δ –7 and –23 ppm.

SiO$_2$-R-PPM-Rh-COD (3): **Method (A)**. A solution of 53.5 mg (53.6 μmol) of R-

PPM-Rh-COD (10) dissolved in 5.0 ml of methylene chloride/toluene (1:4) solution was

added to 0.20 g of SiO$_2$. The resulting slurry was refluxed for 12 h and then stirred overnight

at room temperature. Filtration, followed by washing with 5.0 ml of CH$_2$Cl$_2$ three times, and

drying under vacuum gave **3A**. **Method (B)**. Following the preparation described by Pugin

[5], a 1.0 ml MeOH solution containing 9.9 mg (24.4 μmol) of [Rh(COD)$_2$]$^+$BF$_4^-$ (4) was

added to 0.10 g (~26 μmol of R-PPM (1), based on initial loading) of SiO$_2$-R-PPM (2). The

resulting solid **3B** was then dried under vacuum. Both methods produced nearly identical

surface species as determined by solid-state ^{31}P NMR spectroscopy. ^{31}P CPMAS NMR (Fig.

1b,c): δ 43 and 15 ppm.

SiO$_2$-R-PPM-O$_2$ (11): The tethered phosphine oxide 11 was produced by three

methods: a) A slurry of 50 mg of SiO$_2$-R-PPM (2) in 2.0 ml of acetone was treated with 5

drops of H$_2$O$_2$ (30 wt. %) and stirred for 15 min. The solid was dried under vacuum. b) A

slurry of 50 mg of SiO$_2$-R-PPM-Rh-COD (3) in 2.0 ml of acetone was reacted with 5 drops

of H_2O_2 (30 wt. %) for 15 min. The solid was dried under vacuum. c) A vial of 50 mg of

SiO_2-R-PPM-Rh-COD (3) was exposed to ambient atmosphere for 5 days. All three methods

gave the same product (11), although some starting material (3) was observed in method c)

after only 3 days. ^{31}P CPMAS NMR (Fig. 2): δ 35 ppm.

2.4. Preparation of tethered complexes on palladium silica gel

Pd-SiO_2-R-PPM (12): Similar to the preparation of SiO_2-R-PPM (2), a solution of

23.2 mg (33.1 μmol) of R-PPM (1) in 3.0 ml of toluene was slurried with 0.12 g of Pd-SiO_2

(7). The mixture was stirred at reflux for 12 h and then cooled to room temperature and

stirred overnight. The resulting solid was washed three times with 5.0 ml of toluene and then

dried under vacuum. ^{31}P CPMAS NMR (Fig. 1d): δ −7 and −21 ppm.

Pd-SiO_2-R-PPM-Rh-COD (6): **Method (A).** A solution of 53.5 mg (53.6 μmol) of R-

PPM-Rh-COD (10) dissolved in 5.0 ml of methylene chloride/toluene (1:4) was added to

0.20 g of Pd-SiO_2 (7). The resulting slurry was refluxed for 12 h and then stirred overnight at

room temperature. Filtration, followed by washing three times with 5.0 ml of CH_2Cl_2 and

drying under vacuum gave **6A. Method (B).** A solution consisting of 9.9 mg (24.4 μmol) of

$[Rh(COD)_2]^+BF_4^-$ (4) in 1.0 ml of MeOH was added to 0.10 g (26.8 μmol R-PPM) of Pd-

SiO_2-R-PPM (12). The resulting solid **6B** was then dried under vacuum. Method A produced

the expected surface species, **6**, as established by solid-state ^{31}P NMR spectroscopy (see the

^{31}P CPMAS spectrum of Fig. 1e with two resonances at 45 and 15 ppm). In the

corresponding ^{31}P CPMAS spectrum of the sample prepared using method (B), the

resonances at 45 and 15 ppm are superimposed with additional lines centered at around 35

ppm for the phosphine oxide **13** (see Fig. 1f).

Pd-SiO$_2$-R-PPM-O$_2$ (13): The tethered phosphine oxide on Pd-SiO$_2$ 13 was produced by three methods: a) A slurry of 50 mg of Pd-SiO$_2$-R-PPM (12) in 2.0 ml of acetone was treated with 5 drops of H$_2$O$_2$ (30 wt. %) and stirred for 15 min. The solid was dried under vacuum. b) A slurry of 50 mg of Pd-SiO$_2$-R-PPM-Rh-COD (6) in 2.0 ml of acetone was reacted with 5 drops of H$_2$O$_2$ (30 wt. %) for 15 min. The solid was dried under vacuum. c) A vial of 50 mg of Pd-SiO$_2$-R-PPM-Rh-COD (6) was exposed to ambient atmosphere for 5 days. Again, for all three methods, the product (13) was identical, although starting material (6) was observed after only 3 days in method c). ^{31}P CPMAS NMR: δ 35 ppm (the same as Fig. 2).

2.5. Hydrogenation reactions

2.5.1. Hydrogenation of MAC

A standard hydrogenation run consisted of placing 50 mg of catalyst (~13.4 μmol of Rh) into a three-necked, jacketed vessel containing a Teflon-coated stir bar. One neck of the reaction vessel was capped with a glass stopper. The center neck was fitted with a rubber and Teflon septum to allow for input of solvents and removal of GC samples via syringe. The third neck was fitted with a three arm "Y" stopcock. This allowed the reaction vessel to be attached to a vacuum/argon Schlenk line and a burette filled with hydrogen. After the catalyst was placed in the reaction vessel, the atmosphere in the reaction flask was replaced with Ar using three vacuum/flush cycles. Next, the jacket of the vessel was attached to a constant temperature bath and the temperature was raised to 25.0 (±0.2) °C. While the temperature was being achieved, the hydrogen gas reservoir was filled though a series of three consecutive vacuum and hydrogen gas flush cycles. After the temperature had stabilized at 25.0 °C and the gas burette was full of hydrogen, the reaction vessel itself was evacuated and

filled with hydrogen three times. Immediately after replacing the Ar atmosphere with hydrogen, 5.0 ml of a 0.10 M MAC solution in MeOH were added via syringe. The reaction was opened to the hydrogen gas reservoir, stirring was initiated, and hydrogen uptake was recorded. The rate of reaction was monitored by the volume of hydrogen taken up with time. In addition, conversions based on H_2 uptake were confirmed by GC analysis of the solutions during and after the reaction. In all cases, $MACH_2$ (8) was the only MAC-hydrogenation product observed by GC, and the hydrogen uptake reading from the burette matched the GC analysis [24].

2.5.2. Hydrogenation of toluene

The general procedure used for the hydrogenation of MAC was employed with the following modifications: the temperature of the reaction was held at 40.0 (±0.2) °C, and the solvent (toluene) was also the reactant.

2.5.3. Mercury poisoning studies

The general procedure used for the hydrogenation of MAC or toluene was employed with the following modification: 0.10 ml (6.8 mmol, ~10 eq compared to Rh) of Hg was added prior to or after solvent addition.

2.5.4. Catalyst reuse

Two methods of catalyst reuse were examined. The first consisted of filtering the reaction mixture, washing the solid catalyst with MeOH, drying it, and reweighing it. This inevitably exposed the used catalyst to the atmosphere during the reweighing step. The air sensitivity of the catalyst during and after reaction results in deactivation of the catalyst if it is exposed to air even for a few seconds and prevents reuse by this method. The second method of catalyst reuse involved the *in situ* addition of extra MAC substrate, without

isolation of the used catalyst from the reaction vessel. In this case, the catalyst retained its activity when additional substrate, MAC, was added to the reaction vessel.

3. Results and Discussion

3.1. Characterization of the catalyst and its components before hydrogenation of MAC

3.1.1. Characterization of X-PPM and (X-PPM)Rh(COD)$^+$ species in solution

The parent PPM and R-PPM complexes in solution serve as spectroscopic models for related tethered species. The ^{31}P NMR data (Table 1) for the free ligand PPM (singlets at – 3.7 and –20.3 ppm) are the same as those reported in the literature [20]. Attachment of the linker R to form R-PPM (1), Eq. (2), results in a characteristic shift in the ^{31}P NMR spectra to –8.2 and –22.3 ppm, which is the same as observed by Pugin and Müller [5]. Addition of [Rh(COD)$_2$]$^+$BF$_4^-$ (4) to R-PPM (1) produces the expected but previously unreported R-PPM-Rh-COD (10) species (Scheme 2). Numerous related X-PPM-Rh-COD species have been produced by the displacement of a COD ligand from [Rh(COD)$_2$]$^+$A$^-$ (A$^-$ is a counter anion such as BF$_4^-$ or ClO$_4^-$) with X-PPM, where X-PPM is a PPM derivative with various X groups on the pyrrolidine nitrogen such as H, CO$_2$(t-Bu), and CO(t-Bu) [11,20-23]. The resultant R-PPM-Rh-COD (10) shows ^{31}P NMR signals that are consistent with those of other known X-PPM-Rh-COD complexes: R-PPM-Rh-COD (10) ([R-PPM-Rh-COD]$^+$BF$_4^-$) exhibits a doublet of doublets at 44.2 and 16.8 ppm with J_{Rh-P} = 146 and 140 Hz and J_{P-P} = 38 Hz; [P-PPM-Rh-COD]$^+$ClO$_4^-$ (14), in which P-PPM is an –CO(t-Bu) derivative of PPM, has a doublet of doublets at 43.1 and 12.1 ppm with J_{Rh-P} = 146 and 139 Hz and J_{P-P} = 37 Hz [20]; and [B-PPM-Rh-COD]$^+$ClO$_4^-$ (5), in which B-PPM is a –CO$_2$(t-Bu) derivative of PPM, exhibits a doublet of doublets at 41.6 and 12.6 ppm with J_{Rh-P} = 145 and 140 Hz and J_{P-P} = 37 Hz [20]. Note that the ^{31}P splitting pattern, consisting of two doublets of doublets resulting

from coupling of the phosphines to each other as well as to the spin 1/2 rhodium establishes

the complexation of PPM to rhodium in the compound. In addition, the P-P coupling

constants (38 Hz) and the Rh-P coupling constant (~140 Hz) are consistent with those seen in

other X-PPM-Rh-COD complexes [20].

While PPM appears to be air stable, R-PPM (1) easily forms the phosphine oxide, R-

PPM-O$_2$ (15) in air, Eq (3). This occurs if a solution of R-PPM (1) is exposed to air for a

$$(3)$$

X-PPM		X-PPM-O$_2$		X-PPM	
X= R	1	X= R	15	X= R	10
SiO$_2$-R	2	SiO$_2$-R	11	SiO$_2$-R	3
Pd-SiO$_2$-R	12	Pd-SiO$_2$-R	13	Pd-SiO$_2$-R	6
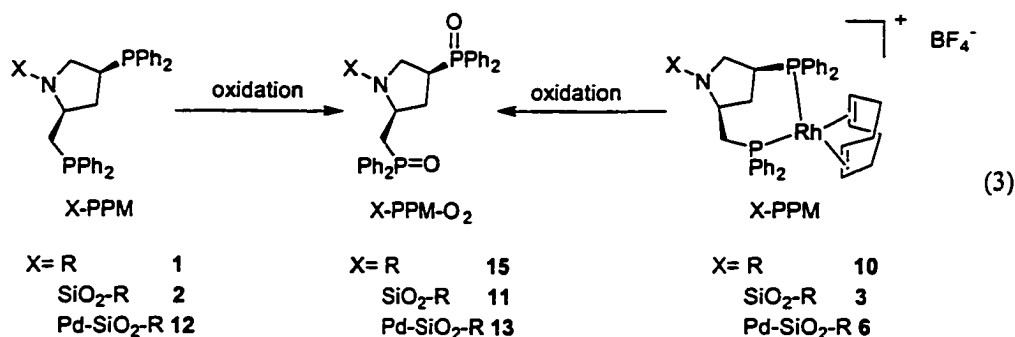
few days at room temperature or overnight at elevated temperature (110 °C). The rhodium

complex R-PPM-Rh-COD (10) is even more air sensitive, oxidizing completely overnight in

solution at room temperature. The oxidation of either compound occurs within 5 min when

reacted with hydrogen peroxide, H$_2$O$_2$ (30 wt. %). Oxidation of 1 or 10 by either method

gives R-PPM-O$_2$ (15), as indicated by the ^{31}P NMR spectrum which contains singlets at 32.4

and 31.6 ppm.

3.1.2. Characterization of R-PPM and (R-PPM)Rh(COD)$^+$ species tethered on SiO$_2$

When R-PPM (1) is tethered to silica by refluxing in toluene with SiO$_2$ for 16 h, the

identity of the resulting product SiO$_2$-R-PPM (2) was established by the similarity of its [31]P

CPMAS NMR spectrum (Fig. 1a) to that of R-PPM (1) in solution. The solid SiO$_2$-R-PPM

(2) shows ^{31}P NMR signals at -7 and -23 ppm; these are nearly identical to those of R-PPM

(1) in solution at -8.2 and -22.3 ppm. This similarity also suggests that the tethering process

does not change the environment of the R-PPM phosphine ligand; that is, the phosphines on the R-PPM ligand do not coordinate to acidic sites on the SiO_2 surface.

SiO_2-R-PPM (2) oxidizes in air to SiO_2-R-PPM-O_2 (11) slowly over a few days, Eq. (3). The oxidation of 2 with H_2O_2 (30 wt. %) in acetone at room temperature occurs completely within 5 min. The ^{31}P CPMAS spectrum of SiO_2-R-PPM-O_2 (11) consists of a broad absorption at 35 ppm (Fig. 2), which compares with two bands at 32.4 and 31.6 ppm for R-PPM-O_2 (15) in $CDCl_3$.

The tethered catalyst, SiO_2-R-PPM-Rh-COD (3), can be produced by two methodologies and is easily characterized by solid-state ^{31}P CPMAS NMR spectroscopy (Fig. 1b,c). Method A involves tethering the preformed complex R-PPM-Rh-COD (10) to the SiO_2 (Scheme 2). In method B, the rhodium is introduced after the phosphine has been tethered to silica gel (Scheme 1). The differences in product 3 prepared by these two methods are negligible, as determined by their ^{31}P CPMAS spectra and catalytic activities (see section 3.2.2.2.). The ^{31}P NMR spectrum of 3, prepared by both methods, shows that the complex on the surface retains the same structure as in solution. This is evidenced by chemical shifts of 43 and 15 ppm for 3 as compared to 44.2 and 16.8 ppm for 10 in solution.

In method A, the rhodium:phosphine ligand ratio is fixed at 1:1 as required by the composition of the reacting R-PPM-Rh-COD (10) complex. This is reflected in the ^{31}P CPMAS spectrum, which shows signals for only SiO_2-R-PPM-Rh-COD (3), 43 and 15 ppm. In method B, various rhodium:phophine ratios can be used depending on the amount of $[Rh(COD)_2]^+BF_4^-$ (4) that is added to the phosphine tethered on the surface (2). When an excess of phosphine is present on the surface, not only is the rhodium complex, SiO_2-R-PPM-Rh-COD (3) detected by its ^{31}P NMR signals at 43 and 15 ppm, but excess ligand,

SiO_2-R-PPM (2), is also present as indicated by ^{31}P NMR signals at –7 and –23 ppm (Fig. 3). If a 1:1 ratio of rhodium to PPM is used, the ^{31}P NMR spectrum shows the presence of only the rhodium complex 3; the absence of signals at -7 and -23 ppm indicates that all of the diphosphine ligand is coordinated. When the rhodium:phosphine ligand ratio is 2:1, the ^{31}P NMR spectrum shows the main species on the surface to be SiO_2-R-PPM-Rh-COD (3), but an unidentified minor complex, ~15% of the sample, exhibits a band at 26 ppm (Fig. 3d).

It should be noted that for all rhodium-phosphine complexes on SiO_2 reported in this paper, the NMR signal from SiO_2-R-PPM-O_2 (11) at 35 ppm is either evident in the spectra of freshly prepared samples or grows in over time. The SiO_2-R-PPM-Rh-COD (3) is moderately to strongly air-sensitive both in the solid state and in solution. This air-sensitivity is evidenced by a decrease in intensity of ^{31}P signals of this complex, an increase in intensity of the phosphine oxide signal (35 ppm), and the appearance of a dark precipitate when 3 is exposed to air. For example, the downfield peak of the spectrum of Fig. 3b consists of two superimposed resonances representing one of the ^{31}P nuclei in 3 (at 45 ppm) and oxide 11 (at 35 ppm). Note that the ^{31}P nuclei in SiO_2-R-PPM-O_2 exhibit large chemical shift anisotropies, which is evidenced by the presence of spinning sidebands in the spectra taken with a lower sample spinning rate (see Fig. 2). The identity of the resonance at 35 ppm in Fig. 3b was verified by measuring the same spectrum at a lower sample spinning rate (not shown), which revealed the presence of similar spinning sidebands associated with this resonance. Solid-state ^{31}P NMR studies indicate that relatively small amounts of oxygen infiltrate the rotor, such that SiO_2-R-PPM-Rh-COD (3) oxidizes to SiO_2-R-PPM-O_2 (11) at a rate of approximately 1% per hour. The air sensitivity of SiO_2-R-PPM-Rh-COD (3) raises the possibility that 3 actually consists of rhodium coordinated to SiO_2-R-PPM-O_2 (11). This

however does not occur since the reaction of H_2O_2 with SiO_2-R-PPM-Rh-COD (**3**) in acetone

at room temperature for 5 min gives a ^{31}P CPMAS spectrum that is identical to that of SiO_2-

R-PPM-O_2 (**11**), which indicates that the rhodium is released from the phosphine ligand

during oxidation. Indeed, when $[Rh(COD)_2]^+BF_4^-$ (**4**) is added to SiO_2-R-PPM-O_2 (**11**), there

is no shift in the ^{31}P NMR signals for **11**, indicating that there are no interactions between

SiO_2-R-PPM-O_2 (**11**) and rhodium. More experimental evidence for this lack of interaction is

presented in section 3.2.2.5.

3.1.3. Characterization of R-PPM and (R-PPM)Rh(COD)$^+$ species tethered on

Pd-SiO$_2$ (7)

The Pd-SiO_2-R-PPM-Rh-COD (**6**) catalyst was prepared by the same two methods

used in the preparation of SiO_2-R-PPM-Rh-COD (**3**). Method A tethers the preformed R-

PPM-Rh-COD (**10**) complex to Pd-SiO_2 (**7**). Method B is a sequential route where the

phosphine, R-PPM (**1**), is tethered to Pd-SiO_2 (**7**) before rhodium is complexed. In method B,

the ^{31}P CPMAS spectrum of Pd-SiO_2-R-PPM (**12**) (Fig. 1d), prior to the addition of rhodium,

exhibits peaks at –7 and –21 ppm, which are very similar to those of SiO_2-R-PPM (**2**) (–7 and

–23 ppm) and R-PPM (**1**) (–8.2 and –22.3 ppm) [25]. Addition of one equivalent of

$[Rh(COD)_2]^+BF_4^-$ (**4**) to **12** produces Pd-SiO_2-R-PPM-Rh-COD (**6B**). The ^{31}P NMR

spectrum of this product is shown in Fig. 1f. The corresponding spectrum of Pd-SiO_2-R-

PPM-Rh-COD prepared using method A (**6A**) is shown in Fig. 1e. As expected, the spectra

of Figs. 1b, 1c and 1e are very similar and consistent with either the presence of **3** or **6**. The

spectrum of Fig. 1f shows the effect of oxidation, as the resonances of **11** centered at 35 ppm

overwhelm the weaker lines at 45 and 15 ppm. More detailed ^{31}P NMR studies revealed that

6 is as air sensitive as **3**, i.e. the oxidation rates in the NMR rotor are approximately 1% per

hour. Again, the oxidation of either **12** or **6** with H_2O_2 produces Pd-SiO_2-R-PPM-O_2 **(13)**, Eq. (3), which exhibits a broad signal at around 35 ppm. Furthermore, the addition of Rh complex **4** to **13** causes no change in the ^{31}P NMR spectrum, confirming that the phosphine oxide of PPM does not coordinate to rhodium.

3.2. Characterization of catalysts after use in the hydrogenation of MAC

3.2.1. Characterization of the catalytic species in solution

The generally accepted catalytic cycle for enantioselective hydrogenation of olefins by cationic rhodium complexes with chelating ligands [20,21,26-32] is shown in the lower part of Scheme 3. In the first step, Eq. (a), open coordination sites on the rhodium are generated by the hydrogenation of the COD ligand [24]. The resulting methanol-solvated species then coordinates the MAC substrate in a bidentate fashion, Eq. (b). Oxidative addition of hydrogen, Eq. (c), is followed by rapid sequential hydrogen transfer, Eq. (d) and (e). The hydrogenated product $MACH_2$ is a poor substrate for binding to the rhodium and is displaced by solvent to regenerate the starting complex in the catalytic cycle.

The ^{31}P NMR spectra of PPM, R-PPM **(1)**, and R-PPM-Rh-COD **(10)** were discussed in section 3.1.1. It is known that the Rh in X-PPM-Rh-COD complexes binds to coordinating solvents after COD is hydrogenated [20,22,26-29,33]. R-PPM-Rh-COD **(10)** also exhibits this behavior. In methanol at room temperature under 1 atm of hydrogen, COD in **10** is hydrogenated to produce the di-methanol complex R-PPM-Rh(MeOH)$_2$ **(16)**, whose ^{31}P NMR spectrum is consistent with other X-PPM-Rh(MeOH)$_2$ species. In particular, R-PPM-Rh(MeOH)$_2$ **(16)** exhibits a doublet of doublets at 69.7 and 46.0 ppm with J_{Rh-P} = 196 and 196 Hz and J_{P-P} = 64 Hz, while the known [20] [P-PPM-Rh(MeOH)$_2$]$^+$ClO$_4^-$ **(17)** exhibits a doublet of doublets at 69.6 and 42.5 ppm with J_{Rh-P} = 201 and 197 Hz and J_{P-P} = 65 Hz, and

[B-PPM-Rh(MeOH)$_2$]$^+$ClO$_4$$^-$ (18) exhibits a doublet of doublets at 68.0 and 42.2 ppm with J_{Rh-P} = 200 and 197 Hz and J_{P-P} = 66 Hz [20]. When 5 equivalents of MAC are added to a methanol solution of R-PPM-Rh(MeOH)$_2$ (16) the ^{31}P NMR spectrum exhibits a doublet of doublets at 50.7 and 22.2 ppm with J_{Rh-P} = 152 and 103 Hz and J_{P-P} = 19 Hz, which is assigned to R-PPM-Rh-MAC (19). The two phosphorus signals move closer to each other when the MeOH-d$_4$ solvent is partially replaced with CDCl$_3$. At 85% CDCl$_3$ and 15% MeOH-d$_4$, the ^{31}P NMR signals are at 40.5 and 32.4 ppm. Because of this dramatic solvent dependency, solid-state NMR spectroscopy of (19) was run and yielded two ^{31}P peaks at 46 and 33 ppm (spectrum not shown).

In order to gain more information about the species present in the catalytic cycle (Scheme 3), we reacted likely intermediates with CO to give more air-stable complexes. Such reactions of rhodium complexes of PPM (or its derivatives) with CO have not been previously reported; however, CO reactions with other cationic rhodium-phosphine complexes are well known [33-35]. When CO is bubbled through a MeOH solution of R-PPM-Rh-COD (10) at room temperature for 10 min (Scheme 3, eq. (f)), R-PPM-Rh-MeOH-CO (20) is produced. During the reaction, the color of the solution bleaches from bright yellow to pale yellow-green. The ^{31}P NMR spectrum of this solution exhibits a doublet of doublets at 35.7 and 24.4 ppm, J_{Rh-P} = 315 and 314 Hz and J_{P-P} = 127 Hz. In the IR spectrum, a v(CO) band appears at 1984 cm^{-1}. This v(CO) band corresponds well with other cationic rhodium(I) carbonyl species such as L$_2$Rh(Solvent)(CO)$^+$, where L = PPh$_3$, PPh$_2$Me and Solvent = DMA, DMF; all of these complexes show v(CO) bands [33] in the same range (1971-2000 cm^{-1}) as that assigned to R-PPM-Rh-MeOH-CO (20). Complex 20 is also formed

when CO is bubbled through a MeOH solution of R-PPM-Rh(MeOH)$_2$ **(16)** (Scheme 3, eq. (g)), as established by its ^{31}P NMR and v(CO) IR spectra.

The reaction of R-PPM-Rh-MeOH-CO **(20)** in MeOH with 5 eq. of MAC gives R-PPM-Rh-MAC-CO **(21)** (Scheme 3, eq. (h)). It is also produced (Scheme 3, eq. (i)) when CO is bubbled for 10 min through a methanol solution of R-PPM-Rh-MAC **(19)** at room temperature. Both methods yield a product identical by IR (v(CO) 1970(s) cm^{-1}) and ^{31}P NMR (doublets of doublets at 54.3 and 47.4 ppm, J_{Rh-P} = 137 and 137 Hz and J_{P-P} = 125 Hz).

The B-PPM-Rh-COD complex **15** is reported to catalyze the hydrogenation of MAC (Eq. (1)) with a TOF of 14.3 min^{-1} and an enantioselectivity of 94.5% ee [5]. Our measured rates and enantioselectivities of R-PPM-Rh-COD **(10)** in solution are slightly lower, TOF 5.01 min^{-1} and 93.5% ee. The enantioselective hydrogenation of MAC using R-PPM-Rh-COD **(10)** and the identification of possible intermediates **16** and **19** described above suggests that **10** catalyzes the hydrogenation of MAC by the mechanism (Scheme 3) indicated for related reactions [20,21,26-32]. Neither of the CO adducts, R-PPM-Rh-MAC-CO **(21)** nor R-PPM-Rh-MeOH-CO **(20)**, exhibit any activity for the hydrogenation of MAC.

3.2.2. Characterization of the catalytic species tethered on SiO$_2$

3.2.2.1. CO derivatives

Unfortunately, the catalytic species present during and after hydrogenation are too air sensitive to be observed by the solid-state ^{31}P NMR techniques used in this study. Although samples from the reactions are handled under argon and loaded into the NMR rotor in a glove bag under nitrogen, the rotor itself is not completely air tight under NMR acquisition conditions. All samples obtained from the hydrogenation reactions gave poor spectra.

Reduced intensities of all signals and an increase in intensity of a peak at 35 ppm

corresponding to SiO_2-R-PPM-O_2 (11) are observed.

Attempts to produce a characterizeable SiO_2-R-PPM-Rh(MeOH)$_2$ (22) species by

hydrogenating off COD in the absence of MAC resulted in poor ^{31}P NMR spectra whose

only discernable signal represented the phosphine oxide 11. If the di-MeOH species (22) is

not separated from the reaction mixture, but instead 5 equivalents of MAC are added under

an atmosphere of argon, SiO_2-R-PPM-Rh-MAC (23) was detected by its solid-state [31]P

signals at 40 and 28 ppm which compare closely to the converging signals of R-PPM-Rh-

MAC (19) in 85% CDCl$_3$/15% MeOH-d$_4$ solution (40.5 and 32.4 ppm) as well as the signals

of solid 19 (46 and 33 ppm), see section 3.2.1.

Reactions of the various rhodium phosphine complexes tethered to SiO_2 with CO give

species that are sufficiently air stable to give observable solid-state ^{31}P NMR and DRIFT

spectra (not shown). As observed for R-PPM-Rh-COD (10), SiO_2-R-PPM-Rh-COD (3) in

MeOH reacts with bubbling CO for 15 min. After solvent removal under vacuum, the

resulting solid gave DRIFT (v(CO) 1990(s) cm^{-1}) and ^{31}P CPMAS NMR spectra (35 and 25

ppm) that are very similar to those of the solution species R-PPM-Rh-MeOH-CO (20) (IR:

v(CO) 1984(s) cm^{-1}; ^{31}P NMR in solution of MeOH-d$_4$: 35.7 and 24.4 ppm). This suggests

that the species on the surface is SiO_2-R-PPM-Rh-MeOH-CO (24).

SiO_2-R-PPM-Rh-MAC-CO (25) is obtained by two independent methods. It is the

product when 5 equivalents of MAC are added to SiO_2-R-PPM-Rh-MeOH-CO (24) in a

methanol solution at room temperature (Scheme 3, eq. (h)). Or, it is formed in the reaction of

SiO_2-R-PPM-Rh-MAC (23) with CO in methanol at room temperature for 15 min (Scheme 3,

eq. (i)). Both methods yield the same product as established by DRIFT spectroscopy.

Assignment of the structure to product **25** is based on the similarity of the DRIFT (v(CO)

1974(s) cm^{-1}) spectrum of **25** to that (IR v(CO) 1970(s) cm^{-1}) of the R-PPM-Rh-MAC-CO

(**21**) complex in solution.

Reaction of CO with SiO$_2$-R-PPM-Rh-COD (**3**) during or after MAC hydrogenation

in methanol results in DRIFT bands readily ascribable to either SiO$_2$-R-PPM-Rh-MeOH-CO

(**24**) or SiO$_2$-R-PPM-Rh-MAC-CO (**25**) depending on when the CO is introduced. If the

hydrogenation of MAC is stopped before MAC is completely hydrogenated and the hydrogen

atmosphere is replaced with CO, the resulting rhodium-CO species exhibits a v(CO) band at

1974 cm^{-1} consistent with SiO$_2$-R-PPM-Rh-MAC-CO (**25**). The absence of additional v(CO)

bands indicates that Rh(0) and Rh(I) on SiO$_2$ are not present since their CO adducts would

give bands at 2095 and 2027 cm^{-1} or 2040-2066 cm^{-1} [36-39]. Replacing the hydrogen

atmosphere with CO after the complete hydrogenation of MAC gives SiO$_2$-R-PPM-Rh-

MeOH-CO (**24**) as indicated by the v(CO) band at 1990(s) cm^{-1}. The ^{31}P CPMAS NMR

spectrum with absorptions at 35 and 25 ppm supports this assignment. This is a reasonable

product as MACH$_2$ is a very weak ligand and only methanol remains for coordination. The

lack of additional DRIFT v(CO) bands conclusively shows that the PPM-Rh unit remains

intact.

Thus, reactions of CO with the tethered catalyst at various stages of the

hydrogenation indicate that the reaction mechanism on the surface mimics that proposed for

the analogous reaction in solution (Scheme 3, eq. (a-e)). These studies also show that the

rhodium remains coordinated to the phosphorus throughout the reaction since no DRIFT

v(CO) bands other than those assignable to SiO$_2$-R-PPM-Rh-MeOH-CO (**24**) or SiO$_2$-R-

PPM-Rh-MAC-CO (25) are observed. Rate data, enantioselectivities, and mercury poisoning experiments, presented below, further support these conclusions.

3.2.2.2. Activity and enantioselectivity studies of the hydrogenation of MAC

Pugin [5] reports that SiO_2-R-PPM-Rh-COD (3) prepared by method B (Scheme 1) gives rates (TOF) varying from 6.25-12.5 min^{-1} with ee values ranging from 89.8 to 94.5% depending on the catalyst batch. Our catalysts prepared by method B give an average TOF value of 11.2 min^{-1} and an average ee of 91.1% (entry 5, Table 2). This indicates that our catalysts are the same as Pugin's. In addition, we observe that the catalyst formed by method A (entry 4) gives a similar average rate (TOF = 13.8 min^{-1}) and enantioselectivity (ee = 93.7%). The comparable rates and enantioselectivities reinforce the previous spectroscopic evidence that the catalysts prepared by either method A or B are the same.

3.2.2.3. Mercury poisoning experiments

In order to exclude the possibility that the hydrogenation of MAC over SiO_2-R-PPM-Rh-COD (3) occurs on metallic rhodium particles deposited from the tethered rhodium complex, studies of the effect of mercury metal were undertaken. It is known that mercury poisons nano-metal catalysts [40] and supported metal catalysts [41] that catalyze olefin and arene hydrogenation reactions. However, mercury does not affect the activities of homogeneous metal catalysts [40]. Thus, the addition of mercury is a standard method for determining whether a reaction is catalyzed by a metal or a metal complex. We observe that mercury has no effect on the rate or enantioselectivity (entry 6, Table 2) of the hydrogenation of MAC catalyzed by SiO_2-R-PPM-Rh-COD (3). Thus, the catalytically active species in SiO_2-R-PPM-Rh-COD (3) is the 'homogeneous' R-PPM-Rh-COD (10) metal complex bound to the silica surface and not rhodium metal.

3.2.2.4. Catalytic activity of [Rh(COD)₂]⁺BF₄⁻/SiO₂(26)

In order to explore the possibility that rhodium metal without phosphine ligands is

able to catalyze the hydrogenation of MAC, $[Rh(COD)_2]^+BF_4^-$ (4) was adsorbed on SiO_2, by

stirring $[Rh(COD)_2]^+BF_4^-$ (4) with SiO_2 for 5 min in the absence of any phosphine. The

resulting solid exhibits (entry 7, Table 2) very low activity (TOF = 0.0600 min⁻¹) for the

hydrogenation of MAC under the usual reaction conditions (25°C, 1atm H_2, MeOH solvent).

The rate of MAC hydrogenation with $[Rh(COD)_2]^+BF_4^-/SiO_2$ (26) is at least two orders of

magnitude slower than the same hydrogenation with SiO_2-R-PPM-Rh-COD (3), and as

expected, $[Rh(COD)_2]^+BF_4^-/SiO_2$ (26) produces racemic $MACH_2$ (8). Moreover, mercury

quenches the hydrogenation reaction completely. This latter experiment also indicates that

the active hydrogenation species must be metallic rhodium resulting from the reduction of

$[Rh(COD)_2]^+BF_4^-$ (4). This is consistent with our observations in studies of $[Rh(COD)_2]^+BF_4^-$

(4) [18] in other hydrogenation reactions.

3.2.2.5. Effect of air on the catalytic activity of SiO₂-R-PPM-Rh-COD (3)

When SiO_2-R-PPM-Rh-COD (3) prepared by method A is partially oxidized by

exposure to air for 5 days, its activity (entry 9, Table 2) for the hydrogenation of MAC is

very low. Interestingly, the remaining activity, TOF = 1.02 min⁻¹, is enantioselective (ee =

90.5%). Presumably a small amount (~2%) of the complex remains unoxidized and is

responsible for the activity. However, when SiO_2-R-PPM-Rh-COD (3) prepared by method

A is oxidized by reaction with a few drops of H_2O_2 in acetone at room temperature for 15

min, the catalyst is completely inactive (entry 10). The addition of $[Rh(COD)_2]^+BF_4^-$ (4) in

methanol to SiO_2-R-PPM-O_2 (11) produces a catalyst (entry 11) with very low activity (TOF

= 0.0135), which exhibits no enantioselectivity. This result supports the ³¹P NMR studies

(see section 3.1.2), which showed that rhodium does not bind to SiO_2-R-PPM-O_2 (11). The poor activity and lack of enantioselectivity of this catalyst (entry 11) is the same as that for $[Rh(COD)_2]^+BF_4^-/SiO_2$ (26) (entry 7).

3.2.2.6. Effect of Rh/PPM ratio on SiO₂-R-PPM-Rh-COD (3) activity

When the catalyst SiO_2-R-PPM-Rh-COD (3) is formed by reaction of the rhodium complex R-PPM-Rh-COD (10) with SiO_2 (method A), the rhodium:phosphorus ratio is fixed at 1:1; the TOF and ee values for this catalyst (entry 4, Table 2) are 13.8 min^{-1} and 93.7% respectively. When 3 is prepared by sequential addition of $[Rh(COD)_2]^+BF_4^-$ (4) to SiO_2-R-PPM (2) (method B), a 0.5:1 ratio of rhodium to PPM yields a catalyst with an activity that reflects the amount of rhodium that is in the form of 3; its TOF and ee values are 8.83 min^{-1} and 90.5%, respectively (Table 3). With a 1:1 ratio of rhodium to PPM the activities are TOF (11.2 min^{-1}) and ee (91.5%). When a 2:1 ratio of rhodium to PPM is incorporated into 3, the enantioselectivity is 90.1%, and if the TOF is calculated based on the total amount of rhodium in the system, the TOF is 6.00 min^{-1}. This value is low in comparison to all of the other TOF values for SiO_2-R-PPM-Rh-COD (3). If the phosphine content, instead of the rhodium content, is used to calculate the amount of 3 present, then a TOF value of 12.0 min^{-1} is obtained, which is consistent with the other TOF values. It is logical to calculate TOF this way since the phosphine is the limiting reagent in the formation of the rhodium-PPM complex and represents the maximum amount of the complex possible. For the catalyst with a 2:1 rhodium to PPM ratio, one equivalent of rhodium is not complexed and presumably deposits on the SiO_2 surface where it is a poor MAC hydrogenation catalyst (see section 3.2.2.4.). For the catalyst with a 4:1 rhodium:PPM ratio, the enantioselectivity (ee = 92.7%) continues to be high and the rate (TOF = 8.84 min^{-1}) based on PPM content is reasonable; on

the other hand, the rate (TOF = 2.21 min^{-1}) based on rhodium content is unreasonably low.

Finally, for **3** prepared by method A or method B with ratios of (Rh:PPM = 0.5:1, 1:1, 2:1, or

4:1), mercury has no effect on the rate or enantioselectivity of the reaction (Table 3). Thus, **3**

containing the [(R-PPM)Rh(COD)]$^+$BF$_4^-$ complex is the only species that catalyzes the

enantioselective hydrogenation of MAC in this system.

3.2.3. Characterization of the catalytic species tethered on Pd-SiO₂ (7)

3.2.3.1. CO derivatives

The species Pd-SiO$_2$-R-PPM-Rh-MeOH-CO (**27**), obtained by stirring a methanol

slurry of Pd-SiO$_2$-R-PPM-Rh-COD (**6**) under a CO atmosphere for 15 min at room

temperature, gives DRIFT (ν(CO) 1990(s) cm^{-1}) and solid-state ^{31}P NMR (35 and 25 ppm)

spectra that are very similar to those of SiO$_2$-R-PPM-Rh-MeOH-CO (**24**) (DRIFT (ν(CO)

1990(s) cm^{-1}) and ^{31}P NMR (35 and 25 ppm)) and R-PPM-Rh-MeOH-CO (**20**) (IR (ν(CO)

1984(s) cm^{-1}) and ^{31}P NMR (35.7 and 24.4 ppm) in solution). Under the same conditions, Pd-

SiO$_2$-R-PPM-Rh-MAC-CO (**28**) is produced from Pd-SiO$_2$-R-PPM-Rh-MAC (**29**) and CO

(Scheme 3, eq. i). The infrared spectrum (DRIFT ν(CO) 1974(s) cm^{-1}) of Pd-SiO$_2$-R-PPM-

Rh-MAC-CO (**28**) is very similar to that (ν(CO) 1974(s) cm^{-1}) of SiO$_2$-R-PPM-Rh-MAC-CO

(**25**) and that (ν(CO) 1970(s) cm^{-1}) of R-PPM-Rh-MAC-CO (**21**). Exposure of Pd-SiO$_2$-R-

PPM-Rh-COD (**6**) to CO prior to MAC addition or after complete hydrogenation of MAC

yields Pd-SiO$_2$-R-PPM-Rh-MeOH-CO (**27**). Exposure to CO during the reaction results in

the formation of Pd-SiO$_2$-R-PPM-Rh-MAC-CO (**29**). This is the same behavior that is

observed with SiO$_2$-R-PPM-Rh-COD (**3**).

3.2.3.2. Catalytic activities

The hydrogenation reactions of MAC catalyzed by Pd-SiO$_2$-R-PPM-Rh-COD (**6A** and **6B**) in which the Rh to PPM ratio is 1:1, prepared by either method A or B are highly enantioselective, ee 90.6% and 88.3%, respectively (entries 13 and 14, Table 2). The sequentially prepared catalyst Pd-SiO$_2$-R-PPM-Rh-COD (**6B**), exhibits rates (TOF) of 11.8 min^{-1}. This is comparable to that of SiO$_2$-R-PPM-Rh-COD (**3B**), where the TOF is 11.2 min^{-1}. Catalyst **6A** (entry 13) shows lower rates of MAC hydrogenation (TOF = 5.69 min^{-1}) compared to that (entry 4) of SiO$_2$-R-PPM-Rh-COD (**3A**) (TOF = 13.8 min^{-1}); the reason for this lower activity is unknown. If the sequentially prepared catalyst (**6B**) contains excess rhodium, i.e. the Rh:PPM ratio is greater than 1:1, then reduced enantioselectivities are observed, see section 4.3. For example, a catalyst prepared with a Rh:PPM ratio of 5:1 provides an ee of 22.0% after the first 5 min of reaction.

Pd-SiO$_2$ (**7**) by itself is a catalyst for the hydrogenation of MAC (TOF$_{eff}$ = 7.06 [42]), but the hydrogenation gives a racemic product (entry 18, Table 2). In order to determine whether rhodium adsorbed on Pd-SiO$_2$ (**7**) without the tethering PPM ligand would be catalytically active, [Rh(COD)$_2$]$^+$BF$_4^-$ (**4**) was adsorbed on Pd-SiO$_2$ (**7**) by stirring a methanol solution of [Rh(COD)$_2$]$^+$BF$_4^-$ (**4**) with Pd-SiO$_2$ (**7**). This system (entry 19) is highly active for the hydrogenation of MAC (TOF = 12.5 min^{-1}) but the product is completely racemic. When Pd-SiO$_2$-R-PPM-O$_2$ (**13**) is reacted with [Rh(COD)$_2$]$^+$BF$_4^-$ (**4**), it gives an active catalyst (TOF = 11.7 min^{-1}) but the product is racemic (entry 21). This rate is very similar to [Rh(COD)$_2$]$^+$BF$_4^-$ (**4**) on Pd-SiO$_2$ (**7**) (entry 19) and reaffirms the spectroscopic results (sections 3.1.2. and 3.1.3.) that PPM-O$_2$ does not coordinate to Rh. Also, while mercury does not decrease the rate or enantioselectivity of Pd-SiO$_2$-R-PPM-Rh-COD (**6**), it quenches the

activity of $[Rh(COD)_2]^+BF_4^-$ (**4**) on $Pd-SiO_2$ (**7**) (entry 22). Thus, the racemic hydrogenation

activity of $[Rh(COD)_2]^+BF_4^-$ (**4**) on $Pd-SiO_2$ (**7**) must be attributed to metallic Rh on the

silica surface. Since Rh on SiO_2 without Pd is not active (entry 7), the activation of the Rh

must be due to the Pd in the system. One possibility is that hydrogen spillover from Pd

reduces the $[Rh(COD)_2]^+BF_4^-$ to Rh metal. This has been shown to occur for related systems

during other hydrogenation reactions [18].

The effect of Pd loading on the surface was explored briefly. A palladium loading

lower than 10% was examined with some 1% w/w Pd catalysts. The 1%-Pd-SiO_2-R-PPM-

Rh-COD (**6B-1%**) catalyst formed using method B exhibited a rate (TOF = 10.2 min^{-1}) and

enantioselectivity (ee = 86.8%) very similar to those of the analogous 10%-Pd catalyst Pd-

SiO_2-R-PPM-Rh-COD (**6B**). The lower palladium content neither significantly raised nor

lowered the MAC hydrogenation activity compared to the catalyst on 10%-Pd-SiO_2 or SiO_2.

Thus from entry 23, Table 2, it can be seen that the Pd loading or even the absence of Pd had

no effect on either the rates or enantioselectivities of MAC hydrogenation.

3.3. Arene hydrogenations studies

3.3.1. SiO_2-R-PPM-Rh-COD (3)

SiO_2-R-PPM-Rh-COD (**3**) exhibits very low, but detectable, hydrogenation activity

(TOF = 0.0135 min^{-1}) for the conversion of toluene to methylcyclohexane (entry 3, Table 4).

However, when the same catalyst is used for toluene hydrogenation in the presence of

mercury, no activity is observed (entry 4). This result indicates that the active *arene*

hydrogenation species is a heterogenized metallic rhodium species resulting from partial

decomposition of SiO_2-R-PPM-Rh-COD (**3**). Support for this interpretation is the higher

activity (TOF = 0.0604 min^{-1}) of the catalyst (entry 1) prepared by adsorbing

$[Rh(COD)_2]^+BF_4^-$ onto SiO_2, **26**. The toluene hydrogenation activity of this catalyst is quenched by the addition of mercury (entry 2); this also indicates that a rhodium metal species is the active arene hydrogenation catalyst.

3.3.2. Pd-SiO₂-R-PPM-Rh-COD (6)

The catalyst $Pd-SiO_2-R-PPM-Rh-COD$ (**6**) is much more active (TOF = 0.124 min^{-1}) for the hydrogenation of toluene (entry 6, Table 4) than $SiO_2-R-PPM-Rh-COD$ (**3**) (TOF = 0.0135 min^{-1}) which does not contain palladium. However, the activity of $Pd-SiO_2-R-PPM-Rh-COD$ (**6**) (TOF = 0.124 min^{-1}) is not much higher than that (entry 5) of simply $Pd-SiO_2$ (**7**) (TOF$_{eff}$ = 0.0785 min^{-1} [42]). Also, mercury quenches the toluene hydrogenation activity of both the palladium and rhodium present in **6** (entry 7).

Oxidation of **6** by reaction with H_2O_2 in acetone at room temperature liberates rhodium from the PPM complex to produce a catalyst that is much more active (TOF = 0.834 min^{-1}) than **6** (entry 8, Table 4). This rate is not much slower than that of the catalyst prepared by adsorbing $[Rh(COD)_2]^+BF_4^-$ (**4**) on $Pd-SiO_2$ (**7**) (TOF = 1.65 min^{-1}; entry 9). The high activity of rhodium species on $Pd-SiO_2$ (**7**) is consistent with the previously observed ability of Pd to activate adsorbed rhodium species for arene hydrogenations [18]. Both the oxidized $Pd-SiO_2-R-PPM-O_2$ (**13**) and $[Rh(COD)_2]^+BF_4^-$ (**4**) on $Pd-SiO_2$ (**7**) catalysts are deactivated when mercury is added to the toluene hydrogenation mixtures. All of these results indicate that a PPM-Rh complex is not active for toluene hydrogenation, but rather metallic rhodium supported on the $Pd-SiO_2$ (**7**) is the catalyst.

4. Conclusions

4.1. Enantioselective hydrogenation of MAC by SiO₂-R-PPM-Rh-COD (3)

One of the goals of these studies was to characterize the form of the tethered R-PPM-Rh-COD (**10**) complex on the silica surface in SiO₂-R-PPM-Rh-COD (**3**), before and during the enantioselective hydrogenation of MAC. On silica, the tethered phosphine, SiO₂-R-PPM (**2**), is shown to retain the same structure and phosphine environment as in solution, R-PPM (**1**). For the tethered metal complex, both Method A (Scheme 2) and Method B (Scheme 1) lead to the same SiO₂-R-PPM-Rh-COD (**3**) surface species as determined by ^{31}P CPMAS NMR spectroscopy, which also establishes that the Rh complex in SiO₂-R-PPM-Rh-COD (**3**) is structurally the same as R-PPM-Rh-COD (**10**) in solution. Consistent with the ^{31}P NMR results, the activities and enantioselectivities for the hydrogenation of MAC are the same whether the SiO₂-R-PPM-Rh-COD (**3**) catalyst is prepared by either method A or B. The activity of this catalyst is also comparable to that of the homogeneous Rh complex, [B-PPM-Rh-COD]⁺, in solution and to that reported earlier by Pugin and Müller [5].

Catalyst **3**, prior to use in MAC hydrogenations, is sensitive to air, undergoing complete oxidation to SiO₂-R-PPM-O₂ (**11**) and depositing rhodium on the SiO₂ within 5 days of air exposure or 15 min by reaction with H₂O₂, Eq. (3). Oxidation also occurs at a rate of ~1% per hour in the NMR rotor used in this study. After use in a MAC hydrogenation, SiO₂-R-PPM-Rh-COD (**3**) is extremely air-sensitive and loss of activity is observed within seconds upon exposure to air.

Exposure of solutions containing MAC and the SiO₂-R-PPM-Rh-COD (**3**) catalyst to CO before, during, and after hydrogenation produces rhodium CO complexes that exhibit strong ν(CO) IR bands diagnostic of complexes that are formed from intermediates in the

catalytic reaction. The identified rhodium-CO complexes are SiO$_2$-R-PPM-Rh-MeOH-CO

(24) and SiO$_2$-R-PPM-Rh-MAC-CO (25). The lack of additional v(CO) bands shows that the

PPM-rhodium complex remains intact throughout the catalytic cycle. Together with solid-

state ^{31}P NMR studies, the IR (and DRIFT) results support a previously proposed mechanism

[20,26-32] (Scheme 3) for the hydrogenation of MAC in the presence of 3 and provide

evidence that the PPM-rhodium unit remains intact throughout the reaction.

Reaction rates, oxidation experiments, and mercury poisoning experiments reinforce

the conclusion that the intact PPM-Rh unit is required for enantioselective hydrogenation of

MAC. On silica, excess [Rh(COD)$_2$]$^+$BF$_4^-$ (4) has no noticeable effect on the rate or

enantioselectivity, because [Rh(COD)$_2$]$^+$BF$_4^-$ (4) by itself is a poor hydrogenation catalyst

[43]. Partial oxidation of SiO$_2$-R-PPM-Rh-COD (3) to SiO$_2$-R-PPM-O$_2$ (11) reduces its

enantioselective activity, while complete oxidation extinguishes it. However, when the PPM-

Rh unit remains intact, mercury does not reduce the rate or enantioselectivity of MAC

hydrogenation. All of these results suggest that during the hydrogenation of MAC, the

phosphine (PPM) remains coordinated to the rhodium throughout the catalytic cycle. Thus,

based on ^{31}P NMR and DRIFT spectroscopic studies, as well as investigations of the catalytic

activity and enantioselectivities of SiO$_2$-R-PPM-Rh-COD (3), it has been established that the

active species in catalyst 3 is the tethered R-PPM-Rh$^+$ unit.

4.2. Enantioselective hydrogenation of MAC by Pd-SiO$_2$-R-PPM-Rh-COD (6)

When metallic Pd is added to the SiO$_2$ surface of SiO$_2$-R-PPM-Rh-COD (3), the

active species of the resulting catalyst Pd-SiO$_2$-R-PPM-Rh-COD (6) is also the SiO$_2$-R-PPM-

Rh-COD complex. In general, the tethered systems on Pd-SiO$_2$ (7) are similar to those on

SiO$_2$. The tethered phosphine Pd-SiO$_2$-R-PPM (12) appears the same by ^{31}P NMR as on

silica, SiO_2-R-PPM (**2**), and in solution, R-PPM (**1**). However, two additional resonances

were observed in **12** that most likely represent a complex of R-PPM with Pd [25]. Also, Pd-

SiO_2-R-PPM-Rh-COD (**6**) catalysts, prepared by either method A or B, are similar to each

other and to **3**. The spectroscopic data are consistent with the observations that the activities

and enantioselectivities of the catalysts (**6** and **3**) with Pd-SiO_2 and SiO_2 supports are very

similar. All of the catalysts (**3A**, **3B**, **6A**, and **6B**) catalyze the enantioselective hydrogenation

of MAC. Solid-state ^{31}P NMR studies show that the R-PPM-Rh-COD complex is the species

present in Pd-SiO_2-R-PPM-Rh-COD (**6**) prior to the hydrogenation of MAC. Exposure to

CO, reaction rates, oxidation experiments, and mercury poisoning experiments indicate that

the intact chelated phosphine-rhodium unit is required for enantioselective hydrogenation of

MAC and this PPM-Rh unit remains intact throughout the reaction.

In all regards discussed so far, the R-PPM-Rh-COD species are the same in **3** and in

6. The same species are observed before, during, and after reaction; and the Pd-SiO_2 catalyst,

6, is as air sensitive as **3** on SiO_2. The only difference between the SiO_2- and Pd-SiO_2-

supported catalysts is the ability of Pd-SiO_2 (**7**) to activate any uncomplexed rhodium, such

as $[Rh(COD)_2]^+BF_4^-$ (**4**), on the silica surface to a highly active racemic hydrogenation

species, presumably rhodium metal. Thus, $[Rh(COD)_2]^+BF_4^-$ (**4**) on Pd-SiO_2 (**7**) is reduced to

an active form of rhodium that catalyzes the hydrogenation of MAC to the racemic $MACH_2$

product; as noted above, $[Rh(COD)_2]^+BF_4^-$ (**4**) on SiO_2 is not very active (TOF = 0.0600

min^{-1}) for MAC hydrogenation. Therefore, excess $[Rh(COD)_2]^+BF_4^-$ (**4**) on Pd-SiO_2-R-PPM-

Rh-COD (**6**) results in reduced enantioselectivities due to concurrent enantioselective and

racemic hydrogenation by the two different species. Also, oxidation of Pd-SiO_2-R-PPM-Rh-

COD (**6**) releases rhodium species that are reduced by the Pd under hydrogenation conditions

to rhodium metal which causes the hydrogenation of MAC to give lower ee values in the MACH$_2$ product. For all of the catalysts containing Pd-SiO$_2$, mercury quenches the part of the reaction catalyzed by metallic rhodium that gives racemic MACH$_2$ yet allows the enantioselective hydrogenation catalyzed by the R-PPM-Rh-COD complex.

4.3. Arene hydrogenation by SiO$_2$-R-PPM-Rh-COD (3) and Pd-SiO$_2$-R-PPM-Rh-COD (6)

Although several Rh complexes tethered on Pd-SiO$_2$ are active TCSM catalysts for the hydrogenation of arenes [7-11], catalysts described in this paper, based on R-PPM-Rh-COD (10), are not. While SiO$_2$-R-PPM-Rh-COD (3) shows trace activity for toluene hydrogenation, the mercury test shows conclusively that the activity cannot be ascribed to the PPM-Rh complex; rather metallic rhodium on the silica is the active species. Somewhat surprisingly, the TCSM catalyst, Pd-SiO$_2$-R-PPM-Rh-COD (6), does not show an increase in toluene hydrogenation activity over that of Pd-SiO$_2$ (7), which suggests that the Pd-SiO$_2$ part of 6 is the active component. When 6 is oxidized to Pd-SiO$_2$-R-PPM-O$_2$ (13) releasing Rh from the complex, toluene hydrogenation activity increases substantially. After extensive oxidation, the rate is the same as that of [Rh(COD)$_2$]$^+$BF$_4^-$ (4) on Pd-SiO$_2$ (7). This increased toluene hydrogenation activity corresponds with reduced enantioselectivities for MAC hydrogenation. Most importantly, mercury stops both the toluene and the racemic MAC hydrogenation activity. This indicates that these activities are due to rhodium metal and not the PPM-Rh complex. Again, the difference in arene hydrogenation activity between [Rh(COD)$_2$]$^+$BF$_4^-$ (4) on Pd-SiO$_2$ (7), which is highly active (TOF = 1.65 min^{-1}), and [Rh(COD)$_2$]$^+$BF$_4^-$ (4) on SiO$_2$, which is much less active (TOF = 0.0604 min^{-1}), is due to Pd facilitating the reduction of [Rh(COD)$_2$]$^+$BF$_4^-$ (4) to a form of rhodium metal that is the

active toluene hydrogenation species. For all of the catalysts examined with the PPM ligand, the intact tethered catalyst is inactive for arene hydrogenation.

References

[1] J.D. Morrison (Ed.), Asymmetric Synthesis, Vol. 5, Chiral Catalysis, Academic Press, Orlando, 1985.

[2] D.E. Vos, I.F.J. Vankelecom, P.A. Jacobs (Eds.), Chiral Catalyst Immobilization and Recycling, Wiley-VCH, New York, 2000.

[3] E.N. Jacobsen, A. Pfaltz, H. Yamamoto (Eds.), Comprehensive Asymmetric Catalysis, Vols. 1 and 3, Springer, New York, 1999.

[4] M.J. Burk, F. Bienewald, Transition Met. Org. Synth. 2 (1998) 13.

[5] B. Pugin, M. Müller, in M. Guisnet et. al. (Ed.), Stud. Surf. Sci. Cat. Part 78: Heterogeneous Catalysis and Fine Chemicals III, Elsevier (1993) 107.

[6] B. Pugin, J. Mol. Catal. A: Chem. 107 (1996) 273.

[7] H. Gao, R.J. Angelici, J. Mol. Catal. A: Chem. 149 (1999) 63.

[8] H. Gao, R.J. Angelici, J. Am. Chem. Soc. 119 (1997) 6937.

[9] H. Gao, R.J. Angelici, Organometallics 18 (1999) 989.

[10] H. Gao, R.J. Angelici, New J. Chem. 23 (1999) 633.

[11] H. Yang, H. Gao, R.J. Angelici, Organometallics 19 (2000) 622.

[12] A.B. Pangborn, M.A. Giardello, R.H. Grubbs, R.K. Rosen, F. J. Timmers, Oganometallics 15 (1996) 1518.

[13] D.D. Perrin, W.L.F. Armarego, D.R. Perrin, Purification of Laboratory Chemicals, 2nd ed., Pergamon, New York, 1980.

[14] J. Suh, E. Lee, Y.C. Myoung, M. Kim, S. Kim, J. Org. Chem. 50 (1985) 977.

[15] R.M. Herbst, D. Shemin, in A.H. Blatt (Ed.), Organic Syntheses, Collect. Vol. 2, Wiley, New York, (1943) 1.

[16] R.R. Schrock, J.A. Osborn, J. Am. Chem. Soc. 93 (1971) 3089.

[17] T. Ioannides, X. Veeykios, J. Catal. 140 (1993) 353.

[18] K.J. Stanger, Y. Tang, J. Anderegg, R.J. Angelici, manuscript in preparation.

[19] S. Hediger, B. H. Meier, and R. R. Ernst, J. Chem. Phys. 102 (1995) 4000.

[20] I. Ojima, T. Kogure, N. Yoda, J. Org. Chem. 45 (1980) 4728.

[21] K. Achiwa, P.A. Chaloner, D. Parker, J. Organomet. Chem. 218 (1981) 249.

[22] M.A. Garralda, L.A. Oro, Transition Met. Chem. 5 (1980) 63.

[23] M. Green, T.A. Kuc, S.H. Taylor, J. Chem. Soc. A (1971) 2334.

[24] During most of the reaction, small amounts of COD, $CODH_2$ (cyclooctene), and $CODH_4$ (cyclooctane) were also observed by GC originating from the Rh complex; the major product was $CODH_2$ After the MAC substrate was consumed, $CODH_4$ became the exclusive product.

[25] Note the presence of two resonances at around 40 and 20 ppm in the spectrum of Fig. 1d. The fact that these resonances were not observed in the corresponding spectrum of sample 2, indicates a complex of R-PPM with Pd. However, on addition of $[Rh(COD)_2]^+BF_4^-$ these signals disappear, Fig. 1f, indicating that any (PPM-Pd) complex is only weakly bound.

[26] J. Halpern. D.P. Riley, A.S.C. Chan, J.J. Pluth, J. Am. Chem. Soc. 99 (1977) 8055.

[27] A.S.C. Chan, J. Halpern, J. Am. Chem. Soc. 102 (1980) 838.

[28] A.S.C. Chan, J.J. Pluth, J. Halpern, J. Am. Chem. Soc. 102 (1980) 5952.

[29] a) C.R. Landis, J. Halpern, J. Organomet. Chem. 250 (1983) 485.

b) C.R. Landis, J. Halpern, J. Am. Chem. Soc. 109 (1987) 1746.

[30] a) I.D. Grdnev, N. Higashi, K. Asakura, T. Imamoto, J. Am. Chem. Soc. 122 (2000) 7194.

b) I.D. Grdnev, N. Higashi, T. Imamoto, J. Am. Chem. Soc. 123 (2001) 4631.

[31] a) C.R. Landis, P. Hilfenhaus, S. Feldgus, J. Am. Chem. Soc. 121 (1999) 8741.

b) S. Feldgus, C.R. Landis, J. Am. Chem. Soc. 122 (2000) 12714.

c) S. Feldgus, C.R. Landis, Organometallics 20 (2001) 2374.

[32] J.P. Collman, L.S. Hegedus, J.R. Norton, R.G. Finke, Principles and Applications of Organotransition Metal Chemistry, University Science Books, Mill Valley, CA, 1987.

[33] R.R. Schrock, J.A. Osborn, J. Am. Chem. Soc. 93 (1971) 2397.

[34] A.D. Zotto, L. Costella, A. Mezzetti, P. Rigo, J. Organomet. Chem. 414 (1991) 109.

[35] L.M. Haines, Inorg. Chem. 10 (1971) 1693.

[36] M.P. Keyes, K.L. Watters, J. Catal. 110 (1988) 96.

[37] C.R. Guerra, J.H. Schulman, Surface Science 7 (1967) 229.

[38] S.D. Worley, C.A. Rice, G.A. Mattson, C.W. Curtis, J.A. Guin, A.R. Tarrer, J. Phys. Chem. 86 (1982) 2714.

[39] C.A. Rice, S.D. Worley, C.W. Curtis, A.J. Guin, A.R. Tarrer, J. Chem. Phys. 74 (1981) 6487.

[40] K.S. Weddle, J.D. Aiken III, R.G. Finke, J. Am. Chem. Soc. 120 (1998) 5653, and references therein.

[41] G. Webb, J.I. Macnab, J. Catal. 26 (1972) 226.

[42] To facilitate comparison, the rates for Pd catalysts are reported in terms of an effective TOF, TOF_{eff}. Since these $Pd-SiO_2$ samples do not contain rhodium, a TOF based on rhodium content cannot be given. The TOF_{eff} value is calculated by assuming that the $Pd-SiO_2$ catalyst contains the standard rhodium loading (13.4 μmol/50mg).

[43] $[Rh(COD)_2]^+BF_4^-$ in solution and on SiO_2 is a poor hydrogenation catalyst, see Table 2 entry 7 and Table 4 entry 1. While the reduced rhodium metal is highly active, the reduction of $[Rh(COD)_2]^+BF_4^-$ to rhodium metal is slow under reaction conditions, taking days at 40°C [18].

Table 1. ^{31}P NMR and IR ν(CO) data for the complexes[a]

Complex	$^{\alpha}$P	$^{\beta}$P	J_{Rh-P}	J_{Rh-P}	J_{P-P}	IRν(CO)
PPM[b]	-3.7	-20.3				
PPM-Rh-COD 9[b]	42.4	32.5	113	110	37	
R-PPM 1[b]	-8.2	-22.3				
R-PPM-O$_2$ 15[b]	32.4	31.6				
R-PPM-Rh-COD 10[b]	44.2	16.8	146	140	38	
R-PPM-Rh(MeOH)$_2$ 16[c]	69.7	46.0	196	196	64	
R-PPM-Rh-MeOH-CO 20[c]	35.7	24.4	315	314	127	1984(s)[d]
R-PPM-Rh-MAC 19[c]	50.7	22.2	152	103	19	
R-PPM-Rh-MAC 19[e]	40.5	32.4	115	112	20	
R-PPM-Rh-MAC 19[f]	46	33				
R-PPM-Rh-MAC-CO 21[c]	54.3	47.4	137	137	125	1970(s)[d]
SiO$_2$-R-PPM 2[f]	-7	-23				
SiO$_2$-R-PPM-O$_2$ 11[f]	35	35				
SiO$_2$-R-PPM-Rh-COD 3[f]	43	15				
SiO$_2$-R-PPM-Rh-MeOH-CO 24[f]	35	25				1990(s)[g]
SiO$_2$-R-PPM-Rh-MAC 23[f]	40	28				
SiO$_2$-R-PPM-Rh-MAC-CO 25[f]						1974(s)[g]
Pd-SiO$_2$-R-PPM 12[f]	-7	-21				
Pd-SiO$_2$-R-PPM-O$_2$ 13[f]	38	38				
Pd-SiO$_2$-R-PPM-Rh-COD 6[f]	45	15				
Pd-SiO$_2$-R-PPM-Rh-MeOH-CO 27[f]	35	25				1990(s)[g]
Pd-SiO$_2$-R-PPM-Rh-MAC-CO 28[f]	.					1974(s)[g]

[a] Chemical shifts (in ppm) are referenced to an external standard of 85% H_3PO_4 and J couplings are given in Hertz. ν(CO) values are given in cm^{-1}.

[b] ^{31}P NMR measured in CDCl$_3$.

[c] ^{31}P NMR measured in MeOH-d$_4$.

[d] Solution IR measured in CH$_2$Cl$_2$.

[e] ^{31}P NMR measured in 85%CDCl$_3$-15%MeOH-d$_4$.

[f] Solid-state (CPMAS) ^{31}P NMR.

[g] DRIFT.

Table 2. Hydrogenation of MAC[a]

Entry	Species	Rate[b](TOF[c], min⁻¹)	ee[d]/%
1	B-PPM-Rh-COD(Lit)[e] **5**	14.3[e]	94.5[e]
2	R-PPM-Rh-COD **10**	5.01	93.5
3	SiO₂-R-PPM-Rh-COD(Lit)[e] **3**	6.25-12.5[e]	89.8-94.5[e]
4	SiO₂-R-PPM-Rh-COD(preformed)[f] **3A**	13.8	93.7
5	SiO₂-R-PPM-Rh-COD(sequential)[g] **3B**	11.2	91.1
6	SiO₂-R-PPM-Rh-COD **3** plus Hg[h]	12.0	92.5
7	SiO₂ plus [Rh(COD)₂]⁺BF₄⁻ **26**	0.0600	Racemic
8	SiO₂ plus [Rh(COD)₂]⁺BF₄⁻ **26** plus Hg[h]	0.00	
9	Oxidized SiO₂-R-PPM-Rh-COD[j]	1.02[k]	90.5[l]
10	Oxidized SiO₂-R-PPM-Rh-COD[m]	0.00	
11	SiO₂-R-PPM-O₂ **11** plus [Rh(COD)₂]⁺BF₄⁻ **4**	0.0135	Racemic
12	Used SiO₂-R-PPM-Rh-COD[f] **3A**	7.51, 4.04[n]	93.0, 94.0[n]
13	Pd-SiO₂-R-PPM-Rh-COD(preformed)[f] **6A**	5.69	90.6
14	Pd-SiO₂-R-PPM-Rh-COD(sequential)[g] **6B**	11.8[e]	88.3
15	Pd-SiO₂-R-PPM-Rh-COD(preformed)[f] **6A** Plus Hg[h]	6.11	92.0
16	Pd-SiO₂-R-PPM-Rh-COD(sequential)[g] **6B** Plus Hg[h]	10.4	85.0
17	Used Pd-SiO₂-R-PPM-Rh-COD(preformed)[f]**6A**	5.02, 4.01[n], 5.04[o]	89.3 ,92.0[n], 92.0[o]
18	Pd-SiO₂ **7**	7.06[p]	Racemic
19	Pd-SiO₂ **7** plus [Rh(COD)₂]⁺BF₄⁻ **4**	12.5	Racemic
20	Oxidized Pd-SiO₂-R-PPM-Rh-COD[j]	3.02	16.0
21	Pd-SiO₂-R-PPM-O₂ **13** plus [Rh(COD)₂]⁺BF₄⁻ **4**	11.7	Racemic
22	Pd-SiO₂ **7** plus [Rh(COD)₂]⁺BF₄⁻ **4** plus Hg[h]	0.00	
23	1%Pd-SiO₂-R-PPM-Rh-COD(sequential)[g] **1%-6B**	10.2	86.8

[a] See Eq. (1). Typical reaction conditions: 14 mg of catalyst (3.75 μmol Rh), 750 μmol (200 eq) MAC, 7.5 ml MeOH, 25°C, 1atm H₂. Data represents the average of 3 or more runs; however, Hg and re-use experiments reflect data from one unique experimental run.

[b] Rate given as TOF [mole H₂/(mole Rh • min)].

[c] TOF calculated after 5 min of reaction, corresponding to the maximum TOF observed.

[d] Enantiomeric excess(ee) determined by GC after complete hydrogenation of MAC, chirasil-val column(50m x 250μm).

[e] Literature reference [5].

[f] The catalyst was prepared using method A.

[g] The catalyst was prepared using method B.

[h] 0.10 mL of Hg added with MAC.

[i] Formed by stirring [Rh(COD)₂]⁺BF₄⁻ and SiO₂ for 5 min at room temperature in MeOH.

[j] Oxidized by exposure to air for 3-5 days.

[k] Activity ceases within 0.5 h of reaction, before complete MAC hydrogenation.

[l] ee for partially reacted substrate.

[m] Oxidized by addition of H₂O₂ to an acetone slurry of the catalyst prior to reaction.

[n] Second use.

[o] Third use.

[p] See footnote [42].

Table 3. Effect of Rh:PPM ratio on the activity and enantioselectivity of SiO_2-R-PPM-Rh-COD (3B), prepared by method B, in the hydrogenation of MAC[a]

Rh:PPM	Rate (TOF, min^{-1})	ee[b]/%
0.5:1	8.83[c]	90.5
plus Hg	9.04[c]	90.0
1:1	11.2[c]	91.5
plus Hg	11.0[c]	92.5
2:1	12.0[d]	90.1
plus Hg	11.0[d]	91.8
4:1	8.84[d]	92.7
plus Hg	10.8[d]	92.4

[a] Reaction conditions are the same as those in Table 2.

[b] Enantiomeric excess determined by GC after complete hydrogenation of MAC.

[c] TOF [mole H_2/(mole Rh • min)] after the first 5 min of reaction, corresponding to the maximum TOF observed.

[d] TOF [mole H_2/(mole PPM • min)] after the first 5 min of reaction, corresponding to the maximum TOF observed.

Table 4. Hydrogenation of toluene to methylcyclohexane[a]

Entry	Species	Rate (TOF[b], min^{-1})
1	SiO$_2$ plus [Rh(COD)$_2$]$^+$BF$_4^{-c}$ 26	0.0604
2	SiO$_2$ plus [Rh(COD)$_2$]$^+$BF$_4^{-c}$ 26 plus Hg^d	0.00
3	SiO$_2$-R-PPM-Rh-COD 3	0.0135
4	SiO$_2$-R-PPM-Rh-COD 3 plus Hg^d	0.00
5	Pd-SiO$_2$ 7	0.0785^e
6	Pd-SiO$_2$-R-PPM-Rh-COD 6	0.124
7	Pd-SiO$_2$-R-PPM-Rh-COD 6 plus Hg^d	0.00
8	Pd-SiO$_2$-R-PPM-Rh-COD oxidized with H$_2$O$_2$^{f}	0.834
9	Pd-SiO$_2$ 7 plus [Rh(COD)$_2$]$^+$BF$_4^{-c}$ 4	1.65
10	Pd-SiO$_2$ 7 plus [Rh(COD)$_2$]$^+$BF$_4^{-c}$ 4 plus Hg^d	0.0182^g

[a] Reaction conditions: 50.0 mg of catalyst (13.4 µmol Rh), 5.0 ml of toluene as both reactant and solvent, 1 atm H$_2$, 40°C.

[b] TOF [mole H$_2$/(mole Rh • min)] after the first 5 min of reaction, corresponding to the maximum TOF observed.

[c] Formed by stirring 5.4 mg (13.4 µmol) of [Rh(COD)$_2$]$^+$BF$_4^-$ (4) and 50.0 mg of SiO$_2$ for 5 min at room temperature in methanol.

[d] 0.10 mL of Hg added.

[e] See footnote [42].

[f] Oxidized by addition of H$_2$O$_2$ to an acetone slurry of the catalyst prior to reaction.

[g] Activity ceases after 10 min.

Scheme 1. Preparation of the tethered catalysts SiO₂-R-PPM-Rh-COD (3B) and Pd-SiO₂-R-PPM-Rh-COD (6B) using method B.

SiO₂-R-PPM-Rh-COD (3)
Pd-SiO₂-R-PPM-Rh-COD (6)
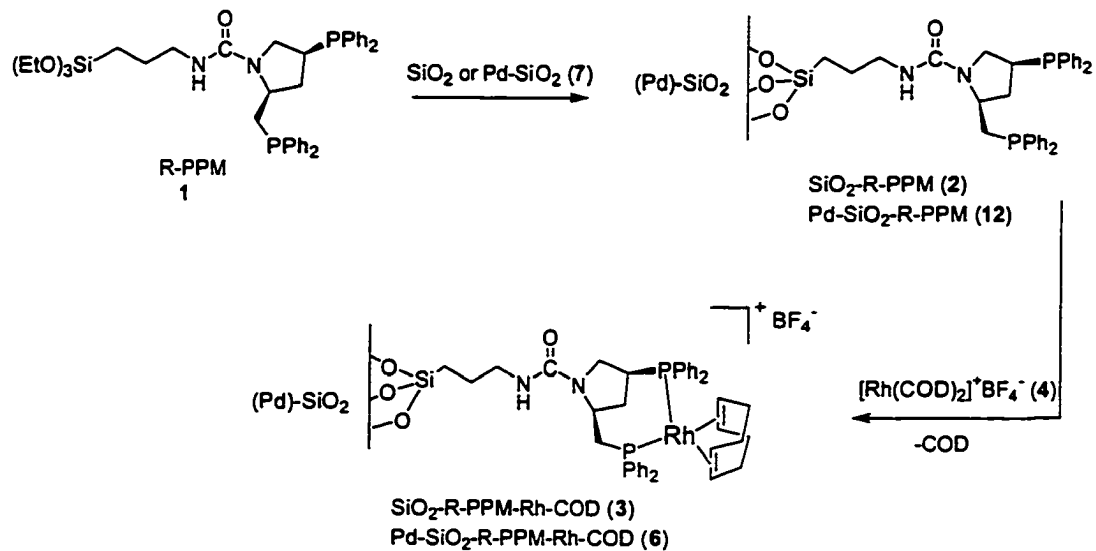
Scheme 2. Preparation of the tethered catalysts SiO₂-R-PPM-Rh-COD (3A) and Pd-SiO₂-R-PPM-Rh-COD (6A) using method A.

R-PPM
1

[Rh(COD)₂]⁺BF₄⁻ (4)
-COD

R-PPM-Rh-COD
10

SiO₂ or
Pd-SiO₂ (7)

SiO₂-R-PPM-Rh-COD (3)
Pd-SiO₂-R-PPM-Rh-COD (6)
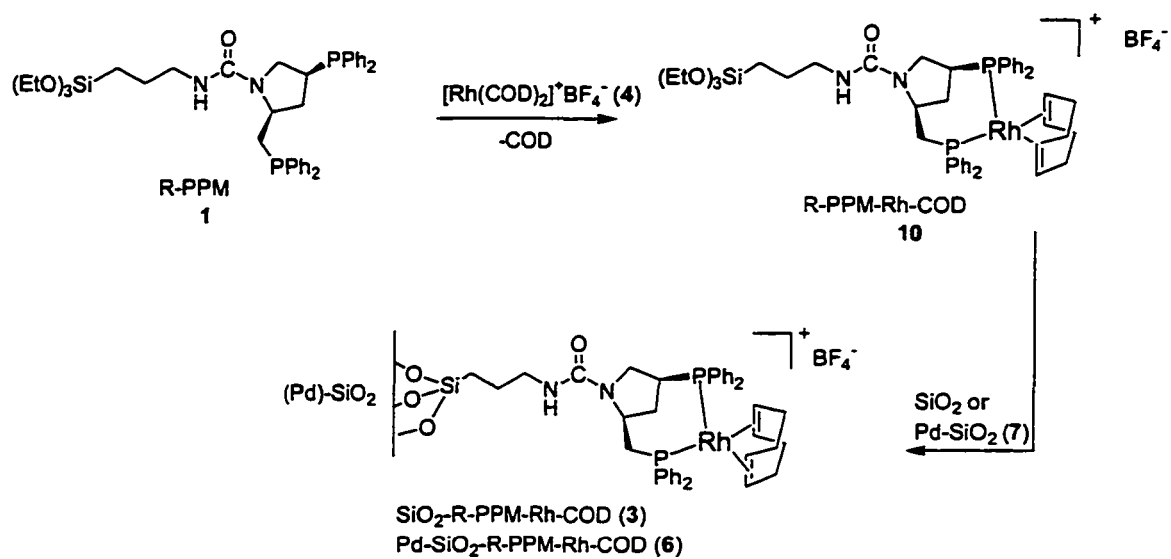
Scheme 3. Catalytic cycle for the hydrogenation of MAC using PPM-Rh and reactions of intermediates with CO
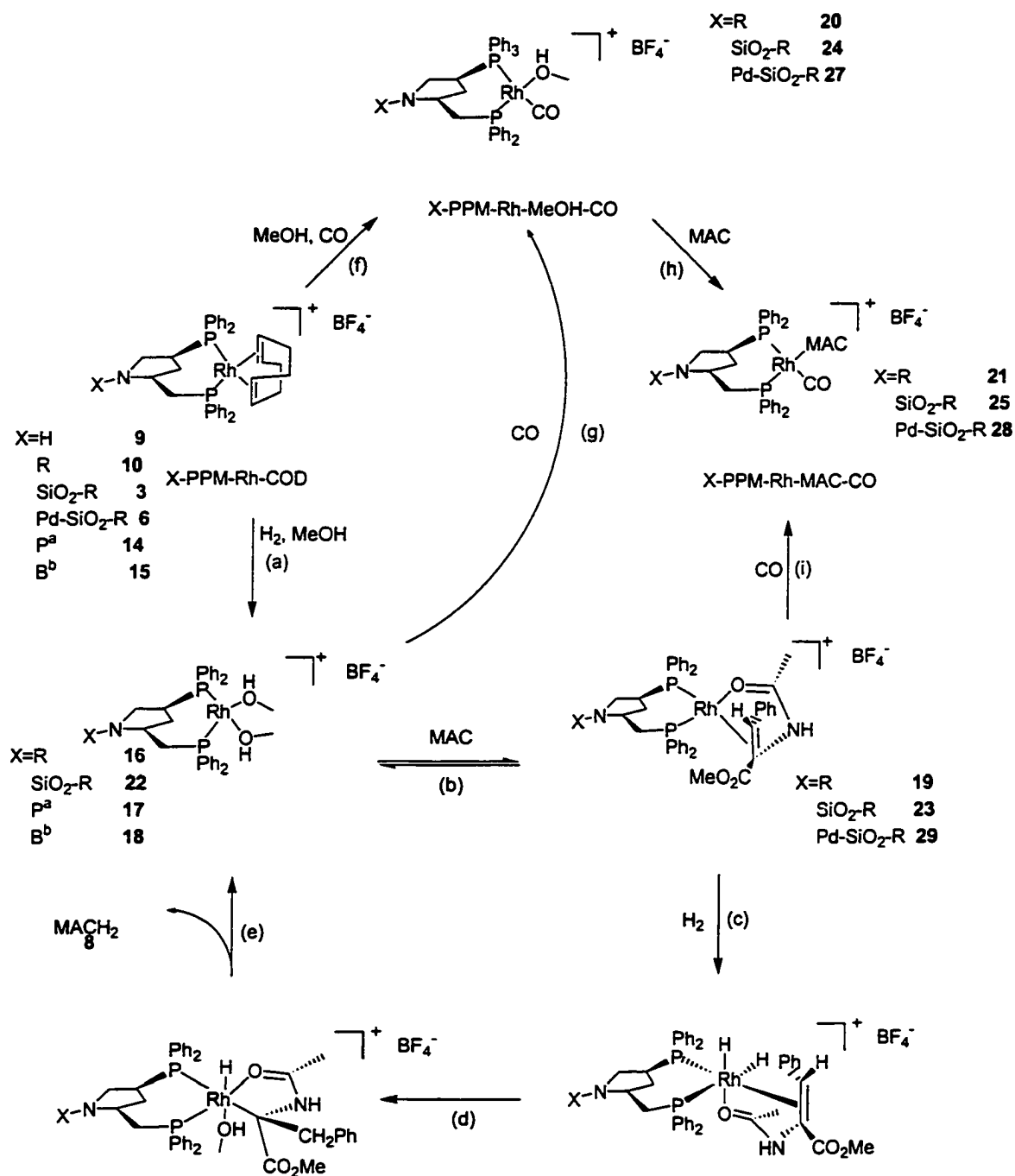
^{a}P = -CO(t-Bu) see ref [20]. ^{b}B = -CO$_2$(t-Bu), see ref [20].

Figure Captions

Fig. 1. ^{31}P CPMAS NMR spectra of (a) chiral phosphine SiO$_2$-R-PPM (2); (b), (c) SiO$_2$-R-PPM-Rh-COD (3) complex prepared by methods A and B, respectively. (d) chiral phosphine Pd-SiO$_2$-R-PPM (12); (e), (f) Pd-SiO$_2$-R-PPM-Rh-COD (6) complex prepared by methods A and B, respectively. Spectrum (f) was acquired using a lower spinning rate of 10kHz. Asterisks (*) denote the spinning sidebands.

Fig. 2. . ^{31}P CPMAS NMR spectrum of SiO$_2$-R-PPM-O$_2$ (11) obtained using a sample rotation rate of 10 kHz. Asterisks (*) denote the spinning sidebands.

Fig. 3. ^{31}P CPMAS NMR spectra of SiO$_2$-R-PPM (2) (a) and its rhodium complex SiO$_2$-R-PPM-Rh-COD (3) obtained by method B (b-d).

Figure 1
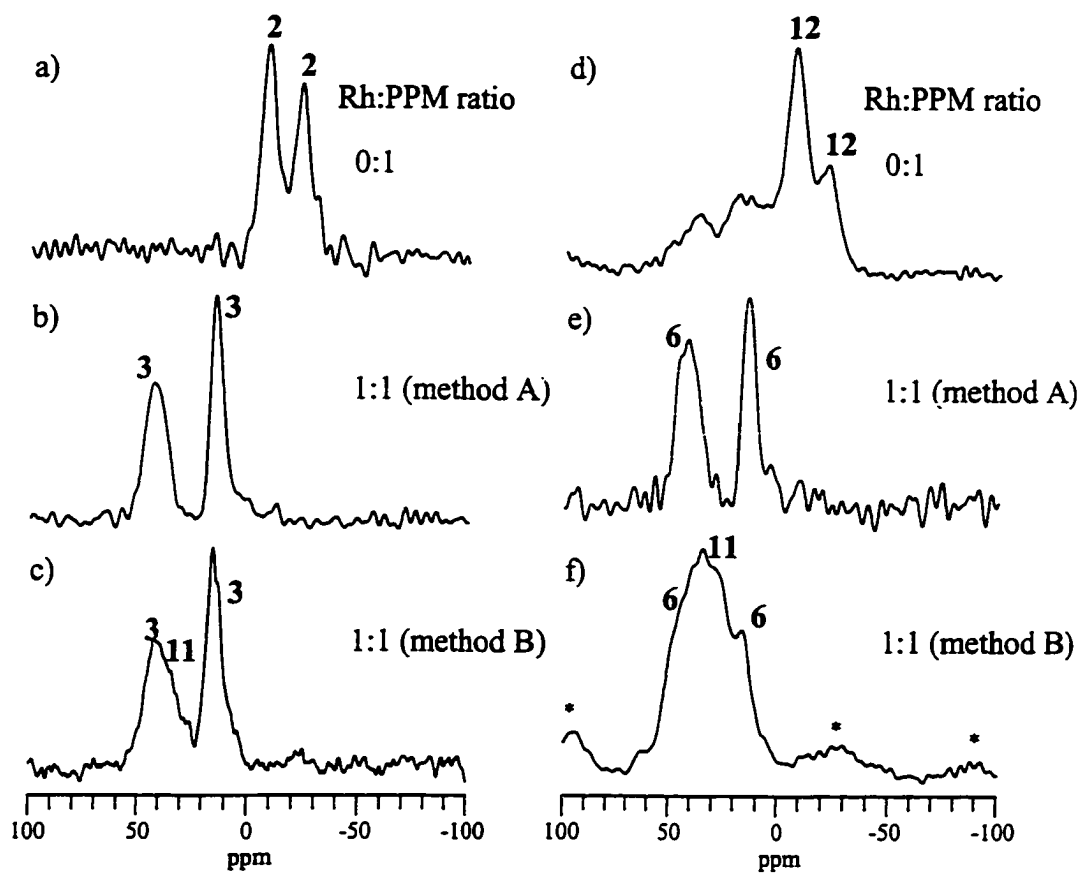
Figure 2
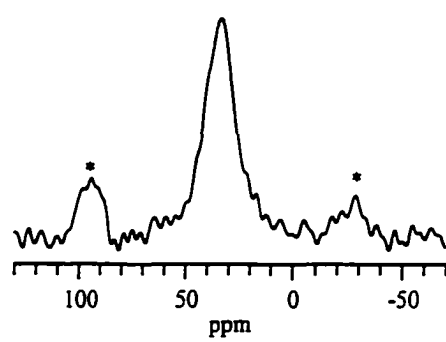
Figure 3
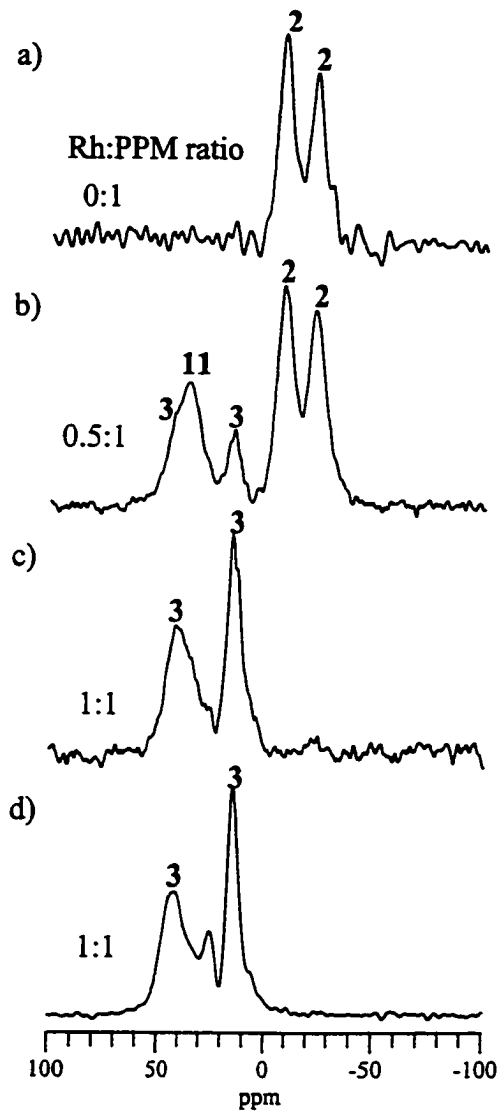
Arene Hydrogenation Using Supported Rhodium Metal Catalysts Prepared from [Rh(COD)H]₄, [Rh(COD)₂]⁺BF₄⁻, and [Rh(COD)Cl]₂ Adsorbed on SiO₂ and Pd-SiO₂

Keith J. Stanger, Yali Tang, James Anderegg, and Robert J. Angelici*

Abstract

Four different rhodium precursors, [Rh(COD)H]₄, [Rh(COD)₂]⁺BF₄⁻, [Rh(COD)Cl]₂, and RhCl₃•3H₂O, adsorbed onto silica (SiO₂) or onto palladium supported on silica (Pd-SiO₂), were examined for their catalytic arene hydrogenation activities. Rates of toluene hydrogenation were compared when the catalysts were pretreated with hydrogen as follows: none, 40 °C for 24 h, and 200 °C for 4 h. With no hydrogen pretreatment, the rhodium precursors adsorbed on Pd-SiO₂ showed higher activities than the corresponding precursors on only SiO₂. As the hydrogen pretreatment temperature was increased, the activities of the catalysts on SiO₂ increased; the highest activity occurred with catalysts pretreated at 200 °C. Conversely, milder pretreatments were more effective for the catalysts on Pd-SiO₂; higher temperature pretreatments reduced activities. The catalysts were characterized by their activities, DRIFTS, transmission electron microscopy (TEM), and X-ray photoelectron spectroscopy (XPS). All of the studies indicate that the active catalytic species is rhodium metal. On silica, H₂ reduction of the rhodium complex to Rh metal under arene hydrogenation conditions was slow in all cases except [Rh(COD)H]₄. However, on Pd-SiO₂, the palladium accelerated the reduction of all of the Rh complex precursors to rhodium metal

under the same conditions. The resulting Rh-Pd-SiO$_2$ bimetallic catalysts exhibited higher activities than catalysts of the same composition prepared by classical methods.

1. Introduction

Our group has shown that catalysts consisting of tethered complexes on supported metals (TCSM) are effective catalysts for various hydrogenation reactions [1-5]. In particular, TCSM catalysts (Fig. 1) that contain a rhodium complex tethered to silica that also has supported palladium metal are highly active for the hydrogenation of arenes under mild conditions (1 atm, 40 °C) [1-5]. Both the tethered rhodium complex and supported palladium contribute to the high activities of the catalysts. Their activities are much greater than either the complex tethered to silica or palladium on silica separately. The specific roles of the tethered complex and supported palladium are not known, but it was suggested, by our group [1-5], that the increased activity is due to hydrogen activation by the palladium, hydrogen spillover [6] to the silica surface, and utilization of the activated hydrogen by the tethered rhodium catalyst. Another possibility is that the activity of the TCSM catalyst is due to rhodium metal on the silica which is formed by palladium-promoted reduction of rhodium that dissociates from the tethered complex. One goal of the work described in the present paper was to determine whether palladium promotes the formation of rhodium metal in catalysts that are prepared by adsorbing Rh complexes on Pd-SiO$_2$.

In the literature, there are reports of rhodium/palladium bimetallic catalysts on silica or alumina supports that exhibit behavior opposite to that of the TCSM systems. Papers by del Angel et. al. [7] and Araya et. al. [8] show that supported bimetallic rhodium/palladium catalysts prepared by impregnation of RhCl$_3$ and PdCl$_2$ in aqueous solutions or bis(acetylacetonato)palladium in dichloromethane onto silica or alumina are less active for

benzene hydrogenation than rhodium-only supported catalysts [7,8]. In contrast, TCSM

catalysts with tethered rhodium complexes and supported palladium metal are more active

for arene hydrogenation than catalysts consisting of the tethered rhodium complexes only [1-

5]. Therefore, we have investigated conditions under which palladium increases or decreases

the arene hydrogenation activity of rhodium catalysts.

Silica- and alumina-supported rhodium is known to be much more active than

supported palladium as an arene hydrogenation catalyst [7-9]. The activity of the palladium-

supported catalyst is known to be structure insensitive and does not depend on the size of the

palladium particles [9]. On the other hand, the activity of supported rhodium catalysts is

structure sensitive and depends on particle size. Rhodium metal clusters of 10 Å or larger are

needed for arene hydrogenation; smaller particles show no arene hydrogenation activity [9-

12].

Considering the structure sensitive nature of supported rhodium catalysts, we also

describe in this report variations in activities of catalysts prepared from different types of

rhodium complexes. Thus, the following four rhodium complexes were examined:

$RhCl_3 \cdot 3H_2O$, $[Rh(COD)Cl]_2$ [13], $[Rh(COD)_2]^+BF_4^-$ [14], and $[Rh(COD)H]_4$ [15,16].

$RhCl_3 \cdot 3H_2O$ was chosen as a Rh catalyst precursor because it is commonly used for the

preparation of supported rhodium metal catalysts by the incipient wetness impregnation

method. It is reduced to metallic rhodium on silica surfaces by exposure to hydrogen gas

above 200 °C [17]. $[Rh(COD)Cl]_2$ is frequently used as a starting material for the synthesis

of homogeneous rhodium hydrogenation catalysts [13], and was chosen for these studies as a

model of surface species that may result from decomposition of rhodium halide catalysts.

Also, Blum and coworkers [18] showed that a sol-gel-entrapped $[Rh(COD)Cl]_2$ becomes an

active arene hydrogenation catalyst if metallic palladium is present in the sol-gel matrix. The

authors suggested the activity of these catalysts arose from a synergy facilitated by the close

proximity of the rhodium and palladium in the matrix. The cationic $[Rh(COD)_2]^+BF_4^-$ is

frequently used to prepare homogeneous rhodium hydrogenation catalysts [14] and is a

precursor for a number of tethered catalysts on silica [1-5,19,20]. In addition, the very

similar $[Rh(COD)(PhCN)_2]^+ClO_4^-$ is reduced to metallic rhodium under hydrogenation

conditions of 25 °C-100 °C in methanol, methylene chloride, or in the solid state [21].

Finally, $[Rh(COD)H]_4$, which catalyzes the hydrogenation of toluene at room temperature

(AR = 0.11 mol MeCy/mol Rh • min), is reduced to rhodium nanoclusters, with an average

size of 2 nm, under the reaction conditions [16].

For the studies reported here, the $RhCl_3•3H_2O$ catalysts were prepared by the standard

impregnation method, while the other catalysts were synthesized by adsorbing the rhodium

complexes onto silica (SiO_2) or palladium supported on silica ($Pd-SiO_2$) under conditions

(refluxing toluene for 4 h) similar to those used in the synthesis of TCSM catalysts [1-5,20].

These catalysts were examined for their activities in toluene hydrogenation, under mild

conditions of 1 atm H_2 and 40 °C (Eq. (1)).

$$\text{toluene} \xrightarrow[\substack{40\,°C}]{\substack{Rh\ catalyst \\ H_2\ (1\ atm)}} \text{methylcyclohexane} \qquad (1)$$
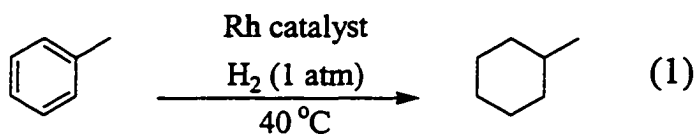
Sometimes the catalysts were studied without pretreatment; at other times, they were

pretreated with hydrogen at 40 °C for 24 h or 200 °C for 4 h. The 40 °C hydrogen

pretreatment was chosen to reflect conditions that would be present under prolonged

hydrogenation reaction times (Eq. (1)). The 200 °C hydrogen pretreatment was chosen to

simulate conditions used in the production of Rh-SiO$_2$ from RhCl$_3$•3H$_2$O. The catalysts were

also characterized by DRIFTS, TEM, and XPS.

2. Experimental

2.1. General considerations

The following chemicals were purchased: RhCl$_3$•3H$_2$O from Pressure Chemicals,

PdCl$_2$ from DFG, silica (SiO$_2$) Merck grade 10184 (B.E.T. surface area, 300 m^2 g^{-1}; pore size

100 Å) and 1,5-cyclooctadiene, COD, from Aldrich. Toluene and methylene chloride were

dried prior to use by passage through an alumina column under argon [22]. The following

compounds were prepared by literature methods: [Rh(COD)Cl]$_2$ [13], [Rh(COD)$_2$]$^+$BF$_4^-$ [14],

and [Rh(COD)H]$_4$ [16]. The preparation of Pd-SiO$_2$ (Pd, 10 wt.%) was described previously

[1].

FTIR and diffuse reflectance infrared Fourier transform spectroscopy (DRIFT)

spectra were obtained on a Nicolet 560 spectrophotometer. The main compartment,

equipped with a TGS detector, was used to take solution IR spectra using a NaCl solution

cell. An auxiliary experiment module (AEM) containing a Harrick diffuse reflectance

accessory with a MCT detector was used to obtain the DRIFT spectra of solid samples. Gas

chromatographic analyses were performed on a Hewlett Packard HP 6890 GC using a 25 m

HP-1 capillary column attached to a FID detector. Rhodium content of the supported

catalysts was determined by ICP-AES conducted by MPC Analytical Services of the Ames

Laboratory. Samples for analysis were prepared by dissolving a 50 mg sample in 5.0 ml of

aqua regia at 90 °C, then 5.0 ml of 5% aqueous HF was added and the mixture was heated to

the same temperature. The resulting solution was diluted to 25 ml in a volumetric flask.

Experimentally determined rhodium compositions (by weight) are listed for representative catalysts in the following sections.

2.2. Preparation of arene hydrogenation catalysts

2.2.1. Preparation of silica-supported metal catalysts (M-SiO₂; M = Rh)

Rh-SiO₂: The preparation of Rh-SiO₂ was similar to that reported in the literature [17]. To 0.234 g of RhCl₃•3H₂O dissolved in 20 ml of water was added 5.0 g of SiO₂ with stirring. After stirring overnight at room temperature, water was removed with a rotary evaporator at 80 °C. The solid was then dried further in an oven at 110 °C overnight. The sample was then placed in a tube furnace, treated with an N₂ flow, and heated to 200 °C for 2 h under the N₂ flow. The sample was cooled to room temperature under N₂, and the gas flow was switched to H₂. Then the sample was reduced for 3 h in a H₂ flow at 200 °C before the temperature was ramped to 250 °C for an additional 5 h. The resulting black solid, Rh-SiO₂, was collected after it had been allowed to cool under H₂ to room temperature. (Rh, 1.17 wt.%)

2.2.2. Preparation of silica-supported bimetallic catalysts (M-M'-SiO₂; M, M' = Pd or Rh)

Rh-(Pd-SiO₂): These catalysts were produced following the procedure for the preparation of Rh-SiO₂ (given above) using Pd-SiO₂ instead of SiO₂. (Rh, 1.65% wt.; Pd, 10% wt.)

Rh/Pd-SiO₂: This catalyst was prepared by the coimpregnation of Rh and Pd. First, 4.6 g of SiO₂ was allowed to stir overnight in an aqueous solution of PdCl₂ (1.0 g, 5.4 mmol) and RhCl₃•3H₂O (0.20 g, 0.90 mmol) in 30 ml of 0.2 M HCl. After rotary evaporation at 80

°C and oven drying at 110 °C overnight, the sample was placed in a tube furnace, where it was reduced in a H_2 flow at 450 °C for 5 h. (Rh, 1.46% wt.; Pd, 10% wt.)

Rh/Pd(O_2)-SiO_2: This catalyst was prepared by the coimpregnation of Rh and Pd by stirring 4.6 g of SiO_2 overnight in an aqueous solution of 1.0 g (5.4 mmol) of $PdCl_2$ and 0.20 g (0.90 mmol) of $RhCl_3 \cdot 3H_2O$ in 30 ml of 0.2 M HCl. After rotary evaporation at 80 °C and oven drying at 110 °C overnight, the sample was placed in a tube furnace and calcined in an air flow at 500 °C for 6 h, before being reduced in an H_2 flow at 500 °C for 6 h. (Rh, 1.56% wt.; Pd, 10% wt.)

Pd-(Rh-SiO_2): This catalyst was prepared by sequential addition of the metals following a literature preparation [8]. A solution of 23 mg (75 μmol) of bis(acetylacetonato)palladium in 5 ml of CH_2Cl_2 was stirred for 1 h with 1.0 g of 0.16% Rh-SiO_2. After vacuum drying, the sample was reduced at 450 °C in a flow of H_2 for 5 h. (Rh, 0.16% wt.; Pd, 0.80% wt.)

2.2.3. Preparation of adsorbed rhodium complexes on SiO_2 and Pd-SiO_2

General procedure

Catalysts were prepared by placing 97 μmol of the rhodium complex and 0.50 g of SiO_2 in a round bottom flask that was attached to a reflux condenser further linked to a Schlenk line. The atmosphere in the apparatus was replaced with nitrogen; 20 ml of toluene and 5.0 ml of CH_2Cl_2, for solubility, were added; and the system was refluxed for 4 h. The mixture was cooled to room temperature and stirred a further 12 h at room temperature. Finally, the solvent and unadsorbed species were filtered off, and the remaining solid was washed at least three times with 20 ml of toluene or until the toluene washings were clear.

The resulting adsorbed catalysts and rhodium contents, determined by ICP-AES, are listed below:

[Rh(COD)Cl]$_2$-SiO$_2$: (Rh, 0.093% wt.); [Rh(COD)$_2$]$^+$BF$_4^-$-SiO$_2$: (Rh, 1.68% wt.);

[Rh(COD)H]$_4$-SiO$_2$: (Rh, 1.68% wt.); [Rh(COD)Cl]$_2$-Pd-SiO$_2$: (Rh, 0.44% wt.; Pd, 10% wt.);

[Rh(COD)$_2$]$^+$BF$_4^-$-Pd-SiO$_2$: (Rh, 1.56% wt.; Pd, 10% wt.); [Rh(COD)H]$_4$-Pd-SiO$_2$: (Rh, 1.84% wt.; Pd, 10% wt.).

2.2.4. Hydrogen pretreatment of adsorbed catalysts

40 °C Treatment: The catalyst (100 mg) was placed in a jacketed vessel, described in section 2.3., with a stir bar. The atmosphere was replaced with hydrogen by performing a series of three vacuum/hydrogen flushes. Under a hydrogen atmosphere (1 atm) in the absence of solvent, the temperature was raised to 40 °C. The dry catalyst was allowed to stir for 24 h at 40 °C under hydrogen. Then, the temperature was lowered to room temperature; the hydrogen atmosphere was removed under vacuum and replaced with nitrogen; and the sample was collected and stored under nitrogen. The resulting catalysts are:

[Rh(COD)Cl]$_2$-SiO$_2$/40°C; [Rh(COD)Cl]$_2$-Pd-SiO$_2$/40°C; [Rh(COD)$_2$]$^+$BF$_4^-$-SiO$_2$/40°C; [Rh(COD)$_2$]$^+$BF$_4^-$-Pd-SiO$_2$/40°C; [Rh(COD)H]$_4$-SiO$_2$/40°C; [Rh(COD)H]$_4$-Pd-SiO$_2$/40°C.

200 °C Treatment: The catalyst (100 mg) was placed in a tube furnace. The atmosphere was replaced with hydrogen using three vacuum/hydrogen flush cycles. Then, hydrogen was passed over the sample for 15 min at room temperature before the temperature was ramped to 200 °C. Hydrogen flow was continued at 200 °C for 4 h. Then, the sample was cooled to room temperature; the atmosphere was switched to nitrogen; and the sample was collected and stored under nitrogen. The resulting catalysts are:

[Rh(COD)Cl]$_2$-SiO$_2$/200°C; [Rh(COD)Cl]$_2$-Pd-SiO$_2$/200°C; [Rh(COD)$_2$]$^+$BF$_4^-$-SiO$_2$/200°C;

[Rh(COD)$_2$]$^+$BF$_4^-$-Pd-SiO$_2$/200°C; [Rh(COD)H]$_4$-SiO$_2$/200°C; [Rh(COD)H]$_4$-Pd-SiO$_2$/200°C.

2.3. Hydrogenation reactions

2.3.1. Hydrogenation of toluene

A standard hydrogenation run consisted of placing 50 mg of catalyst (~10 μmol of Rh) into a three-neck jacketed vessel containing a Teflon-coated stir bar (Fig. 2). One neck of the reaction vessel was capped with a glass stopper. The center neck was fitted with a rubber and Teflon septum to allow for input of solvents and removal of GC samples via syringe. The third neck was fitted with a three-arm "Y" stopcock. This allowed the reaction vessel to be attached to a vacuum/argon Schlenk line and the burette to be filled with hydrogen.

After the catalyst was placed in the reaction vessel, the atmosphere in the reaction flask was replaced with Ar using three vacuum/flush cycles. Next, the jacket of the vessel was attached to a constant temperature bath and the temperature was raised to 40.0 °C (±0.2 °C). While the temperature was being achieved, the hydrogen gas reservoir was filled though a series of three consecutive vacuum and hydrogen gas flush cycles. After the temperature had stabilized at 40 °C and the gas burette was full of hydrogen, the reaction vessel itself was evacuated and filled with hydrogen three times. Immediately after replacing the nitrogen atmosphere with hydrogen, 5.0 ml of toluene were added via syringe. The reaction was opened to the hydrogen gas reservoir and stirring was initiated. Generally, less then 5 min were required for the toluene to warm to 40 °C and for the burette to stabilize after addition of solvent to the reaction vessel; after this time, hydrogen uptake readings were made. The

rate of reaction was monitored by the volume of hydrogen taken up with time. In all cases, methylcyclohexane (CyMe) was the only product observed, and hydrogen uptake readings from the burette matched the amount of CyMe product determined by GC analysis. Solvent and reaction vessel volumes were the same for all runs. The stirring speed (600 rpm) was held constant in the reported reactions, but changes in stirring speeds (300-1200 rpm) did not change the observed rates indicating that effects of hydrogen mass transfer were not significant and rates were not diffusion limited. Rates were calculated as atomic rates (AR) [23] based on the total moles of methylcyclohexane produced (1/3 of the moles of hydrogen gas consumed) divided by the moles of rhodium in the catalyst and the time of the reaction in minutes, Eq. (2).

$$AR = \frac{\text{(Total Moles of Methylcyclohexane produced)}}{\text{(Total Moles of Rh in the catalyst)(minutes)}} \qquad (2)$$

2.3.2. Hydrogenation of 1-hexene

The same hydrogenation setup and procedure used for toluene hydrogenation were utilized with the following modifications. The amount of catalyst was reduced to 25 mg (~5 μmol of Rh); the temperature was held at 0.0 °C (±0.2°C); and 1-hexene (5.0 ml) was used as both solvent and substrate. Rates, as atomic rates (AR) [23], were calculated as in Eq. (2), but based on the total moles of hexane produced (the same as the number of moles of hydrogen gas consumed).

2.3.3. Hydrogenation in the presence of mercury

After initial rates of hydrogenation of toluene or 1-hexene were determined, 0.2 ml (14 mmol) of Hg was added to the reaction via syringe. The rate of hydrogen uptake was continuously monitored. In cases where the effect of mercury on the rate was not complete

in 1 h, the hydrogen atmosphere was replaced with argon and the mercury was stirred with the catalyst under the inert atmosphere of argon for a period of time. After this time (2 or 17 h), the argon atmosphere was replaced with hydrogen via three quick vacuum/hydrogen flush cycles, and rates of the mercury-treated reactions were measured by following the hydrogen uptake with time.

2.4. IR studies of CO treated catalysts

The catalyst (50 mg) was placed in 1.0 ml of toluene and stirred under 1 atm of CO for 18 h. The samples were then filtered, washed three times with 1.0 ml of toluene, and vacuum dried before being analyzed by DRIFTS.

2.5. TEM analysis of catalysts

Samples were crushed using an agate mortar and pestle. The finely separated samples were then floated using methanol over a holey carbon grid supported on a copper grid. The samples were air dried and then analyzed with a Philips CM 30 transmission electron microscope (TEM) equipped with a LINK energy dispersive spectrometer (EDS) system. Both selected-area electron diffraction (SAED) and micro-diffraction patterns were obtained from the samples for phase identification. Visual images were manipulated with Photoshop and distances measured with Image-Pro Plus®. In order to obtain accurate statistical results of size distribution of nano particles, more than 120 particles were measured for analysis. MS Excel was used to tabulate distances and produce distribution curves.

2.6. XPS analysis of catalysts

Samples were heated to 150 °C under vacuum for 12 h prior to analysis. The samples were then mounted on two-sided tape and analyzed with a Physical Electronics 5500 Multi-technique system using the standard Mg source. An initial survey was conducted from the

range 0 - 1100 eV and then multiple elemental regions were examined including Rh, Pd, C, Si, and O regions. Physical Electronics' MultiPak® software was used to analyze the data. For all samples, peaks were referenced to C (1s, 284.5 eV) and/or Si (2p,103.3 eV).

3. Results

3.1. Activities of [Rh(COD)H]₄-based catalysts

The rates of toluene hydrogenation to methylcyclohexane at 40 °C under 1 atm of H_2 in the presence of [Rh(COD)H]₄-based catalysts are summarized in Table 1. In solution, [Rh(COD)H]₄ is active from the outset (AR = 1.83 min⁻¹) (entry 1). When adsorbed onto silica, [Rh(COD)H]₄ activity (entry 2) appears to increase with time, as is evident in the higher rate at 6 h (AR = 2.26 min⁻¹) than at 1 h (AR = 1.59 min⁻¹); in contrast, the activity of [Rh(COD)H]₄ in solution decreases with time. Hydrogen pretreatments enhance the activity of the silica-supported catalyst. Pretreatment at 40 °C (entry 3) causes the initial activity to nearly double (AR = 3.33 min⁻¹) and to remain elevated even after 6 h (AR = 2.64 min⁻¹). A 200 °C pretreatment (entry 4) causes the initial rate to triple (AR = 5.13 min⁻¹) and remain high even after 6 h (AR = 4.17 min⁻¹).

The catalyst [Rh(COD)H]₄-Pd-SiO₂ consisting of [Rh(COD)H]₄ adsorbed onto Pd-SiO₂ shows high activity from the outset, AR = 4.80 min⁻¹ (entry 5). For this system, hydrogen pretreatments provide no benefit. A 40 °C pretreatment (entry 6) slightly decreases the activity (AR = 3.77 min⁻¹), and a 200 °C pretreatment reduces the activity by a factor of nearly five (AR = 1.07 min⁻¹) (entry 7).

3.2. Activities of [Rh(COD)₂]⁺BF₄⁻-based catalysts

Rates of toluene hydrogenation for [Rh(COD)₂]⁺BF₄⁻-based catalysts are summarized in Table 1. The cationic [Rh(COD)₂]⁺BF₄⁻ is insoluble in toluene; when it is dissolved in a

1:4 vol/vol mixture of CH_2Cl_2:toluene, the resulting solution is only weakly active (AR =

0.02 min^{-1}) (entry 8). The silica-supported catalyst $[Rh(COD)_2]^+BF_4^--SiO_2$ (entry 9) requires

a long induction period, ~1 d, before achieving a steady AR of 0.67 min^{-1}, which is

maintained for over three days. If this catalyst is pretreated with H_2 at 40 °C, it shows an

increased initial rate (AR = 1.58 min^{-1}) (entry 10) that decreases to a steady AR of 0.67 min^{-1}

after 10 h. In contrast, 200 °C pretreatment provides a highly active catalyst,

$[Rh(COD)_2]^+BF_4^--SiO_2/200°C$ (AR = 4.10 min^{-1}) (entry 11).

For the catalyst $[Rh(COD)_2]^+BF_4^--Pd-SiO_2$, prepared by adsorbing $[Rh(COD)_2]^+BF_4^-$

onto $Pd-SiO_2$, an initial activity is observed that is very high (AR = 3.83 min^{-1}) (entry 12).

Hydrogen pretreatments of this catalyst appear to have no beneficial effects. A 40 °C

pretreatment produces no appreciable change in rate (AR = 3.50 min^{-1}) (entry 13). A 200 °C

hydrogen pretreatment (entry 14) severely reduces the catalytic activity by almost five-fold

(AR = 0.76 min^{-1}).

3.3. Activities of $[Rh(COD)Cl]_2$-based catalysts

The activities of $[Rh(COD)Cl]_2$-based catalysts for the hydrogenation of toluene are

given in Table 1. In solution and on silica, $[Rh(COD)Cl]_2$ shows little activity even after

three days (AR<0.01 min^{-1}) (entries 15, 16). However, if the rhodium catalyst on silica is

treated with hydrogen gas at elevated temperatures, the system becomes active (entries 17,

18). With one day of hydrogen pretreatment at 40 °C, the catalyst, $[Rh(COD)Cl]_2$-

$SiO_2/40°C$, exhibits an AR of 0.72 min^{-1}. When the system is pretreated at 200 °C for 4 h, a

nearly ten-fold rate increase is observed: the initial AR is 7.00 min^{-1} and the extended AR is

5.67 min^{-1} after 6 h.

When the same rhodium precursor is adsorbed onto Pd-SiO$_2$, the catalyst,

[Rh(COD)Cl]$_2$-Pd-SiO$_2$, is highly active (entry 19) from the outset (AR = 3.87 min^{-1}). Once

again hydrogen pretreatments provide no benefit for rhodium complexes on Pd-SiO$_2$;

pretreatment of [Rh(COD)Cl]$_2$-Pd-SiO$_2$ with H$_2$ at 40 °C has little effect on the activity (AR

= 5.13 min^{-1}) (entry 20), while H$_2$ pretreatment at 200 °C nearly eliminates the activity (entry

21) of the catalyst (after 6 h, the rate is only AR = 0.60 min^{-1}).

3.4. Activities of RhCl$_3$-based catalysts

The rates of hydrogenation of toluene to methylcyclohexane at 40 °C under 1 atm of

H$_2$ catalyzed by catalysts prepared by impregnation with RhCl$_3$ are summarized in Table 1.

The activity (entry 22) of Rh-SiO$_2$ is very good (AR = 2.52 min^{-1}). When RhCl$_3$ and

palladium are combined on SiO$_2$ using several different methods of preparations (see section

2.2.2), all resulting catalysts are less active then Rh-SiO$_2$. Impregnation of RhCl$_3$ onto Pd-

SiO$_2$ gives a catalyst {Rh-(Pd-SiO$_2$)} with a very low activity (AR = 0.31 min^{-1}) (entry 23).

A catalyst prepared by coimpregnation of rhodium and palladium (Rh/Pd-SiO$_2$) exhibits a

modest activity (AR = 0.52 min^{-1}) (entry 24), but it is still slower than that of Rh-SiO$_2$; if in

the preparation of this catalyst, the reduction is preceded by a calcination step (Rh/Pd(O$_2$)-

SiO$_2$), the catalyst is nearly inactive (AR = 0.03 min^{-1}) (entry 25). Palladium supported on

Rh-SiO$_2$ {Pd-(Rh-SiO$_2$)} is also dramatically slower (AR = 0.43 min^{-1}) (entry 26) than the

parent Rh-SiO$_2$.

3.5. Activities of catalysts in the presence of mercury

3.5.1. Toluene hydrogenation

A number of catalysts that are active for toluene hydrogenation were examined for their activities in the presence of mercury metal, Table 2. For all of the catalysts studied, the reactions are quenched completely within 20 min of mercury addition.

3.5.2. 1-Hexene hydrogenations

The $[Rh(COD)_2]^+BF_4^-$ series of catalysts were examined for 1-hexene hydrogenation activity at 0.0 °C both in the absence and presence of mercury (Table 3). In the absence of mercury, $[Rh(COD)_2]^+BF_4^-$ in solution (1ml CH_2Cl_2 : 4 ml 1-hexene) and adsorbed on SiO_2, $[Rh(COD)_2]^+BF_4^-$-SiO_2, are very poor hydrogenation catalysts of 1-hexene (AR = 0.0 min^{-1}). The addition of mercury to these systems has no activating effect, AR = 0.0 min^{-1}. In contrast, the hydrogen-pretreated catalysts, $[Rh(COD)_2]^+BF_4^-$-SiO_2/40°C and $[Rh(COD)_2]^+BF_4^-$-SiO_2/200°C, both show similar high activities (AR~34 min^{-1}). The addition of mercury to these systems results in no immediate change in activity. However, a slow deactivation is apparent. After 2 h of contact time, activity has dropped by a third or more; and after 17 h of mercury exposure, the catalysts are completely deactivated (AR = 0.0 min^{-1}).

The activity of Pd-SiO_2 for 1-hexene hydrogenation, unlike toluene hydrogenation, is comparable to the rhodium complexes on SiO_2. The initial rate for Pd-SiO_2 is AR_{eff} = 65.2 min^{-1} [24]. Mercury poisoning of supported palladium is slow but more pronounced than for supported rhodium; after 2 h, activity has decreased more than 60 fold (AR_{eff} = 1.62 min^{-1} [24]). After 17 h of contact, mercury exposure completely quenched the hydrogenation ability of Pd-SiO_2 (AR_{eff} = 0.0 min^{-1} [24]).

The catalysts prepared by adsorbing $[Rh(COD)_2]^+BF_4^-$ on $Pd-SiO_2$ are very active for

1-hexene hydrogenation at 0 °C. Without hydrogen pretreatment, $[Rh(COD)_2]^+BF_4^--Pd-SiO_2$

shows an initial activity of 116 min^{-1}. Both pretreated samples, $[Rh(COD)_2]^+BF_4^--Pd-$

$SiO_2/40°C$ and $[Rh(COD)_2]^+BF_4^--Pd-SiO_2/200°C$ show similar initial activities (AR~160

min^{-1}). Addition of mercury to all $[Rh(COD)_2]^+BF_4^--Pd-SiO_2$-based catalysts causes a slow

decrease in 1-hexene hydrogenation activity. After 2 h, the activities decrease by a factor of

~8, and complete quenching is observed after 17 h.

3.6. Characterization of catalysts by IR, TEM, and XPS

After exposure to CO, all catalysts showed distinctive $v(CO)$ bands in their DRIFT

spectra. For all of the $[Rh(COD)Cl]_2$ catalysts, the concentration of rhodium carbonyl

species on the surface of the fresh catalysts was too low for DRIFT detection. For all of the

catalysts shown in Figs. 3, the catalysts used in a toluene hydrogenation show CO bands that

are the same as those observed in the unused catalyst, but the intensities of the bands are

reduced. For all the CO-treated catalysts in Figs. 3, no surface rhodium carbonyl species are

removed by toluene or CH_2Cl_2 washes, as determined by the absence of IR bands in the

washes.

TEM studies of the $[Rh(COD)H]_4-SiO_2/40°C$ and $[Rh(COD)H]_4-SiO_2/200°C$

catalysts clearly indicate that rhodium crystallites are present. Visual inspection of the

electron micrographs reveals rhodium rafts with a wide range of sizes, Figs. 4 and 5. The

nature of these particles is confirmed by micro-chemical analysis and electron diffraction of

the crystallites, Fig. 6. The diffraction patterns, Fig. 6 (a) and (b), are explicit for face

centered cubic (fcc) rhodium metal. For example, distances of 2.2 Å are measured for the

(111) plane and 1.9 Å for the (200) plane, which match the literature values for the distances found in fcc rhodium metal [25].

XPS data obtained from many of the catalysts are collected in Table 4. Further discussion of these data will be presented in section 4.1.3.

4. Discussion

4.1. Catalyst characterization

4.1.1. IR studies of the catalysts

Although $v(CO)$ spectra of catalyst samples treated with CO are often useful for identifying species present on the surface, this identification may be complicated by similar $v(CO)$ spectra of the various species. For supported metallic rhodium, two main species have been identified (Fig. 7). The rhodium(I) dicarbonyl species, $Rh^I(CO)_2$, exhibits CO bands at 2096(s) and 2038(s) cm^{-1}, although the bands are shifted slightly depending on the support [26-33]. The CO linearly bound to bulk islands of rhodium metal show a coverage dependent signal, which ranges from 2040 cm^{-1} (at low coverages) to 2066 cm^{-1} (at high coverages) [26,27]. The situation is further complicated by the possible formation of several surface-constrained homogeneous species such as $[Rh(CO)_2Cl]_2$, $[Rh(CO)_2Cl(H_2O)]$, and even $Rh(CO)_x$ that are known to exhibit IR bands similar to those of surface bound rhodium dicarbonyl or linearly bound CO on rhodium metal [34,35].

For the catalysts in this work, the $v(CO)$ signals may be interpreted to indicate the presence of surface bound $Rh^I(CO)_2$ species and adsorbed CO on bulk rhodium (Fig. 3). All of the CO-containing rhodium complexes on the surface are strongly bound to the silica surface as toluene and CH_2Cl_2 extractions fail to yield solutions containing species with $v(CO)$ bands. Thus, soluble complexes such as $[Rh(CO)_2Cl]_2$, $[Rh(CO)_2Cl(H_2O)]$, or

$Rh(CO)_x$, which are known to be readily soluble in pentane, toluene, or CH_2Cl_2 and easily washed from silica surfaces [34,35], are not present or formed upon CO adsorption.

Attempts to characterize rhodium sites on the CO-treated catalysts, by correlating catalyst activity with specific v(CO) bands gave no consistent correlations. Unused Rh-SiO$_2$ (Fig. 3, trace a) shows the characteristic $Rh^I(CO)_2$ bands (2092(vs) and 2027(m) cm^{-1}). $[Rh(COD)_2]^+BF_4^-$-SiO$_2$ (Fig. 3, trace b) and $[Rh(COD)_2]^+BF_4^-$-Pd-SiO$_2$ (Fig. 3, trace e) show very similar IR signatures (2089(vs) and 2030(m) cm^{-1}). For $[Rh(COD)_2]^+BF_4^-$ on SiO$_2$ and Pd-SiO$_2$, a CO band at 2055 cm^{-1} appears as a shoulder with hydrogen pretreatments (Fig. 3 traces c, d, f, and g). Also, for the hydrogen-treated catalysts containing $[Rh(COD)_2]^-BF_4^-$ on SiO$_2$ and Pd-SiO$_2$, the relative intensities of the 2089 and 2030 cm^{-1} bands are changed from those of the untreated catalysts (Fig. 3, trace b and e). These changes may be due to the appearance of rhodium metal clusters. However, the similarities of these spectra to those of the samples that had not been hydrogen-treated complicate interpretation. Thus, the observed DRIFTS of hydrogen-pretreated samples may result from signals from both residual starting complex (with a large extinction coefficient) and CO on metallic rhodium. Similar results were obtained from DRIFT studies of [Rh(COD)H]$_4$ on SiO$_2$ and Pd-SiO$_2$ (not shown).

4.1.2. TEM studies of the catalysts

For [Rh(COD)H]$_4$-SiO$_2$/40°C and [Rh(COD)H]$_4$-SiO$_2$/200°C, TEM micrographs (Fig. 4) and electron diffraction patterns (Fig. 6) clearly show the presence of rhodium crystallites, which suggests the active species is supported rhodium metal. The mean size (9.8 nm) of the rhodium particles of the [Rh(COD)H]$_4$-SiO$_2$/200°C sample is slightly smaller than those (13.8 nm) of the [Rh(COD)H]$_4$-SiO$_2$/40°C sample (Fig. 5). Thus, dispersion may play a vital role in the greater activity of the 200 °C hydrogen pretreated sample; smaller

particles will have more surface area, more active sites, and therefore higher observed activity.

4.1.3. XPS analyses

4.1.3.1. [Rh(COD)$_2$]$^+$BF$_4^-$

For the series of catalysts containing [Rh(COD)$_2$]$^+$BF$_4^-$ on SiO$_2$, distinct Rh 3d$_{5/2}$ signals are observed (Table 4). The solid complex [Rh(COD)$_2$]$^+$BF$_4^-$ exhibits a signal at 308.6 eV, which corresponds well to literature values for Rh(I) complexes (~308 eV) [36]. The [Rh(COD)$_2$]$^+$BF$_4^-$-SiO$_2$ catalyst exhibits a very similar signal at 308.4 eV; this is both diagnostic for Rh(I) and suggests that the [Rh(COD)$_2$]$^+$BF$_4^-$ complex remains intact. Thus, the initial adsorbed complex is still Rh(I) prior to pretreatment with hydrogen and/or use in hydrogenation reactions. After hydrogen pretreatment, the Rh 3d$_{5/2}$ signals for [Rh(COD)$_2$] $^+$BF$_4^-$-SiO$_2$/40°C (307.4 eV) and [Rh(COD)$_2$]$^+$BF$_4^-$-SiO$_2$/200°C (307.1 eV) are in the correct range for Rh(0) (307 eV) [36] and match well with Rh-SiO$_2$ (307.2 eV).

When the catalyst [Rh(COD)$_2$]$^+$BF$_4^-$-SiO$_2$ is examined after 30 min of toluene hydrogenation, the main Rh peak is seen at 307.9 eV. Even after 2 h of reaction, the Rh signal is at 308.3 eV. These signals indicate the presence of Rh(I) and reflect the poor activity of the [Rh(COD)$_2$]$^+$BF$_4^-$-SiO$_2$ catalyst during the induction period, which continues for at least six hours. After 7.5 h of reaction, the Rh peak has clearly shifted to 307.0 eV, in the correct range for Rh(0) metal, and the catalyst is nearly fully active.

4.1.3.2. [Rh(COD)H]$_4$

For the [Rh(COD)H]$_4$ complex (Table 4) the XPS signal is at 308.2 eV. For the [Rh(COD)H]$_4$-SiO$_2$ catalyst, the signal (308.3 eV) suggests the presence of Rh(I). After hydrogen pretreatments, however, the Rh signal indicates the presence of Rh(0):

[Rh(COD)H]$_4$–SiO$_2$/40°C (307.0 eV) and [Rh(COD)H]$_4$–SiO$_2$/200°C (307.0 eV). This result directly confirms the TEM results, in section 4.1.2.

4.1.3.3. [Rh(COD)$_2$]$^+$BF$_4^-$-Pd-SiO$_2$

The XPS spectra of [Rh(COD)$_2$]$^+$BF$_4^-$ on Pd-SiO$_2$ are similar to those on SiO$_2$ (Table 4). For the untreated [Rh(COD)$_2$]$^+$BF$_4^-$-Pd-SiO$_2$ catalyst, the Rh signals are virtually the same as those of the untreated [Rh(COD)$_2$]$^+$BF$_4^-$-SiO$_2$: Rh at 308.0 eV and Pd at 335.3 eV [37]. Hydrogen pretreatments had a discernable effect on the Rh signal but almost no effect on the Pd signal; compare [Rh(COD)$_2$]$^+$BF$_4^-$-Pd-SiO$_2$/40°C (Rh at 307.3 eV and Pd at 334.7 eV) and [Rh(COD)$_2$]$^+$BF$_4^-$-Pd-SiO$_2$/200°C (Rh at 306.9 eV and Pd at 334.9 eV). This indicates that, as for [Rh(COD)$_2$]$^+$BF$_4^-$-SiO$_2$, the complex is reduced to Rh(0) only after hydrogen pretreatment or reaction.

4.2. Mercury poisoning experiments

The ability of mercury to poison heterogeneous metal catalysts, but not homogeneous metal catalysts, is documented in the literature [38,39]. The observation that mercury completely quenches toluene hydrogenation (Table 2) supports the conclusion that metallic rhodium is the active catalyst. Similarly, 1-hexene hydrogenation activity (Table 3) is quenched by mercury. The observation that [Rh(COD)$_2$]$^+$BF$_4^-$ in solution and [Rh(COD)$_2$]$^+$BF$_4^-$-SiO$_2$ without pretreatment are inactive for 1-hexene hydrogenation, together with the XPS results (Table 4), demonstrates that the active catalyst for both 1-hexene and toluene hydrogenation is metallic rhodium.

4.3. 1-Hexene hydrogenation rates

It is interesting to compare the initial 1-hexene hydrogenation activity of the catalysts formed from [Rh(COD)$_2$]$^+$BF$_4^-$ on SiO$_2$ and on Pd-SiO$_2$. In particular, 40 °C and 200 °C

hydrogen-pretreated catalysts on the same support have similar 1-hexene hydrogenation

activities (Table 3). The rates for $[Rh(COD)_2]^+BF_4^--SiO_2/40°C$ (AR = 34.6 min^{-1}) and

$[Rh(COD)_2]^+BF_4^--SiO_2/200°C$ (AR = 34.0 min^{-1}) suggest the same numbers of rhodium sites

are present on both the 40 °C and 200 °C pretreated catalysts. Also, the overall rates for

$[Rh(COD)_2]^+BF_4^--Pd-SiO_2/40°C$ (AR = 160 min^{-1}) and $[Rh(COD)_2]^+BF_4^--Pd-SiO_2/200°C$

(AR = 161 min^{-1}) suggest approximately the same number of rhodium sites for these two

catalysts, assuming the palladium on both catalysts contributes the same amount to the

overall rate. Finally, the absence of 1-hexene hydrogenation activity with $[Rh(COD)_2]^+BF_4^--$

SiO_2 (AR = 0.0 min^{-1}) in contrast to the substantial activity of $[Rh(COD)_2]^+BF_4-Pd-SiO_2$ (AR

= 116 min^{-1}) [40] points to a facile reduction of the rhodium complex to metallic rhodium in

the presence of palladium and H_2, even at 0 °C.

4.4. General activity trends

Several general trends in toluene hydrogenation activity are the same for catalysts

prepared from all of the rhodium precursors ($[Rh(COD)H]_4$, $[Rh(COD)_2]^+BF_4^-$, and

$[Rh(COD)Cl]_2$). On silica, the adsorbed species (entries **2, 9, 16** in Table 1) start out no more

active than they are in solution (entries **1, 8, 15**), but over time the adsorbed catalysts either

come close or out-perform the solution species. The activities of the catalysts (entries **2, 9,**

16) are improved by hydrogen pretreatments prior to reaction. The activity increases with

the temperature of the hydrogen pretreatment, 200 °C (entries **4, 11, 18**) being better than 40

°C (entries **3, 10, 17**). For rhodium catalysts on Pd-SiO$_2$ (entries **5, 12, 19**), a different trend

is observed. The catalysts (entries **5, 12, 19**) are more active from the outset and show higher

activities than the same metal complex on SiO$_2$ (entries **2, 9, 16**). Furthermore, on Pd-SiO$_2$,

the higher temperature (200 °C) pretreatment reduces the activity of the catalyst (entries **7,**

14, 21). For these catalysts on Pd-SiO₂ (entries **5, 12, 19**), the untreated catalyst is the most

active of the series, and hydrogen pretreatments do not have a beneficial effect.

Although there are pronounced differences in toluene hydrogenation activity of the

rhodium complexes in solution ([Rh(COD)H]₄>>[Rh(COD)₂]⁺BF₄⁻>[Rh(COD)Cl]₂), their

activities are similar when adsorbed on SiO₂ and treated with H₂ at 200 °C (entries **4, 11, 18**).

In addition, all of the adsorbed rhodium complexes on Pd-SiO₂ have comparable activities

(entries **5, 12, 19**). Also, the catalysts pretreated at 200 °C on SiO₂ (entries **4, 11, 18**) and

those on Pd-SiO₂ (entries **5, 12, 19**) all have similar activities (AR~4 min⁻¹) regardless of the

rhodium precursor. The one exception is the unusually active [Rh(COD)Cl]₂-SiO₂/200°C

(**18**); perhaps the very low loading (Rh, 0.093% wt.) of rhodium in this case leads to much

greater rhodium dispersion and thus higher observed activity per total rhodium content.

Finally, it is instructive to consider the catalysts prepared by impregnation with

RhCl₃•H₂O (Table 1, entries **22-26**). The only catalyst prepared from RhCl₃•3H₂O with

good activity is the standard rhodium on silica, Rh-SiO₂ (entry **22**). Any catalyst that is

prepared from both RhCl₃•3H₂O and PdCl₂ has substantially lower activity no matter which

metal is introduced first or even if they are co-impregnated (entries **23-26**). One common

aspect of these catalysts and similar rhodium-palladium bimetallic examples in the literature

[7, 8] is that their preparations involve a high temperature (>200 °C) reduction step with

hydrogen. Also, the adsorbed catalysts ([Rh(COD)H]₄, [Rh(COD)₂]⁺BF₄⁻, and

[Rh(COD)Cl]₂) on Pd-SiO₂ (entries **5, 12, 19**) that are pretreated at 200°C with hydrogen

have relatively low activities (entries **7, 14, 21**).

4.5. Interpretation of hydrogenation activity

All methods of characterization (DRIFTS, TEM, XPS, and mercury poisoning experiments) suggest that the toluene hydrogenation activity of these rhodium-containing catalysts is due to the formation of rhodium metal. This metal formation could occur by reduction pathways similar to those proposed for the reduction of Rh nanoparticles on supports [23] or in solution [41]. The conclusion that the active catalyst is rhodium metal is supported by the observation that the activities of the bimetallic systems ([Rh(COD)H]$_4$, [Rh(COD)$_2$]$^+$BF$_4^-$, and [Rh(COD)Cl]$_2$ on Pd-SiO$_2$) are very similar to that of reduced rhodium on silica (Rh-SiO$_2$) in the absence of palladium (compare entries **5** and **4**; **12** and **11**; **19** and **18**). The similar activities of [Rh]-Pd-SiO$_2$ and [Rh]-SiO$_2$/200°C, where [Rh] is [Rh(COD)H]$_4$, [Rh(COD)$_2$]$^+$BF$_4^-$, and [Rh(COD)Cl]$_2$, suggest that both contain similar amounts of reduced rhodium species. The effect of the palladium in the [Rh]-Pd-SiO$_2$ systems is to facilitate the reduction of the Rh complex to active rhodium metal species. Perhaps, the palladium reduces the rhodium precursors to rhodium metal by providing highly active spillover hydrogen [6]. It is interesting to note that the process is very quick and effective, as no induction period is observed (less than 5 min), and it is equivalent to 4 h of hydrogen pretreatment at 200 °C. Furthermore, the resulting Rh-Pd-SiO$_2$ catalysts are more active than those of the same composition prepared by classical impregnation methods [7,8]. The scope, utility, and mechanism of the palladium-assisted reduction requires further investigation.

Toluene hydrogenation activities of the [Rh]-Pd-SiO$_2$ catalysts are reduced by high temperature (200 °C) pretreatment with hydrogen (entries **7, 14, 21**, as well as **23-26**). For example, the 200 °C pretreatment reduced the toluene hydrogenation activity of

[Rh(COD)$_2$]$^+$BF$_4^-$-Pd-SiO$_2$/40°C (AR = 3.50 min^{-1}) to [Rh(COD)$_2$]$^+$BF$_4^-$-Pd-SiO$_2$/200°C (AR = 0.76 min^{-1}). This treatment apparently changes the structure of the catalyst perhaps to a form similar to that of other bimetallic rhodium-palladium catalysts supported on silica or alumina, which are substantially less active for arene hydrogenation than just rhodium on the same supports [7,8]. This lower activity was attributed either to the formation of a rhodium-palladium alloy or to the formation of rhodium clusters that are smaller than the 10 Å size required for this activity. In contrast to the structure sensitivity of toluene hydrogenation, 1-hexene hydrogenation rates are the same for both [Rh(COD)$_2$]$^+$BF$_4^-$-Pd-SiO$_2$/40°C (AR = 160 min^{-1}) and [Rh(COD)$_2$]$^+$BF$_4^-$-Pd-SiO$_2$/200°C (AR = 161 min^{-1}). This observation is consistent with the structure-insensitive nature of supported rhodium-palladium catalysts reported for other alkene hydrogenation reactions [8].

5. Conclusions

In conclusion, the adsorption of homogeneous rhodium complexes ([Rh(COD)H]$_4$, [Rh(COD)$_2$]$^+$BF$_4^-$, and [Rh(COD)Cl]$_2$) onto silica produces catalysts that are more active than those (Rh-SiO$_2$) produced by the standard incipient wetness method utilizing RhCl$_3$•H$_2$O. The most active of these, those pretreated with hydrogen at 200 °C or adsorbed onto Pd-SiO$_2$, are nearly twice as active as Rh-SiO$_2$. In addition, the use of Pd-SiO$_2$ as a support for rhodium complexes gives catalysts that have no induction period. Such induction periods in the [Rh]-SiO$_2$ catalyst can also be eliminated by pretreatment of the catalysts at 200 °C under H$_2$. The only real difference in catalytic behavior among the three rhodium precursors is their rate of reduction to rhodium metal: [Rh(COD)H]$_4$ >[Rh(COD)$_2$]$^+$BF$_4^-$ >[Rh(COD)Cl]$_2$. Finally, it is shown for [Rh]-SiO$_2$ catalysts that Rh(0) is the active catalytic species for toluene and 1-hexene hydrogenation. For [Rh]-Pd-SiO$_2$, Rh(0) is the active

toluene hydrogenation catalyst, while both palladium and rhodium metal are responsible for

1-hexene hydrogenation activity. The [Rh]-Pd-SiO$_2$ catalysts that were not pretreated with

hydrogen exhibit toluene hydrogenation activities that are greater than other Rh-Pd bimetallic

catalysts in the literature [7,8].

References

[1] H. Gao, R.J. Angelici, J. Mol. Catal. A: Chem. 149 (1999) 63.

[2] H. Gao, R.J. Angelici, J. Am. Chem. Soc. 119 (1997) 6937.

[3] H. Gao, R.J. Angelici, Organometallics 18 (1999) 989.

[4] H. Gao, R.J. Angelici, New J. Chem. 23 (1999) 633.

[5] H. Yang, H. Gao, R.J. Angelici, Organometallics 19 (2000) 622.

[6] W.C. Conner Jr., J.L. Falconer, Chem. Rev. 95 (1995) 759.

[7] G. del Angel, B. Coq, F. Figueras, J. Catal. 95 (1985) 167.

[8] P.E. Araya, E.E. Miro, L. Cornaglia, J. Chem. Research (S) (1997) 258.

[9] G.A. del Angel, B. Coq, G. Ferrat, F. Figueras, Surface Science 156 (1985) 943.

[10] W.F. Graydon, M.D. Langan, J. Catal. 69 (1981) 180.

[11] T. Ioannide, X.E. Verykios, J. Catal. 143 (1993) 175.

[12] F. Fajardie, J-F. Tempere, G. Djega-Mariadassou, G. Blanchard, J. Catal. 163 (1996) 77.

[13] G. Giordano, R.H. Crabtree, Inorg. Synth. 19 (1979) 218.

[14] R.R. Schrock, J.A. Osborn, J. Am. Chem. Soc. 93 (1971) 3089.

[15] M. Kulzick, R.T. Price, E.L. Muetterties, V.W. Day, Organometallics 1 (1982) 1256.

[16] Z. Duan, M.J. Hampden-Smith, A.P. Sylwester, Chem. Mater. 4 (1992) 1146.

[17] T. Ioannides, X. Veeykios, J. Catal. 140 (1993) 353.

[18] a) R. Abu-Reziq, D. Avnir, I. Miloslavski, H. Schumann, J. Blum, J. Mol. Catal. A:

Chem. 185 (2002) 179.

b) R. Abu-Reziq, D. Avnir, J. Blum, J. Mol. Catal. A: Chem. 187 (2002) 277.

[19] B. Pugin, M. Müller, in M. Guisnet et. al. (Ed.), Stud. Surf. Sci. Cat. Part 78:

Heterogeneous Catalysis and Fine Chemicals III, Elsevier (1993) 107.

[20] K.J. Stanger, J.W. Wiench, M. Pruski, R.J. Angelici, J. Mol. Catal. A: Chem. in press.

[21] C.S. Chin, B. Lee, J. Moon, J. Song, Y. Park, Bull. Korean Chem. Soc. 16 (1995) 528.

[22] A.B. Pangborn, M.A. Giardello, R.H. Grubbs, R.K. Rosen, F. J. Timmers,

Oganometallics 15 (1996) 1518.

[23] M. Che, C.O. Bennett, Advances in Catalysis, 36 (1989) 55. Atomic Rates (AR) are

discussed on p. 72, reduction to metal particles on supports on p. 71.

[24] To facilitate comparison, the rates for Pd-SiO$_2$ catalysts are reported in terms of an

effective AR, AR$_{eff}$. Since these catalysts do not contain rhodium, a AR based on rhodium

content cannot be given. The AR$_{eff}$ value is calculated by assuming that the Pd-SiO$_2$ catalyst

contains the standard rhodium loading (9.8 μmol).

[25] J. Haeglund, A.F. Guillermet, G. Grimvall, M. Kaerling, Phys. Rev. B. 48 (1993) 11685.

[26] C.R. Guerra, J.H. Schulman, Surface Science 7 (1967) 229.

[27] S.D. Worley, C.A. Rice, G.A. Mattson, C.W. Curtis, J.A. Guin, A.R. Tarrer, J. Phys.

Chem. 86 (1982) 2714.

[28] C.A. Rice, S.D. Worley, C.W. Curtis, A.J. Guin, A.R. Tarrer, J. Chem. Phys. 74 (1981) 6487.

[29] T.T.T. Wong, A.Y. Stakheev, W.M.H. Sachtler, J. Chem. Phys. 96 (1992) 7733.

[30] P. Basu, D. Panayotov, J.T. Yates, Jr., J. Chem. Phys. 91 (1987) 3133.

[31] J.L. Robbins, J. Phys. Chem. 90 (1986) 3381.

[32] H.F. J. van't Bilk, J.B.A.D. van Zon, T. Huizinga, J.C. Vis, D.C. Koningsberger, J. Am. Chem. Soc. 107 (1985) 3139.

[33] M.P. Keyes, K.L. Watters, J. Catal. 110 (1988) 96.

[34] R. Pasaro, R.R. Ugo, C. Dossi, A. Fusi, J. Mol. Cat. 74 (1992) 391.

[35] D. Roberto, R. Pasaro, R. Ugo, Organometallics 12 (1993) 2292.

[36] J.F. Moulder, W.F. Stickle, P.E. Sobol, K.D. Bomben, Handbook of X-ray Photoelectron Spectroscopy, J. Chastain (Ed.), Perkin-Elmer Corporation Physical Electronics Division, 1992.

[37] Additional $[Rh(COD)_2]^+BF_4^-$-Pd-SiO_2 catalysts were examined with different Rh:Pd loadings. For Rh:Pd (wt. % : wt. %) ratios of 2:10, 2:5, 2:2.5, and 2:1, the XPS spectra were all the same, consistent with Rh(I) (~308 eV) and Pd(0) (~335 eV) [36].

[38] K.S. Weddle, J.D. Aiken III, R.G. Finke, J. Am. Chem. Soc. 120 (1998) 5653, and references therein.

[39] G. Webb, J.I. Macnab, J. Catal. 26 (1972) 226.

[40] Note that the activity of $[Rh(COD)_2]^+BF_4^-$-Pd-SiO_2 is not due solely to the Pd in the system as the observed AR (116 min^{-1}) is well above that for Pd-SiO_2 alone ($AR_{eff} = 65.2$ min^{-1} [24]).

[41] R.G. Finke, in D.L. Feldheim, C.A. Foss Jr. (Eds.), Metal Nanoparticles: Synthesis, Characterization, and Applications, Marcel Dekker, Inc., New York, 2001, pages 17-54 and references therein.

Table 1. Rates of toluene hydrogenation to methylcyclohexane[a]

Entry	Catalyst	AR[b] 1 h	AR[b] 6 h	AR[b] (X h)
1	[Rh(COD)H]$_4$[c]	1.83	1.43	
2	[Rh(COD)H]$_4$-SiO$_2$	1.59	2.26	
3	[Rh(COD)H]$_4$-SiO$_2$/40°C	3.33	2.64	
4	[Rh(COD)H]$_4$-SiO$_2$/200°C	5.13	4.17	
5	[Rh(COD)H]$_4$-Pd-SiO$_2$	4.80	4.10	
6	[Rh(COD)H]$_4$-Pd-SiO$_2$/40°C	3.77	3.03	
7	[Rh(COD)H]$_4$-Pd-SiO$_2$/200°C	1.07	0.85	
8	[Rh(COD)$_2$]$^+$BF$_4$$^-$[c]	0.02	0.02	0.03(24)
9	[Rh(COD)$_2$]$^+$BF$_4$$^-$-SiO$_2$	0.02	0.47	0.67(100)
10	[Rh(COD)$_2$]$^+$BF$_4$$^-$-SiO$_2$/40°C	1.58	0.99	0.67(10)
11	[Rh(COD)$_2$]]$^+$BF$_4$$^-$-SiO$_2$/200°C	4.10	3.05	
12	[Rh(COD)$_2$]$^+$BF$_4$$^-$-Pd-SiO$_2$	3.83	3.07	
13	[Rh(COD)$_2$]$^+$BF$_4$$^-$-Pd-SiO$_2$/40°C	3.50	3.11	
14	[Rh(COD)$_2$]$^+$BF$_4$$^-$-Pd-SiO$_2$/200°C	0.76	0.69	
15	[Rh(COD)Cl]$_2$[c]	0.00	0.01	
16	[Rh(COD)Cl]$_2$-SiO$_2$	0	0	0.01(72)
17	[Rh(COD)Cl]$_2$-SiO$_2$/40°C	0.72	0.75	
18	[Rh(COD)Cl]$_2$-SiO$_2$/200°C	7.00	5.67	
19	[Rh(COD)Cl]$_2$-Pd-SiO$_2$	3.87	3.60	
20	[Rh(COD)Cl]$_2$-Pd-SiO$_2$/40°C	5.13	3.93	4.00(24)
21	[Rh(COD)Cl]$_2$-Pd-SiO$_2$/200°C	0.00	0.60	
22	Rh-SiO$_2$	2.52	2.32	
23	Rh-(Pd-SiO$_2$)	0.31	0.31	
24	Rh/Pd-SiO$_2$	0.52	0.50	0.44(24)
25	Rh/Pd(O$_2$)-SiO$_2$	0.03	0.03	0.02(24)
26	Pd-(Rh-SiO$_2$)	0.43	0.37	

[a] Reaction conditions: 50 mg (~9.8 μmol Rh)of solid catalyst, 5 ml of toluene, 40.0 °C, 1 atm of H$_2$ (Eq. (1)).

[b] AR: Atomic rate is defined as moles of methylcyclohexane produced per total moles of rhodium per min (Eq. (2)).

[c] 9.2 μmol of homogeneous catalyst.

Table 2. Rates[a] of toluene hydrogenation in the presence of mercury[b]

Catalyst	AR 1 h	with Hg[c]
$[Rh(COD)_2]^+BF_4^-$-SiO$_2$/40°C	1.58	0
$[Rh(COD)_2]^+BF_4^-$-SiO$_2$/200°C	4.10	0
$[Rh(COD)_2]^+BF_4^-$-Pd-SiO$_2$	3.83	0
$[Rh(COD)H]_4$-SiO$_2$/200°C	5.13	0
$[Rh(COD)H]_4$-Pd-SiO$_2$	4.80	0
Rh-SiO$_2$	2.52	0

[a] Rates given as AR [mol CyMe/(mol Rh • min)] based on total Rh content.

[b] Reaction conditions: 40.0 °C, 1 atm H$_2$, 5.0 ml toluene, and 25 mg (~4.9 μmol Rh) of supported catalyst.

[c] Rate after addition of 0.2 ml (14 mmol) Hg.

Table 3. Rates[a] of 1-hexene hydrogenation[b]

Catalyst	AR[c]	Hg[d] 2 h[e]	Hg[d] 17 h[f]
[Rh(COD)$_2$]$^+$BF$_4^-$[g]	0.0	0.0	--
[Rh(COD)$_2$]$^+$BF$_4^-$-SiO$_2$[h]	0.0	0.0	--
[Rh(COD)$_2$]$^+$BF$_4^-$-SiO$_2$/40°C[h]	34.6	14.5	0.0
[Rh(COD)$_2$]$^+$BF$_4^-$-SiO$_2$/200°C[h]	34.0	2.70	0.0
[Rh(COD)$_2$]$^+$BF$_4^-$-Pd-SiO$_2$[h]	116	14.6	0.0
[Rh(COD)$_2$]$^+$BF$_4^-$-Pd-SiO$_2$/40°C[h]	160	20.6	0.0
[Rh(COD)$_2$]$^+$BF$_4^-$-Pd-SiO$_2$/200°C[h]	161	27.3	0.0
Pd-SiO$_2$[i]	65.2	1.62	0.0

[a] Rates given as AR [mol hexane/(mol Rh • min)] based on total Rh content.
[b] Reaction conditions: 0.0 °C, 1 atm H$_2$, 5.0 ml 1-hexene.
[c] AR measured over the first 5 min of reaction.
[d] 0.2 ml (14 mmol) of Hg added.
[e] Rate 2 h after Hg addition.
[f] Rate 17 h after Hg addition.
[g] 4.0 mg (9.9 μmol Rh) of homogeneous complex in 4.0 ml 1-hexene and 1.0 ml of CH$_2$Cl$_2$.
[h] 25 mg (~4.9 μmol Rh) of supported catalyst.
[i] 25 mg of 10% Pd-SiO$_2$, rate given as AR$_{eff}$, see footnote [24].

Table 4. XPS[a] analysis of catalysts

Catalyst	Use[b]	Rh $3d_{5/2}$	Pd $3d_{5/2}$
[Rh(COD)$_2$]$^+$BF$_4^-$	New	308.6	--
[Rh(COD)$_2$]$^+$BF$_4^-$-SiO$_2$	New	308.4	--
[Rh(COD)$_2$]$^+$BF$_4^-$-SiO$_2$/40°C	New	307.4	--
[Rh(COD)$_2$]$^+$BF$_4^-$-SiO$_2$/200°C	New	307.1	--
[Rh(COD)$_2$]$^+$BF$_4^-$-SiO$_2$	0.5 h	307.9	--
[Rh(COD)$_2$]$^+$BF$_4^-$-SiO$_2$	2.0 h	308.3	--
[Rh(COD)$_2$]$^+$BF$_4^-$-SiO$_2$	7.5 h	307.0	--
[Rh(COD)H]$_4$	New	308.2	--
[Rh(COD)H]$_4$-SiO$_2$	New	308.3	--
[Rh(COD)H]$_4$-SiO$_2$/40°C	New	307.0	--
[Rh(COD)H]$_4$-SiO$_2$/200°C	New	307.0	--
[Rh(COD)$_2$]$^+$BF$_4^-$-Pd-SiO$_2$[c]	New	308.0	335.3
[Rh(COD)$_2$]$^+$BF$_4^-$-Pd-SiO$_2$/40°C	New	307.3	334.7
[Rh(COD)$_2$]$^+$BF$_4^-$-Pd-SiO$_2$/200°C	New	306.9	334.9
Rh-SiO$_2$	New	307.2	--
Pd-SiO$_2$	New	--	334.7

[a] For experimental details see section 2.6. Signals are given in eV.

[b] "New" denotes freshly prepared catalysts examined by XPS prior to toluene hydrogenation. Listed times indicate the reaction times that the catalysts were used for toluene hydrogenation under standard reaction conditions (40.0 °C, 1 atm H$_2$) prior to XPS analysis.

[c] See footnote [37].

Figure Captions

Fig. 1. Conceptual illustration of a TCSM catalyst consisting of a tethered homogeneous complex on a supported metal heterogeneous catalyst.

Fig. 2. Hydrogenation apparatus.

Fig. 3. DRIFT spectra of CO-exposed catalysts: a) Rh-SiO$_2$, b) [Rh(COD)$_2$]$^+$BF$_4^-$-SiO$_2$, c) [Rh(COD)$_2$]$^+$BF$_4^-$-SiO$_2$/40°C, d) [Rh(COD)$_2$]$^+$BF$_4^-$-SiO$_2$/200°C, e) [Rh(COD)$_2$]$^+$BF$_4^-$-Pd-SiO$_2$, f) [Rh(COD)$_2$]$^+$BF$_4^-$-Pd-SiO$_2$/40°C, g) [Rh(COD)$_2$]$^+$BF$_4^-$-Pd-SiO$_2$/200°C.

Fig. 4. TEM micrographs of [Rh(COD)H]$_4$-SiO$_2$/40°C (a) and [Rh(COD)H]$_4$-SiO$_2$/200°C (b).

Fig. 5. Size distributions of rhodium crystallites determined by TEM and imaging analyses of [Rh(COD)H]$_4$-SiO$_2$/40°C (a) and [Rh(COD)H]$_4$-SiO$_2$/200°C (b). Note the change in length(nm) scale for particle sizes larger than 20nm.

Fig. 6. Electron diffraction patterns of polycrystalline [Rh(COD)H]$_4$-SiO$_2$/40°C (a) and single crystallite [Rh(COD)H]$_4$-SiO$_2$/200°C (b) samples.

Fig. 7. Reported CO-containing species on Rh-SiO$_2$.

Fig. 1. Conceptual illustration of a TCSM catalyst consisting of a tethered homogeneous complex on a supported metal heterogeneous catalyst.

Fig. 2. Hydrogenation apparatus.

Fig. 3. DRIFT spectra of CO-exposed catalysts: a) Rh-SiO$_2$, b) [Rh(COD)$_2$] $^+$BF$_4^-$-SiO$_2$,
c) [Rh(COD)$_2$] $^+$BF$_4^-$-SiO$_2$/40°C, d) [Rh(COD)$_2$] $^+$BF$_4^-$-SiO$_2$/200°C, e) [Rh(COD)$_2$] $^+$BF$_4^-$-
Pd-SiO$_2$, f) [Rh(COD)$_2$] $^+$BF$_4^-$-Pd-SiO$_2$/40°C, g) [Rh(COD)$_2$] $^+$BF$_4^-$-Pd-SiO$_2$/200°C.

Fig. 4. TEM micrographs of [Rh(COD)H]$_4$-SiO$_2$/40°C (a) and [Rh(COD)H]$_4$-SiO$_2$/200°C (b).

Fig. 5. Size distributions of rhodium crystallites determined by TEM and imaging analyses of [Rh(COD)H]$_4$-SiO$_2$/40°C (a) and [Rh(COD)H]$_4$-SiO$_2$/200°C (b). Note the change in length(nm) scale for particle sizes larger than 20nm.

Fig. 6. Electron diffraction patterns of polycrystalline [Rh(COD)H]$_4$-SiO$_2$/40°C (a) and single crystallite [Rh(COD)H]$_4$-SiO$_2$/200°C (b) samples.

v(CO):   2096 and 2038 cm^{-1} 2040 to 2066 cm^{-1}

Fig. 7. Reported CO-containing species on Rh-SiO$_2$.

Hydrodefluorination of Fluorobenzene Catalyzed by Rhodium Metal Prepared from [Rh(COD)$_2$]$^+$BF$_4^-$ and Supported on SiO$_2$ and Pd-SiO$_2$

Keith J. Stanger and Robert J. Angelici*

Abstract

The effects of solvent, pH, temperature, and hydrogen pressure were determined for the reaction of fluorobenzene with hydrogen gas catalyzed by supported rhodium metal on silica. Non-polar and aprotic solvents, heptane and 1,2-dichloroethane, favor hydrogenation to fluorocyclohexane. Polar and protic solvents, heptane/methanol and heptane/water, favor hydrodefluorination to benzene and subsequent hydrogenation to cyclohexane. The hydrodefluorination and hydrogenation of fluorobenzene to cyclohexane via benzene was found to proceed best in heptane/water under acidic conditions. For the hydrodefluorination of fluorobenzene in heptane/water, the hydrodefluorination product, benzene, inhibited further hydrodefluorination of fluorobenzene. In DCE or heptane, a side reaction between fluorocyclohexane and hydrogen fluoride, not catalyzed by rhodium, was discovered that provides an alternate pathway to cyclohexane. Reaction conditions can be modified to yield primarily fluorocyclohexane, benzene, or cyclohexane.

1. Introduction

Carbon-fluorine bonds are the strongest that carbon can form [1]. There are several examples of stoichiometric cleavage of C-F bonds by organometallic complexes, but few complexes have been reported that are capable of catalytic transformations of C-F bonds [2-11]. Even fewer systems are capable of catalytic hydrodefluorination to remove fluorine

from non-activated monofluoroarenes [12-23]. Palladium on carbon (Pd/C), in the presence

of NaOH at 82 °C, hydrodefluorinates fluorobenzene (PhF) to benzene (PhH) by hydrogen-

transfer from isopropanol [14,15], but palladium was unable to catalyze the same reaction by

hydrogen-transfer from HCOOK in ethanol/water (1:3) or under 4 atm of H_2 at 37 °C in

methanol [15]. The first example of hydrodefluorination of a monofluoroarene by hydrogen

gas over a heterogeneous metal was reported in 1920 by Swarts [16], who used Pt(black) in

water to hydrodefluorinate PhF to cyclohexane (CyH) and p-fluorobenzoic acid to

cyclohexanecarboxylic acid. Renoll utilized Swarts' conditions to hydrodefluorinate 2-

fluoro-4'-acetylbiphenyl to p-cyclohexylethylbenzene [17]. Pattison and Saunders reported

the hydrodefluorination of p-fluorophenylacetic acid to ethyl cyclohexylphenylacetate with

Raney Ni at 180-200 °C under 160-180 atm H_2 in ethanol [18]. Tashiro et.al. used Raney Ni-

Al and Raney Cu-Al alloys for the hydrodefluorination of p-fluoroacetophenone to 1-

phenylethanol at 50 °C in 10% NaOH(aq) [19]. The first reported use of rhodium metal for

the hydrodefluorination of a monofluoroarene was by Freedman et. al. [20] who converted

fluoroarylphosphonic acids to cyclohexylphosphonic acids under 4 atm of H_2 at room

temperature in 95% ethanol. Young and Grushin used [$(Cy_3P)_2Rh(H)Cl_2$] to catalytically

hydrodefluorinate 1-fluoronapthalene to naphthalene under 80 psi hydrogen at 95 °C in the

presence of 40% NaOH [D21]. However, [$(Cy_3P)_2Rh(H)Cl_2$] was incapable of

hydrodefluorinating PhF, 4-fluorotoluene, 3- or 4-fluoroanisole, or 4-fluoroaniline. Under

identical conditions, metallic rhodium nanoparticles [21] catalyzed the hydrodefluorination

of the C-F bond in 1-fluoronapthalene, PhF, 4-fluorotoluene, 3- or 4-fluoroanisole, and 4-

fluoroaniline while catalyzing only trace amounts of hydrogenation of the resulting arenes.

Blum et. al. reports that sol-gel encapsulated $RhCl_3$-Aliquat 336 catalyzes the

hydrodefluorination and hydrogenation of fluorobenzene (PhF), 2- or 4-fluorotoluene, and 2-, 3-, or 4-fluoroanisole in 1,2-dichloroethane (DCE) at 80 °C under 16 atm of hydrogen to the corresponding dehalogenated, substituted cyclohexanes [22]. Our initial hydrodefluorination studies showed that rhodium pyridylphosphine and bipyridyl complexes tethered to Pd-SiO$_2$ under 4 atm of hydrogen at 70 °C efficiently converted PhF to a mixture of CyH and CyF [23]. The relative amounts of these products were influenced by the solvent. In heptane, fluorocyclohexane (CyF) was the major product, but in heptane/ethanol, with added base (NaOAc being the best), benzene (PhH) was formed initially but was subsequently hydrogenated to cyclohexane (CyH).

Our examination of supported bimetallic rhodium and palladium catalysts for arene hydrogenation [24] prompted us to explore their hydrodefluorination capabilities. These catalysts were prepared by adsorbing, various rhodium complexes including [Rh(COD)$_2$]$^+$BF$_4^-$ on SiO$_2$ or Pd-SiO$_2$ (10% Pd wt/wt) to give a ~ 2% Rh (wt/wt) loading. These materials were used as obtained or pretreated with H$_2$ for 24 h at 40 °C or for 4 h at 200 °C. The actual catalysts consisted of highly active rhodium(0) metal supported on SiO$_2$ formed by the reduction of the rhodium complex precursor by the hydrogen pretreatment or during the hydrogenation reaction (1 atm H$_2$ at 40 °C). Palladium, in the [Rh]-Pd-SiO$_2$ systems, served to facilitate the reduction of the Rh complex to active rhodium metal species *in situ*. On SiO$_2$ without Pd, activities were improved by hydrogen pretreatments prior to reaction, but on Pd-SiO$_2$, the rhodium catalysts were less active when pretreated by hydrogen.

In the present paper, we describe the use of the Rh-SiO$_2$ catalysts in the hydrogenation of PhF to CyF, PhH, and/or CyH as shown in Scheme 1. The effects of

solvent, pH, added base, temperature, and hydrogen pressure on product selectivity and reaction rates were determined. The relative amounts of the products can be controlled by choosing the proper conditions. The catalytic reactions described in this paper, when used with the proper solvent and pH, catalyze the hydrodefluorination of PhF under the mildest reported conditions (1 atm H_2 at 40 °C) while still providing rates that are faster than those of other hydrodefluorination systems.

2. Experimental

2.1. General considerations

Ethanol, 1,2-dichloroethane (DCE), NaH_2PO_4, Na_2HPO_4, Na_3PO_4, 85% phosphoric acid, sodium acetate (NaOAc), glacial acetic acid, heptane, fluorobenzene (PhF), fluorocyclohexane (CyF), and benzene (PhH) were purchased from commercial sources and used as received. Methanol was distilled from Mg/I_2 under nitrogen [25]. The catalysts $[Rh(COD)_2]^+BF_4^--SiO_2/200°C$ (Rh-SiO$_2$(A)), $[Rh(COD)_2]^+BF_4^--SiO_2/40°C$, Rh-SiO$_2$, $[Rh(COD)_2]^+BF_4^--Pd-SiO_2$, $[Rh(COD)_2]^+BF_4^--Pd-SiO_2/40°C$, $[Rh(COD)_2]^+BF_4^--Pd-SiO_2/200°C$, and Pd-SiO$_2$ were prepared and characterized as described previously [24,26]. Briefly, the catalysts were prepared by adsorbing $[Rh(COD)_2]^+BF_4^-$ on SiO$_2$ or Pd-SiO$_2$ (10% Pd wt/wt) to give a ~ 2% Rh (wt/wt) loading. These materials were used as obtained or pretreated with H_2 for 24 h at 40 °C or for 4 h at 200 °C. The resulting catalysts consist of highly active rhodium(0) metal on supported SiO$_2$. Gas chromatographic (GC) analyses were performed on a Hewlett Packard HP 6890 GC using a J&W 30 m alumina capillary column and an FID (flame ionization detector).

2.2. Preparation of buffer solutions

The 1.0 M buffers were prepared [27] by dissolving 0.10 mmol of acid in 80 ml of water and then adding NaOH until the pH, monitored by a pH meter, had reached the desired value. This solution was rinsed into a 100 ml volumetric flask and diluted to volume. Other concentration buffers were obtained by this same procedure modifying the amount of acid added as appropriate. Acetate buffers were prepared for pH = 4.8 solutions, and phosphate buffers were prepared for pH = 11.2, 7.1, and 2.2 solutions.

2.3. Hydrodefluorination reactions

The general experimental procedures for both atmospheric pressure and high pressure reactions are outlined below. A number of different solvent systems, pressures, and temperatures were examined. The specifics of the reaction conditions will be discussed in detail as required in the discussion of the results.

2.3.1. Hydrodefluorination reactions at 1 atmosphere pressure

A standard hydrogenation run consisted of placing 50.0 mg of catalyst (containing ~9.7 μmol of Rh) and base into the reaction vessel (described previously [24,28-31]) and replacing the atmosphere with Ar using three vacuum/flush cycles. Next, the jacket of the vessel was attached to a constant temperature bath and the temperature was raised to reaction temperature, 40.0 (±0.2) °C. While the temperature was being achieved, a hydrogen gas reservoir was filled by a series of three consecutive vacuum and hydrogen gas flush cycles so that the system could be held at 1 atm H_2 throughout the reaction. After the temperature had stabilized at 40.0 °C and the gas burette was full of hydrogen, the reaction vessel itself was evacuated and filled with hydrogen three times. Next, solvent (5.0 ml) was added via syringe; when the solvent mixture was heptane (3.0 ml) and water (2.0 ml), the heptane layer

was on top. After the system had achieved the reaction temperature, fluorobenzene 0.10 ml

(1.1 mmol) was added via syringe. The reaction was opened to the hydrogen gas reservoir,

stirring was initiated, and hydrogen uptake was recorded. The reaction was monitored by

periodic GC analyses of samples of the organic layer removed with a syringe.

2.3.2. Higher pressure hydrodefluorination reactions (15-58 psi of hydrogen)

The reagents, 30.0 mg (containing ~5.8 μmol of Rh) of catalyst, 0.36 g (4.4 mmol) of

NaOAc, and 0.40 ml (4.3 mmol) of PhF, were added to a Fischer-Porter high-pressure tube

containing a Teflon-coated stir bar. After the solvent (5.0 ml) was added, the atmosphere

was replaced with hydrogen using three freeze-pump-thaw cycles. After purging the

atmosphere with hydrogen, the hydrogen pressure was raised while being monitored by the

regulator on the hydrogen gas cylinder. Upon reaching the desired reaction pressure, the

system was closed and immersed in an oil bath at 70 (±1) °C. After the reaction was stirred

for 30 min, the tube was removed from the oil bath, cooled to room temperature in water, and

vented to the atmosphere. After the layers were separated, the organic layer was dried over

sodium sulfate and filtered prior to GC analysis. GC analysis showed that PhF and products

were present in the upper organic layer and drying with sodium sulfate had no effect on their

concentrations. No corrections were made for pressure changes due to heating or reaction

progress.

3. Results

3.1. Effects of solvent on the reaction of PhF with H_2

3.1.1. Heptane

In heptane solution, the reaction of fluorobenzene (PhF) with 1 atm H_2 at 40 °C

catalyzed by Rh-SiO$_2$(A) produces a mixture of fluorocyclohexane (CyF) and cyclohexane

(CyH) (entry 1, Table 1). The ratio of CyF to CyH is constant throughout the course of the reaction (Fig. 1) indicating concurrent competing reaction pathways (paths a and bc, in Scheme 1). The reaction is essentially complete within 30 minutes. Fluorocyclohexane is not converted to CyH during the catalytic reaction as the ratio (3.3:1.0 for CyF:CyH) of these products remains constant at longer reaction times (Fig. 1). The ratio of CyF:CyH produced by the reaction is temperature-dependent and the following ratios were observed for the following temperatures: 5.0:1.0 (20 °C), 3.3:1.0 (40 °C), and 9.9:1.0 (70 °C).

3.1.2. 1,2-Dichloroethane (DCE)

In the more polar, aprotic solvent DCE, the reaction of PhF with 1 atm H_2 at 40 °C catalyzed by Rh-SiO$_2$(A) also produces a mixture of CyF and CyH (entry 2, Table 1). However, the reaction is much slower (95% complete after 5880 min) than in heptane, and the CyF:CyH ratio decreases from 6.6:1 in the initial stages, during the first 150 min, to a final ratio of 1.7:1 (Fig. 1). At 70 °C with 4 times the normal amount of catalyst (200 mg), the ratio of CyF:CyH was 2.3:1 and did not significantly change until after the reaction was over 95% complete (270 min). After the reaction of PhF to CyF and CyH, a much slower reaction (~3% per hour) was observed that converted CyF to CyH. The changing ratios of CyF:CyH suggests that CyF is converted to CyH during the catalytic reaction. Further experiments (Section 3.6) show that the conversion of CyF to CyH in DCE is not catalyzed by rhodium, silica, or hydrogen gas but is due to a reaction between CyF and HF, produced during the hydrodefluorination reaction.

3.1.3. Heptane/methanol

In the polar, protic heptane/methanol (3 ml/2 ml) solvent system, where two phases are present, no CyF is produced (entry 3, Table 1), and CyH is the only final product

observed (after 600 min) in the reaction (Fig. 1) of PhF with 1 atm H_2 at 40 °C catalyzed by

Rh-SiO$_2$(A). However, under these conditions the intermediate benzene (PhH) is detected in

small amounts (<2%) before it is hydrogenated to CyH (path b and c, Scheme 1).

3.1.4. Heptane/water

The more polar, protic heptane/water (3 ml/2 ml) solvent system produces only CyH

as the final product (entry 4, Table 1) in the reaction of PhF with 1 atm H_2 at 40 °C catalyzed

by Rh-SiO$_2$(A). As in heptane/methanol, PhH (path b and c, Scheme 1) is observed (~10%)

as an intermediate during the course of the reaction (Fig. 1). The reaction is faster in

heptane/water, where it is essentially complete in 180 min, compared to heptane/methanol,

where 600 min are required.

3.2. Effects of base and pH on the hydrodefluorination of PhF

3.2.1. Heptane/methanol

A number of different bases were used in the heptane/methanol solvent system for the

reaction of PhF with 1 atm H_2 at 40 °C catalyzed by Rh-SiO$_2$(A) (Fig. 2). The rate of PhF

hydrodefluorination (path bc, Scheme 1) decreased as the strength of the base increased:

none>NaOAc>>NaOH>>NaOMe. For heptane/methanol without a base, the reaction is

complete after 600 min and only small amounts (<2%) of the intermediate PhH are detected

as it is hydrogenated to CyH (path b and c, Scheme 1; Fig. 2). The reaction takes almost

twice as long (1130 min) in the presence of NaOAc, and the intermediate PhH reaches a

concentration of 36.4% during the course of the reaction (Fig. 2). With added NaOH, the

first 310 min produce PhH (37%) with only trace hydrogenation to CyH (2%). After this

point, conversion of PhF to PhH and PhH to CyH slows considerably and only 13%

conversion of PhF occurs over the next 1100 min to provide PhH (47%) and CyH (5%).

NaOMe deactivated the catalyst as only trace amounts of PhH (5%) and CyH (3%) were produced, even after 1500 min of reaction (Fig. 2).

3.2.2. Heptane/water

The rate of the Rh-SiO$_2$(A) catalyzed reaction of PhF with 1 atm H$_2$ at 40 °C in buffered solutions depends on the pH of the aqueous phase (Table 2 and Fig. 3). In general, slightly faster initial defluorination rates (path b, Scheme 1) were obtained in more basic media (Table 2). However, initial rates do not comprehensively describe the overall course of the reaction. In contrast to defluorination, the hydrogenation of benzene (PhH) (path c, Scheme 1) is slower under more basic conditions (Table 2). The pH dependence of PhH hydrogenation accounts for the greater build-up of the PhH intermediate in the hydrodefluorination of PhF at higher pH (Fig. 3). The rate of benzene hydrogenation also affects the rate of hydrodefluorination of PhF, as the increase in PhH concentration decreases the rate of PhF reaction. This was shown in reactions of PhF in the presence of added PhH using the heptane/water (3 ml/2 ml) system buffered at pH = 2.2 under 1 atm H$_2$ at 40 °C catalyzed by Rh-SiO$_2$(A) (Table 3). As the concentration of PhH was increased, the rate of hydrodefluorination of PhF decreased. Thus, it appears that, because of inhibition by PhH, hydrodefluorination of PhF proceeds faster at lower pH's where PhH concentrations are low because of the rapid hydrogenation of PhH to CyH.

A series of hydrodefluorination reactions of PhF with 1 atm H$_2$ at 40 °C catalyzed by Rh-SiO$_2$(A) in heptane (3 ml) over aqueous buffered solutions of NaOAc/HOAc (2 ml, pH = 4.8) showed that the buffer concentration (1.0, 2.0, and 4.0 M) caused almost no variation in reaction rates or concentration of PhH intermediate (see Fig. 3, pH = 4.8 for a typical

reaction profile). This indicates that the rate is independent of the acetate base concentration, but depends on the pH of the solution (Table 2, Fig. 3).

3.3. Reuse of Rh-SiO₂(A) in the hydrodefluorination of PhF

The catalyst, Rh-SiO$_2$(A), after use in the heptane/water reactions can be filtered in air, washed with water (5x10 ml/50 mg SiO$_2$), and re-used with no apparent loss of activity (not shown). This has been repeated two more times. Alternatively, the catalyst can be reused by removal of solvent and substrate under vacuum followed by addition of fresh solvent and substrate without washing the catalyst. When this method of reuse was applied to the Rh-SiO$_2$(A)-catalyzed hydrodefluorination of PhF to CyH in heptane/water under 1 atm H$_2$ at 40 °C, three successive hydrodefluorinations were performed with no apparent catalyst deactivation. The unbuffered hydrodefluorination reactions in this example were more rapid (180 min to 95% completion) than the buffered reaction at pH = 2.2 (280 min to 95% completion) under the same conditions. The increased activity of the unbuffered reactions can easily be explained by the low pH (~1) of the solution at the end of the reaction; this low pH is presumably due to the HF produced during the reaction (see Scheme 1). Since lower pH values increase the rate of benzene hydrogenation (path c, Scheme 1) and the overall conversion of PhF (path bc, Scheme 1) (section 3.2.), the rate increase can be attributed to the more acidic conditions in the unbuffered reactions.

3.4. Effect of hydrogen pressure on the hydrodefluorination of PhF

The effect of hydrogen pressure on the reaction was examined for a heptane/ethanol/water (3 ml/1.2 ml/0.6 ml) solvent system with added NaOAc (0.36 g, 4.4 mmol) using the high-pressure tube (section 2.3.2.) using Rh-SiO$_2$(A) with hydrogen pressures ranging from 15 to 58 psi at 70 °C. The following rates [32] were observed under

the following pressures: 451 h^{-1} (58psi), 410 h^{-1} (44 psi), 381 h^{-1} (40 psi), 399 h^{-1} (36 psi),

350 h^{-1} (29 psi), 348 h^{-1} (22 psi), 295 h^{-1} (18 psi), 276 h^{-1} (15 psi). The rate of reaction

increases with increasing hydrogen pressure, and over the range of 15-58 psi (~1-4 atm) of

H$_2$, the rates vary by a power of 1/3, i.e. rate $\propto$ P$_{H2}$$^{1/3}$ (Fig. 4).

The effect of hydrogen pressure on the ratio of CyF to CyH was examined for

heptane (5 ml) using Rh-SiO$_2$(A) with hydrogen pressures ranging from 15 to 58 psi at 70 °C.

All, reactions were complete within 30 min and the following ratios of CyF:CyH were

observed under the following pressures: 9.8:1.0 (15 psi), 12.0:1.0 (29 psi), and 8.2:1.0 (58

psi). Thus, it was observed that variations in hydrogen pressure over 1-4 atm caused very

little change in the ratio of CyF to CyH although a slight decrease in selectivity for CyF was

observed as the pressure was increased (care must be utilized to prevent the reaction from

proceeding past complete conversion of PhF, as the resulting solution containing HF is

capable of transforming CyF to CyH and this will affect the CyF:CyH ratio at longer times,

Section 3.6).

3.5. Other catalysts for the hydrodefluorination of PhF

The [Rh(COD)$_2$]$^+$BF$_4$$^-$-SiO$_2$/40°C, Rh-SiO$_2$, [Rh(COD)$_2$]$^+BF_4$$^-$-Pd-SiO$_2$,

[Rh(COD)$_2$]$^+$BF$_4$$^-$-Pd-SiO$_2$/40°C, [Rh(COD)$_2$]$^+BF_4$$^-$-Pd-SiO$_2$/200°C, and Pd-SiO$_2$ catalysts

were examined for their PhF hydrodefluorination activity under 29 psi H$_2$ at 70 °C with

NaOAc base in the heptane/ethanol/water solvent system (Table 4). The activities of the

various rhodium and rhodium/palladium catalysts in the hydrodefluorination of PhF to PhH

and CyH approximately parallels their toluene hydrogenation activities [24]. Detailed

characterization (DRIFTS, TEM, XPS, and mercury poisoning experiments) of the rhodium

containing catalysts showed that they all consist of rhodium metal on silica, which is

responsible for their toluene hydrogenation activity [24]. The effect of the palladium in the [Rh]-Pd-SiO$_2$ systems is to facilitate the reduction of the Rh complex to active rhodium metal. The catalytic activity of supported rhodium catalysts is structure sensitive and depends on particle size with metal clusters of ~10 Å or larger needed for arene hydrogenation [33-38]. For catalysts prepared from the rhodium precursor [Rh(COD)$_2$]$^+$BF$_4^-$ on silica, toluene hydrogenation activities are improved by hydrogen pretreatments prior to reaction. The activity increases with the temperature of the hydrogen pretreatment, 200 °C (Rh-SiO$_2$(A), Rate = 246 h^{-1}) being better than 40 °C (Rh-SiO$_2$(B), Rate = 95 h^{-1}). For [Rh(COD)$_2$]$^+$BF$_4^-$ on Pd-SiO$_2$, a different trend is observed as the catalysts are more active when they are not pretreated. The untreated catalyst (Rh-Pd-SiO$_2$(A), Rate = 230 h^{-1}) is the most active of the series. A 40 °C H$_2$-pretreatment produces no appreciable change in rate (Rh-Pd-SiO$_2$(B), Rate = 210 h^{-1}). A 200 °C hydrogen pretreatment severely reduces the catalytic activity by almost five-fold (Rh-Pd-SiO$_2$(C), Rate = 46 h^{-1}). This treatment apparently changes the structure of the catalyst to a form that is substantially less active for arene hydrogenation than just rhodium on the same support. This lower activity was attributed either to the formation of a rhodium-palladium alloy or to the formation of rhodium clusters that are smaller than the 10 Å size required for arene hydrogenation activity [24, 33, 34]. Since the most active hydrogenation catalysts are also the most active hydrodefluorination catalysts (Table 4) and benzene is observed to inhibit the hydrodefluorination reaction, the same catalytic sites on rhodium metal are probably used for both toluene hydrogenation and fluorobenzene hydrodefluorination.

3.6. Attempted hydrodefluorination of CyF

Hydrodefluorination of CyF was attempted using Rh-SiO$_2$(A) as a catalyst under all of the reaction conditions (heptane, DCE, heptane/water; pH = 11.2-2.2; 1-4 atm H$_2$; 40 °C-70 °C) examined in this study, but CyF remained unreacted even after 24 h of treatment. However, a few of the PhF hydrodefluorination reactions (see Section 3.1.2.) suggested that CyF could be converted to CyH. Also, Blum et. al. reported that thermal defluorination of fluorocyclohexane to cyclohexene occurs in DCE at 80 °C under 16 atm H$_2$ [22]. Since CyF was converted to CyH in DCE with 1 atm H$_2$ at 70 °C over Rh-SiO$_2$ (A) during the hydrodefluorination of PhF but identical conditions failed to converted commercial CyF to CyH, 10 drops of HF (49% aqueous solution) were added to a commercial sample of CyF in DCE with 1 atm H$_2$ at 70 °C over Rh-SiO$_2$ (A), and a rapid conversion of CyF to CyH was observed (<40 min). The slower process (~3% per hour) seen during the hydrodefluorination of PhF in DCE indicates that the rate of conversion of CyF depends on the amount of HF added, however changing the amount of Rh-SiO$_2$(A) did not change the rate of CyF conversion. Furthermore, in the absence of rhodium, CyF reacted with HF to form cyclohexene in DCE at 70 °C. Thus, the conversion of CyF to CyH is a two-step process consisting of conversion of CyF to cyclohexene by HF (path d, Scheme 1) followed by catalytic hydrogenation of cyclohexene to CyH by rhodium (path e, Scheme 1). This interconversion of CyF to CyH by HF (path de, Scheme 1) also occurs in heptane, but is more rapid in DCE.

4. Discussion

4.1. Effect of solvent on the Rh-SiO₂(A)-catalyzed reaction of PhF with H₂

For the Rh-SiO_2(A)-catalyzed hydrodefluorination of fluorobenzene (PhF), the

solvent system affects the product distribution (path *a* or path *bc*, Scheme 1). The non-polar

solvent heptane produces mixtures of CyF and CyH (3.3:1.0 at 40 °C or 9.9:1.0 at 70 °C).

DCE, an aprotic but more polar solvent than heptane, still favors initial arene hydrogenation

over hydrodefluorination, but decreases the ratio of CyF to CyH because the conversion of

CyF to CyH by HF (path *de*, Scheme 1) occurs at a rate similar to the rate of the rhodium

catalyzed reaction of PhF and H_2 (path *a* and path *bc*, Scheme 1). In contrast, reactions in

polar protic solvent systems, heptane/methanol and heptane/water, proceed only by path *bc*,

Scheme 1. The reaction is faster in heptane/water than in heptane/methanol.

Prior to this work, there were only a limited number of reports of the catalytic

hydrodefluorination of monofluoroarenes [12-23] and fewer by rhodium metal [20-23]. No

studies of solvents on these reactions have been reported. However, solvent effects in

hydrodehalogenation reactions of other aryl halides (Cl, Br, I) using several supported metal

catalysts (Pd, Rh, Pt, Ni) are observed: more polar solvents accelerate hydrodehalogenation

while non-polar solvents retard the loss of halogen [39,40]. This general trend of more polar

solvents facilitating hydrodehalogenation of arylhalides (Cl, Br, I) over supported metals (Pd,

Rh, Pt, Ni) [39,40] is consistent with our results and is dramatically illustrated by our system

for PhF hydrodefluorination over supported rhodium metal. Furthermore, the ability of our

system to catalyze the formation of CyF from PhF in heptane is notable as in all other

examples the hydrodehalogenation of aryl halides [12-22,39-43], even fluorides, occurs at

rates greater than or equal to ring hydrogenation, and the reduction of an aryl ring to the

corresponding cyclohexyl halide with considerable retention of halogen was not possible.

4.2. Effect of pH on the hydrodefluorination of PhF in heptane/methanol and heptane/water

The $Rh-SiO_2(A)$-catalyzed hydrodefluorination of PhF in the polar protic solvents of

heptane/methanol and heptane/water follow path *bc* in Scheme 1. The hydrodefluorination

step *b* is slightly faster when the solution is basic (initial rate = 54.5 h^{-1} at pH = 11.2

compared to an initial rate of 28.6 h^{-1} at pH = 2.2, Table 2), but the overall reaction (path *bc*,

Scheme 1), including arene hydrogenation to CyH (step *c*, Scheme 1), is much faster under

acidic conditions (Table 2 and Fig. 3). Benzene inhibits defluorination, confirmed by

competition reactions between PhF and PhH using the heptane/water system buffered at pH =

2.2 (Table 3), and can slow the overall process to the point where PhH hydrogenation

determines the rate of PhF hydrodefluorination (see pH = 7.1 and 11.2, Fig. 3). Therefore,

the conversion of PhF to CyH is fastest under acidic conditions (Fig. 3) because PhH

hydrogenation is fastest under these conditions (Table 2).

At first glance, this result seems to contradict the conventional wisdom for

hydrodehalogenation (F, Cl, Br, I) reactions over supported metals (Pd, Rh, Pt, Ni), where

base has traditionally been used to neutralize the hydrogen halide acid as it is formed [40,43],

and where the presence of a base may accelerate the rate of dehalogenation [39,40,43].

However, arene hydrogenation catalyzed by rhodium metal is inhibited by the presence of

strong bases [39-43] (especially strong nitrogen bases such as amines and pyridines) while

acids have been observed to both promote and inhibit the reaction [39-43]. For example,

Stocker observed that acetic acid in methanol increased the rate of reduction of certain

aromatics over rhodium on alumina [40,44]; but the hydrogenation of toluene or benzoic acid

in methanol over 5% rhodium on carbon was neither promoted nor inhibited by the addition

of several weak or strong acids, except HCl which was a strong inhibitor [39-43,45].

For the hydrodefluorination of PhF by Rh-SiO$_2$(A) in polar protic solvents the

hydrodefluorination product (PhH) interacts strongly enough with the catalyst to inhibit

further hydrodefluorination of PhF. In this case, the effects of base and solvent on both

steps, hydrodefluorination and hydrogenation (steps *a* and *b*, Scheme 1), must be considered.

Acidic conditions promote the hydrogenation of PhH to CyH (step *b*, Scheme 1), and remove

PhH which would otherwise inhibit the hydrodefluorination of PhF to PhH (step *a*, Scheme

1). Thus, the overall reaction (path *bc*, Scheme 1) experiences an effective acid promotion

and base inhibition. This leads to a situation where conventional hydrodefluorination

conditions, i.e. presence of strong bases to neutralize the hydrogen halide acid as it is formed,

become detrimental to the rhodium catalyzed hydrodefluorination, and the absence of a base

or the presence of an acidic buffer actually facilitates the overall reaction (path *ab*, Scheme

1)! The inhibition of hydrodefluorination by PhH and the low rate of PhH hydrogenation

under basic conditions may explain the much lower rates of reaction observed by Young and

Grushin for rhodium nanoparticle hydrodefluorination where reaction with 3 M

fluorobenzene under 40 psi H$_2$ at 95 °C in a very basic 40% NaOH aqueous solvent provided

88 TO's in 1 day with minimal hydrogenation of the resulting benzene [21].

5. Conclusions

In these studies of the Rh-SiO$_2$(A)-catalyzed reactions of PhF with H$_2$, non-polar,

aprotic solvents (heptane and DCE) favor arene hydrogenation (path *a*, Scheme 1), while

polar, protic solvents (heptane/methanol and heptane/water) favor hydrodefluorination (path

bc, Scheme 1). A benzene (PhH) intermediate, on the way to CyH, was detected in the

heptane/methanol and heptane/water reactions confirming the pathways shown in Scheme 1. The complete hydrodefluorination of fluorobenzene (PhF) to cyclohexane (CyH) was found to proceed best in heptane/water under acidic conditions. This is because PhH inhibits the hydrodefluorination of fluorobenzene (PhF) to benzene (PhH) (path *b*), and the hydrogenation of benzene (PhH) to cyclohexane (CyH) is fastest under acidic conditions. Since the supported rhodium catalysts most active for toluene hydrogenation are also the most active hydrodefluorination catalysts (Table 4) and benzene is observed to inhibit the hydrodefluorination reaction, the same catalytic sites on rhodium metal are probably used for both arene hydrogenation and fluorobenzene hydrodefluorination. To the best of our knowledge, the systems described in this paper, when used in heptane/water at low pH, catalyze the hydrodefluorination of PhF under the mildest reported conditions, 1 atm H_2 at 40 °C, while still providing rates that are faster than those of other hydrodefluorination systems which utilize more pressing conditions.

References

[1] M. Hudlicky, Chemistry of Organic Fluorine Compounds, Prentice-Hall, New York, 1992, p. 175.

[2] J.L. Kiplinger, T.G. Richmond, C.E. Osterberg, Chem. Rev. 94 (1994) 373.

[3] J. Burdeniuc, B. Jedlicka, R.H. Crabtree Chem. Ber./Recl. 130 (1997) 145.

[4] E. Murphy, R. Murugavel, H. W. Roesky, Chem. Rev. 97 (1997) 3425.

[5] T.G. Richmond, Topics in Organomet. Chem. 3 (1999) 243.

[6] R. Bosque, E. Clot, S. Fantcci, F. Maseras, O. Eisenstein, R.N. Perutz, K.B. Renkema, K.G. Caulton, J. Am. Chem. Soc. 120 (1998) 12634.

[7] N.Y. Adonin, V.F. Starichenko, Mendeleev Commun. 2 (2000) 60.

[8] D. Huang, P.R. Koren, K. Folting, E.R. Davidson, K.G. Caulton, J. Am. Chem. Soc. 122 (2000) 8916.

[9] K.M. Bradley, R.J. Lachicotte, W.D. Jones, J. Am. Chem. Soc. 123 (2001) 10973.

[10] K.M. Bradley, W.D. Jones, J. Am. Chem. Soc. 124 (2002) 8681.

[11] R.P. Huges, S. Willemsen, A. Williamson, D. Zhang, Organometallics 21 (2002) 3085.

[12] M. Hudlicky, J. Fluorine Chem. 44 (1989) 345.

[13] F.J. Urbano, J.M. Marinas, J. Mol. Catal. A: Chem 173 (2001) 329.

[14] Y. Ukisu, T. Miyadera, J. Mol. Catal. A: Chem. 125 (1997) 135.

[15] M.A. Aramendia, V. Borua, I.M. Garcia, C. Jimenez, A. Marinas, J.M. Marinas, F.J. Urbano, C. R. Acad. Sci. Paris, Serie IIC, Chimie, 3 (2000) 465.

[16] a) F. Swarts, Bull. Acad. Roy. Belg. (1920) 399; Chem. Abstr. 16 (1922) 2316.

a) F. Swarts, Bull. Acad. Roy. Belg. (1936) 122; Chem. Abstr. 30 (1936) 4154.

[17] M.W. Renoll, J. Am. Chem. Soc. 68 (1946) 1159.

[18] F.L.M Pattison, B.C. Saunders, J. Chem. Soc. (1949) 2745.

[19] M. Tashiro, H. Nakamura, K. Nakayama, Org. Prep. Proc. Int. 19 (1987) 442.

[20] L.D. Freedman, G.O. Doak, E.L. Petit, J. Am. Chem. Soc. 77 (1955) 4262.

[21] R.J. Young, V.V. Grushin, Organometallics 18 (1999) 294.

[22] J. Blum, A. Rosenfeld, F. Gelman, H. Schumann, D. Avnir, J. Mol. Catal. A: Chem. 146 (1999) 117.

[23] H. Yang, H. Gao, R.J. Angelici, Organometallics 18 (1999) 2285.

[24] K.J. Stanger, Y. Tang, J. Anderegg, R.J. Angelici, J. Mol. Catal. A: Chem., accepted for publication.

[25] D.D. Perrin, W.L.F. Armarego, D.R. Perrin, Purification of Laboratory Chemicals, 2nd ed., Pergamon, New York, 1980.

[26] The catalysts are referred to by the notation [Rh]-(Pd)-SiO$_2$/T°C (where [Rh] designated the rhodium precursor, (Pd)-SiO$_2$ indicated whether the support contained reduced Pd metal, and T°C described the temperature of any hydrogen pretreatments) [D24]. For this paper, the most widely used catalyst [Rh(COD)$_2$]$^+$BF$_4^-$-SiO$_2$/200°C is referred to as Rh-SiO$_2$(A).

[27] D.C. Harris, Quantitative Chemical Analysis, 3rd ed., W.H. Freeman and Company, New York, 1991, p 202.

[28] H. Gao, R.J. Angelici, J. Mol. Catal. A: Chem. 149 (1999) 63.

[29] H. Gao, R.J. Angelici, Organometallics 18 (1999) 989.

[30] H. Gao, R.J. Angelici, New J. Chem. 23 (1999) 633.

[31] K.J. Stanger, J.W. Wiench, M. Pruski, R.J. Angelici, J. Mol. Catal. A: Chem. 195 (2003) 63.

[32] Rate given as [Δ mole PhF/(mole Rh • h)] over the first 30 min of reaction

[33] G. del Angel, B. Coq, F. Figueras, J. Catal. 95 (1985) 167.

[34] P.E. Araya, E.E. Miro, L. Cornaglia, J. Chem. Research (S) (1997) 258.

[35] G.A. del Angel, B. Coq, G. Ferrat, F. Figueras, Surface Science 156 (1985) 943.

[36] W.F. Graydon, M.D. Langan, J. Catal. 69 (1981) 180.

[37] T. Ioannide, X.E. Verykios, J. Catal. 143 (1993) 175.

[38] F. Fajardie, J-F. Tempere, G. Djega-Mariadassou, G. Blanchard, J. Catal. 163 (1996) 77.

[39] R.L. Augustine, Catalytic Hydrogenation, Marcel Dekker, Inc. New York, 1965.

[40] P.N. Rylander, Catalytic Hydrogenation over Platinum Metals, Academic Press, New York, 1967.

[41] M. Freifelder, Practical Catalytic Hydrogenation, Wiley-Interscience, New York, 1971.

[42] M. Freifelder, Catalytic Hydrogenation in Organic Synthesis Procedures and Commentary, Wiley-Interscience, New York, 1978.

[43] S. Nishimura, Handbook of Heterogeneous Catalytic Hydrogenation for Organic Synthesis, Wiley-Interscience, New York, 2001.

[44] J.H. Stocker, J. Org. Chem. 27 (1962) 2288.

[45] M. Freifelder, J. Org. Chem. 26 (1961) 1835.

Scheme 1. Reaction of PhF with H_2 catalyzed by Rh-SiO$_2$(A).

Table 1. Effect of solvent on the rate and product selectivity of the reaction of PhF with H_2.[a]

Entry	Solvent	95% Completion time (min)	% CyH	% CyF
1	Heptane	30	23.4	76.6
2	DCE	5880	36.7	63.3
3	Heptane/Methanol[b]	600	100	0
4	Heptane/Water[c]	180	100	0

[a] Reaction conditions: 50.0 mg (containing ~9.7 μmol Rh) of Rh-SiO$_2$(A) catalyst, 1.1 mmol PhF, 5.0 ml solvent, 40.0 (±0.2) °C, 1 atm H$_2$.

[b] 3.0 ml of heptane over 2.0 ml of methanol.

[c] 3.0 ml of heptane over 2.0 ml of water.

Table 2. Effect of pH on the hydrodefluorination of PhF[a] and hydrogenation of PhH[b] with H_2

in heptane/water solutions.

pH	Initial Rate[c]	95% Completion time (min)[a] PhF Hydrodefluorination	95% Completion time (min)[b] PhH Hydrogenation
11.2[d]	54.5	1008 (68%)[e]	293
7.1[d]	81.8	790	272
4.8[f]	28.7	600	226
2.2[d]	28.6	280	183

[a] Reaction conditions: 50.0 mg (containing ~9.7 μmol Rh) of Rh-SiO$_2$(A) catalyst, 1.1 mmol

PhF, 3.0 ml of heptane over 2.0 ml of 1.0 M aqueous buffer solution, 40.0 (±0.2) °C, 1 atm

H_2.

[b] Reaction conditions: 50.0 mg (containing ~9.7 μmol Rh) of Rh-SiO$_2$(A) catalyst, 0.36

mmol PhH, 3.0 ml of heptane over 2.0 ml of 1.0 M aqueous buffer solution, 40.0 (±0.2) °C, 1

atm H_2.

[c] Initial rate calculated after 5 min of reaction by [Δ mole PhF/(mole Rh • h)].

[d] Phosphate buffer.

[e] Reaction was only 68% complete after 1008 min.

[f] Acetate buffer.

Table 3. Effect of PhH on the rate of PhF hydrodefluorination in heptane/water buffered (pH = 2.2) solution.[a]

PhH$_i$[b] (mmol)	Initial Rate (ΔPhF)[c]	Initial Rate (ΔPhH)[d]
0	28.3	--
0.55	10.4	9.48
1.1	7.50	15.2
2.4	2.90	47.9

[a] Reaction conditions: 50.0 mg (containing ~9.7 μmol Rh) of Rh-SiO$_2$(A) catalyst, 1.1 mmol PhF, 0-2.4 mmol PhH, 3.0 ml of heptane over 2.0 ml of 1.0 M aqueous acetate buffer solution at pH = 2.2, 40.0 ($\pm$0.2) °C, 1 atm H$_2$.

[b] Initial amount of benzene (PhH$_i$).

[c] Rate given as [Δ mole PhF/(mole Rh • h)] over the first 60 min of reaction.

[d] Rate given as [Δ mole PhH/(mole Rh • h)] over the first 60 min of reaction.

Table 4. Rates of hydrodefluorination of PhF[a] and hydrogenation of toluene[b] using various catalysts.

Catalyst	Rate (PhF)[c]	Rate (PhMe)[d]
Rh-SiO$_2$(A)	350	246
[Rh(COD)$_2$]$^+$BF$_4^-$-SiO$_2$/40°C	244	95
Rh-SiO$_2$	280	151
[Rh(COD)$_2$]$^+$BF$_4^-$-Pd-SiO$_2$	371	230
[Rh(COD)$_2$]$^+$BF$_4^-$-Pd-SiO$_2$/40°C	369	210
[Rh(COD)$_2$]$^+$BF$_4^-$-Pd-SiO$_2$/200°C	135	46
Pd-SiO$_2$	12.1[e]	

[a] Reaction conditions: 30.0 mg (containing ~5.8 μmol Rh) of catalyst indicated, 4.3 mmol PhF, 0.36 g (4.4 mmol) NaOAc, 3.0 ml of heptane over 1.2 ml ethanol and 0.8 ml water, 70 °C, P$_{H2}$ = 29 psi, 30 min reaction time, Fischer-Porter reaction vessel.
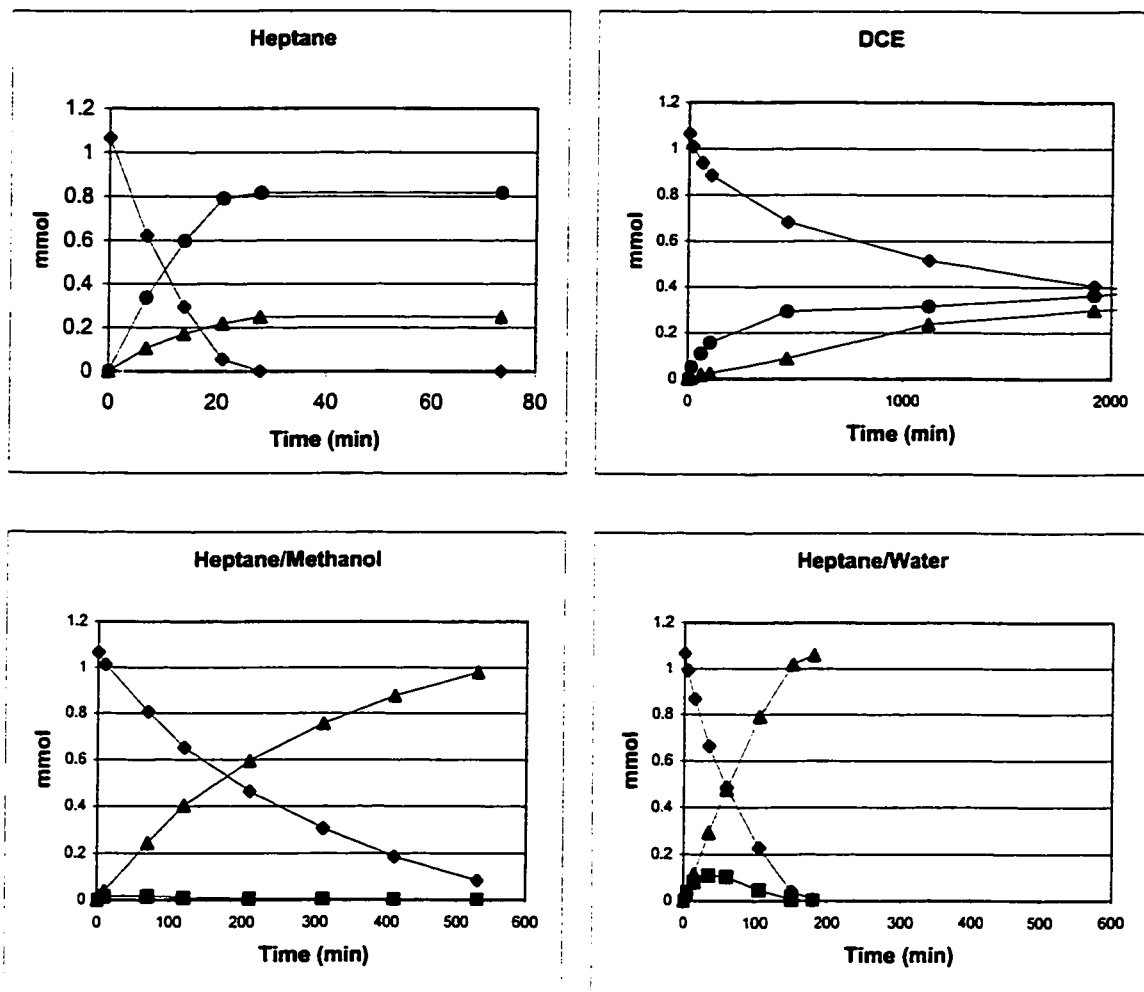
[b] Reaction conditions: 50 mg of solid catalyst, 5 ml of toluene, 40.0 °C, 1 atm of H$_2$ from [C18].

[c] Rate given as [Δ mole PhF/(mole Rh • h)] over 30 min of reaction.

[d] Rate given as [Δ mole PhH/(mole Rh • h)] over the first hour of reaction [C18].

[e] To facilitate comparison, the rate for the Pd-SiO$_2$ catalyst is reported in terms of an effective rate. Since, it does not contain rhodium, a rate based on rhodium cannot be given. The rate value here is calculated by assuming the Pd-SiO$_2$ catalyst contains the standard rhodium loading (5.8 μmol/30.0 mg).

Fig. 1. Effect of solvent on the rate and selectivity of the reaction of PhF with H_2.[a]

[a] Reaction conditions are the same as those in Table 1. ($\blacklozenge$) PhF, ($\bullet$) CyF, ($\blacksquare$) PhH,

($\blacktriangle$) CyH.

127

Fig. 2. Effect of base on the hydrodefluorination of PhF in heptane/methanol.[a]

[a] Reaction conditions: 50.0 mg (containing ~9.7 μmol Rh) of catalyst, Rh-SiO$_2$(A), 1.1 mmol

PhF, 1.2 mmol base, 3.0 ml of heptane over 2.0 ml of methanol, 40 °C, 1 atm H$_2$. (♦) PhF,

(●) CyF, (■) PhH, (▲) CyH.

Fig. 3. Effect of pH on the hydrodefluorination of PhF in heptane/water solutions.[a]

[a] Reaction conditions are the same as those in Table 2. Phosphate buffers were used for pH

11.2, 7.1, and 2.2; an acetate buffer for pH 4.8. (♦) PhF, (■) PhH, (▲) CyH.

Fig. 4. Effect of hydrogen pressure on the hydrodefluorination of PhF.[a]

[a] Reaction conditions: 30.0 mg (containing ~5.8 μmol Rh) of Rh-SiO$_2$(A) catalyst, 4.3 mmol

PhF, 0.36 g (4.4 mmol) NaOAc, 3.0 ml of heptane over 1.2 ml ethanol and 0.8 ml water, 70

°C, 30 min reaction time, P$_{H2}$ = 15-58 psi, Fischer-Porter reaction vessel. The equation for

the best-fit line is y = 0.35 x + 2.05. Thus, over the range 1-4 atm, rate $\propto$ P$_{H2}$$^{1/3}$.
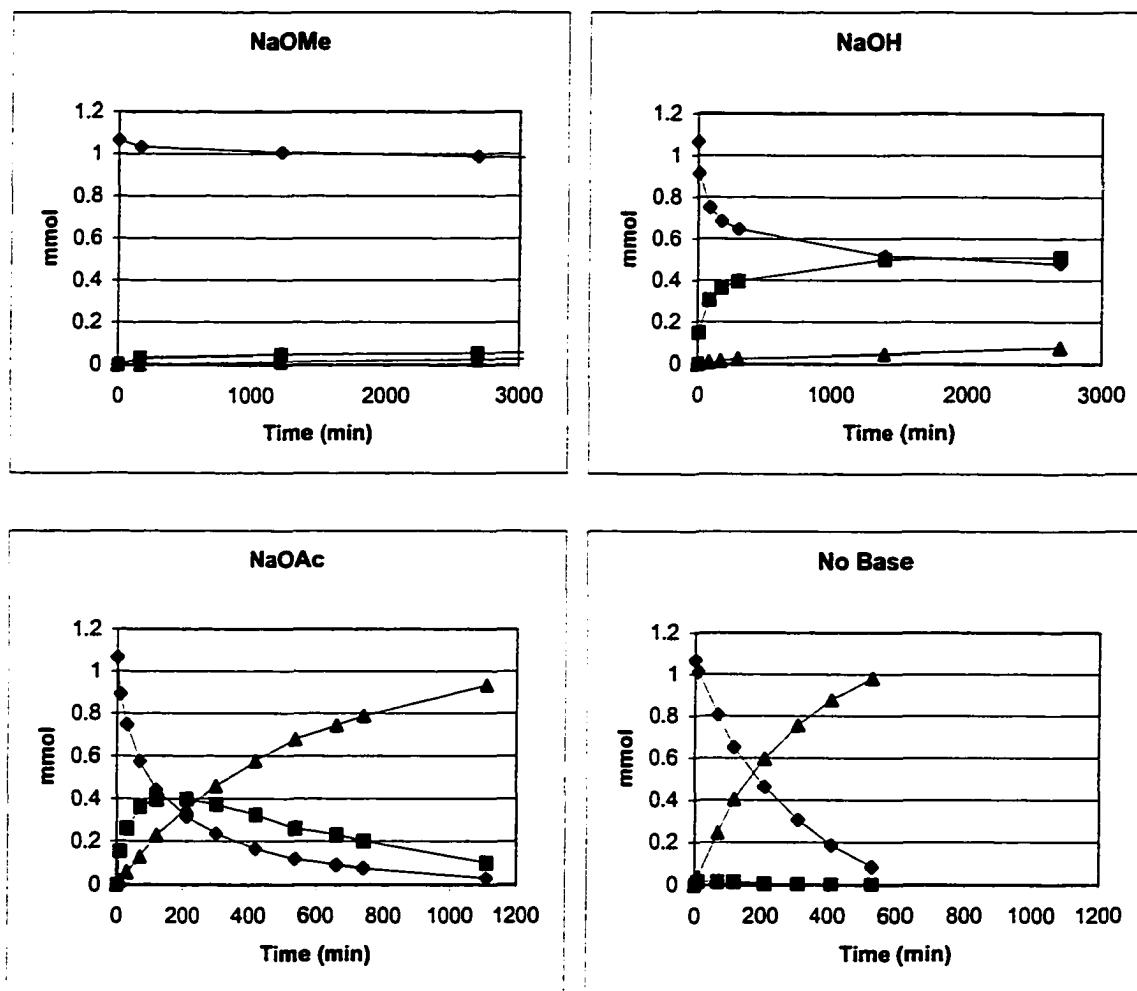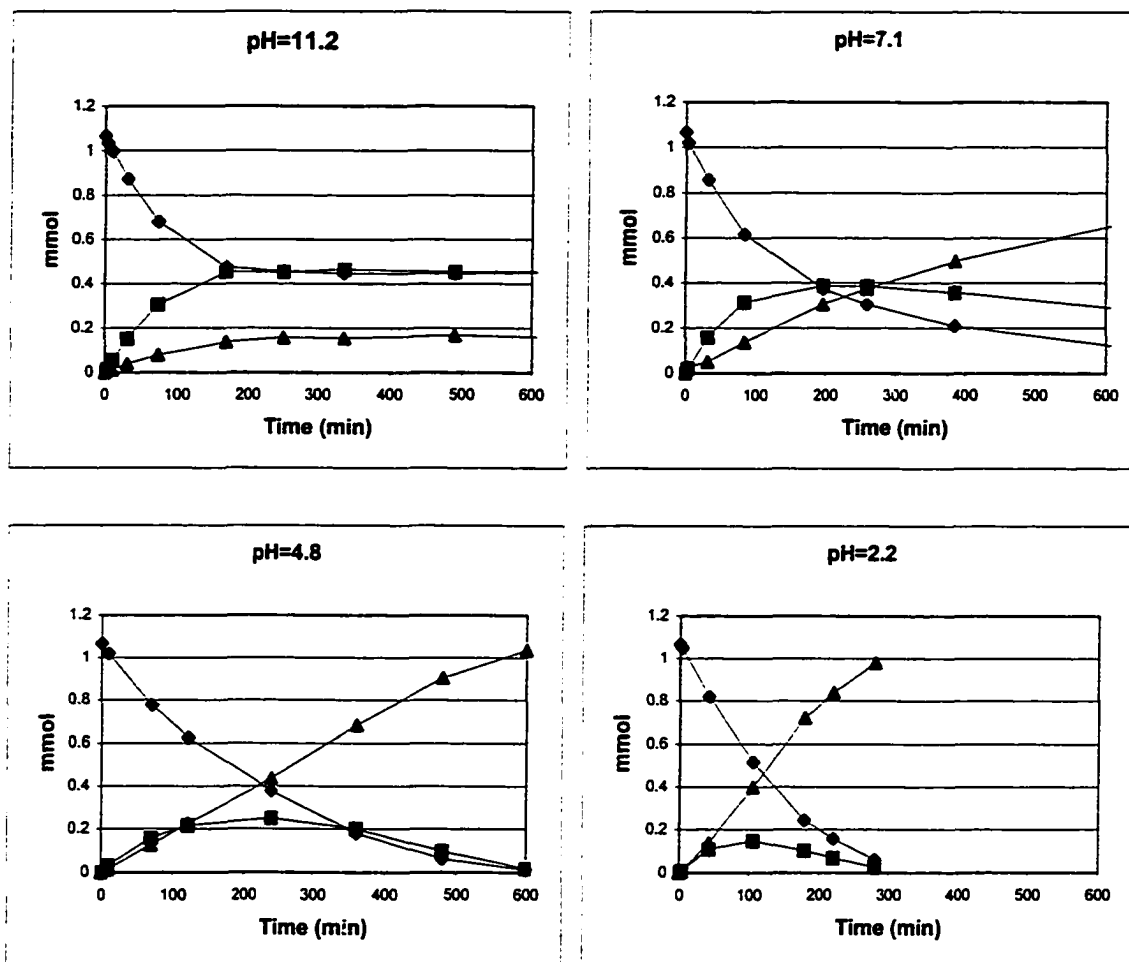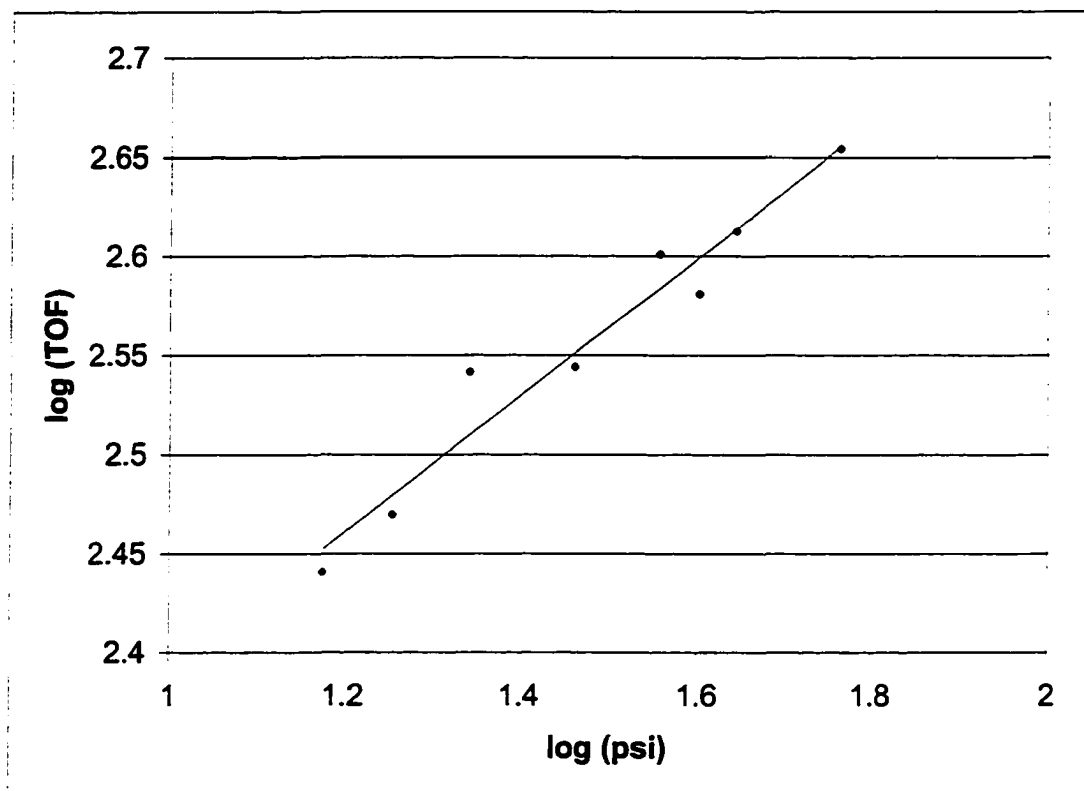
Oxidation of Sulfides Relevant to HDS with Oxorhenium(V) Dithiolates Catalysts Tethered on Silica

Keith J. Stanger, Jerzy W. Wiench, Marek Pruski, James H. Espenson, George Kraus, and

Robert J. Angelici*

Abstract

Oxorhenium(V) dithiolate catalysts [-S(CH$_2$)$_n$S-]Re(O)(Me)(PPh$_3$) were modified to

allow immobilization via tethering to silica supports. The resulting (SiO$_2$-

RTA)Re(O)(Me)(PPh$_3$), Fig. 2, is the first example of a tethered oxorhenium(V) dithiolate

catalyst. The anchored complex and homogeneous analogs were used for the selective

oxidation of sulfides (methyltolylsulfide (MTS), dibenzothiophene (DBT), and 4,6

dimethyldibenzothiophene (4,6-Me$_2$DBT)) to the corresponding sulfoxides and sulfones by

tert-butylhydroperoxide (TBHP) in various solvents (benzene, chloroform, etc.) and

temperatures (20, 50, and 100 °C). Catalytic oxidation reactions showed the heterogenized

catalyst to be similar to its homogeneous analog in regards to reactivity. However, the

immobilized catalyst offered additional advantages of recycleability, extended stability, and

increased resistance to deactivation over the homogeneous catalyst.

1. Introduction

The EPA has mandated by 2006 the reduction in total sulfur content of gasoline to 25

ppm from the current allowed level of 400 ppm [1]. This removal will need to come from

refractory sulfides not currently removed by the first stages of hydrodesulfurization (HDS)

[2]. Oxidative chemistry could be utilized for further sulfur reduction in oil as the oxides of

sulfides exhibit different solubility and reactivity properties [3,4-7]. While the oxidation of

sulfides to sulfoxides and sulfones can be achieved by a variety of biological and laboratory

methods [8-11], the class of oxorhenium(V) dithiolate compounds stand out as highly

effective and desirable oxygen atom transfer (OAT) catalysts from both kinetic as well as

selectivity standpoints with many aspects of their mechanism and activities recently

elucidated [3,12-21]. However, the utility of the catalysts would be increased if they could

be more easily recycled and re-utilized after reactions. Furthermore, the homogeneous

oxorhenium(V) dithiolate compounds have already been shown to be very effective catalysts

for *tert*-butylhydroperoxide (TBHP) oxidation of refractory sulfides, such as

dibenzothiophene (DBT) and 4,6 dimethyldibenzothiophene (4,6-Me$_2$DBT), Eq. (1) [3].
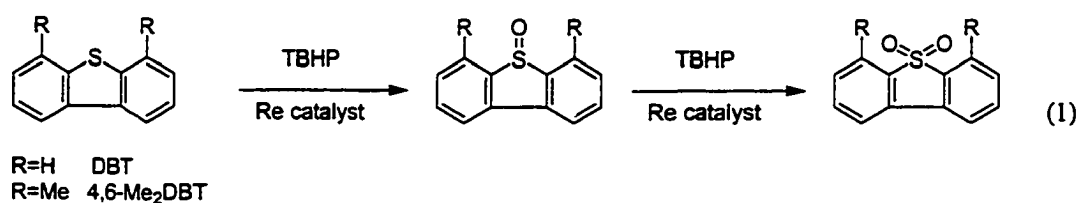
R=H   DBT
R=Me 4,6-Me$_2$DBT

Catalyst immobilization is a viable method to achieve the best possible combination of

catalyst activities, rates, and lifetimes. When catalysts are tethered on solid supports, the

resulting catalysts can combine the advantages of both homogeneous (selectivity, tuneability,

and homogeneous sites) and heterogeneous (recovery and separation) catalysts [10,11].

Furthermore, additional benefits often occur which arise from site-isolation of the catalyst

centers. Therefore, the immobilization of homogeneous catalysts is a highly desirable goal.

Thus, it was decided that the immobilization of oxorhenium(V) dithiolate catalysts be

undertaken with particular emphasis on their oxidation activities for HDS relevant sulfides.

Within, we report our findings for the first example of a tethered oxorhenium(V) dithiolate catalyst.

2. Experimental

2.1. General considerations

The chemicals TBHP (5-6 M solution in nonane) (Aldrich), 3-chloropropyltriethoxysilane (RCl) (Fluka), 1,3 propanedithiol (pdt) (Aldrich), 1,2 ethanedithiol (edt) (Aldrich), DBT (Aldrich), 4,6-Me$_2$DBT (Aldrich), methyltolylsulfide (MTS) (Aldrich), thioctic acid (TA) (Aldrich), chloroform (CHCl$_3$) (Fischer), deuterated chloroform (CDCl$_3$) (Cambridge) were purchased from commercial sources and used as received. Silica gel Merck grade 10184 (B.E.T. surface area, 300 m^2 g^{-1}; pore size 100 Å) (Aldrich) was dried under vacuum at 150 °C for 12 h and kept under argon before use. Toluene, hexanes, and methylene chloride were dried prior to use by passage through an alumina column under argon [22]. Benzene was distilled from CaH$_2$ under nitrogen [23]. The compound 3-iodopropyltriethoxysilane (RI) was prepared from a literature synthesis [24]. The preparation of (PhS)$_4$Re$_2$(O)$_2$(Me)$_2$ followed a literature method [25]. Gas chromatographic (GC) analyses were performed on a Hewlett Packard HP 6890 GC using a 25 m HP-5 capillary column at 190 °C isotherm and an FID (flame ionization detector).

2.2.1. Preparation of ligands

(EtO)$_3$SiCH$_2$CH$_2$CH$_2$OC(O)CH$_2$CH$_2$CH$_2$CH$_2$CH(S-)CH$_2$CH$_2$(S-), RTA: Fig. 1. To a solution of 0.10 g (0.48 mmol) of TA dissolved in 5.0 ml of dry acetonitrile, 0.07 ml (0.5 mmol) of Et$_3$N and then 0.15 ml (0.45 mmol) of RI were added via syringe. The reaction was refluxed under argon at 70 °C for 3 days. Upon cooling to room temperature, the reaction mixture was flash-columned (2.5 cm x 63 cm) on silica (25% EtOAc:hexanes)

Fractions were monitored by silica TLC and RTA collected, $R_f = 0.25$. Yield 50%. ^{1}H NMR (CDCl$_3$) δ 4.00 (t, J=8.0 Hz, 2H, CO$_2$CH$_2$), 3.78 (q, J = 8.0 Hz, 6H, OCH$_2$CH$_3$), 3.53 (m, 1H, CH), 3.12 (m, 2H, CH(S-)CH$_2$CH$_2$(S-)),2.42 (m, 1H, CH(S-)CH$_2$CH$_2$(S-)), 2.3 (t, J = 7.4 Hz, 2H, O$_2$CCH$_2$), 1.88 (m, 1H, CH(S-)CH$_2$CH$_2$(S-)), 1.7 (m, 6H, O$_2$CCH$_2$CH$_2$CH$_2$CH$_2$, O$_2$CCH$_2$CH$_2$CH$_2$CH$_2$, and SiCH$_2$-CH$_2$-CH$_2$O$_2$C-), 1.4 (m, 2H, O$_2$CCH$_2$CH$_2$CH$_2$CH$_2$), 1.19 (t, J = 8.0 Hz, 9H, OCH$_2$CH$_3$), 0.60 (m, 2H, SiCH$_2$). ^{13}C NMR (CDCl$_3$) δ 173.7 (CO$_2$), 66.5 (CO$_2$CH$_2$), 58.5 (OCH$_2$CH$_3$), 56.4 (CH), 40.2 (CH(S-)CH$_2$CH$_2$(S-)), 38.5 (CH(S-)CH$_2$CH$_2$(S-)), 34.6 (O$_2$CCH$_2$CH$_2$CH$_2$CH$_2$), 34.1 (O$_2$CCH$_2$), 28.8 (O$_2$CCH$_2$CH$_2$CH$_2$CH$_2$), 24.7 (O$_2$CCH$_2$CH$_2$CH$_2$CH$_2$), 22.3 (SiCH$_2$-CH$_2$-CH$_2$O$_2$C), 18.3 (OCH$_2$CH$_3$), 6.6 (SiCH$_2$). High resolution mass Anal. calcd for C$_{17}$H$_{34}$O$_5$S$_2$Si: 410.16170. Found: 410.16265, deviation 2.3 ppm.

(EtO)$_3$SiCH$_2$CH$_2$CH$_2$OC(O)CH$_2$CH$_2$CH$_2$CH$_2$CH$_2$(SH)CH$_2$CH$_2$SH, RTAH$_2$: Fig. 1. Solid NaBH$_4$, 8.8 mg (0.23 mmol), was added to a solution of 80 mg (0.20 mmol) of RTA dissolved in 2.0 ml of dry ethanol at 0 °C and stirred at that temperature for 2 h. After complete reaction, the majority of ethanol was removed under vacuum. Then, the reaction mixture was worked up with the addition of 20 ml of 0.01 M HCl. Extraction with CH$_2$Cl$_2$, followed by drying over MgSO$_4$, yielded the desired reduced product in 75% yield judged pure by ^{1}H NMR and ^{13}C NMR. ^{1}H NMR (MeOH-d$_4$) δ 4.05 (t, J = 6.9 Hz, 2H, CO$_2$CH$_2$), 3.82 (q, J = 7.2 Hz, 6H, OCH$_2$CH$_3$), 2.91 (m, 1H, CH), 2.67 (m, 2H, (CH(S-)CH$_2$CH$_2$(S-)), 2.34 (m, 1H, (CH(S-)CH$_2$CH$_2$(S-)), 2.0-1.4 (m, 13H), 1.20 (t, J = 7.2 Hz, 9H, OCH$_2$CH$_3$), 0.64 (m, 2H, SiCH$_2$). ^{13}C NMR (MeOH-d$_4$) δ 175.6 (CO$_2$), 67.6 (CO$_2$CH$_2$), 59.6 (OCH$_2$CH$_3$), 44.4, 40.2, 39.9, 35.1, 27.7, 25.9, 23.5, 22.9, 18.8 (OCH$_2$CH$_3$), 7.5 (SiCH$_2$).

(SiO$_2$-RTAH$_2$): A mixture of 0.5 g of SiO$_2$ and 0.12 g (0.29 mmol) of RTA were slurried together in 10.0 ml of dry toluene. The mixture was refluxed for 4 h and then stirred overnight at room temperature. The resulting solid was washed with 4x10 ml of toluene and dried under vacuum to give SiO$_2$-RTA. This solid was then treated with 0.3 g of NaBH$_4$ in 5.0 ml of EtOH at 0 °C for 4 h. Quenching with 0.01M HCl, filtration, and extensive washing with H$_2$O was followed by 2x10 ml EtOH wash prior to vacuum drying. The resulting solid was recovered and stored under argon prior to use.

2.2.2. Preparation of rhenium complexes

(pdt)Re(O)(Me)(PPh$_3$): A mixture of 25.0 mg (57.4 μmol Re) of (PhS)$_4$Re$_2$(O)$_2$(Me)$_2$ and 15.0 mg (57.4 μmol) of PPh$_3$ were dissolved in 1.0 ml of chloroform, benzene, or toluene. After stirring for 10 min at room temperature, 6.0 μl (59.8 μmol) of pdt was added to the green solution. After 8 h, solvent was removed under vacuum, the green solid was washed with hexanes and recrystalized by layering hexane over toluene. ^{1}H NMR (C$_6$D$_6$) δ 7.78 (m, 6H, PPh$_3$), 6.95 (m, 9H, PPh$_3$), 3.16 (m, 2H, CH$_2$), 3.13 (m, 1H, CH$_2$-S), 2.90 (d, J$_{P-H}$ = 8.7 Hz, 3H, Re-CH$_3$), 2.75 (m, 1H, CH$_2$-S), 2.40 (m, 1H, CH$_2$-S), 2.30 (m, 1H, CH$_2$-S). ^{13}C NMR (C$_6$D$_6$) δ 134.73 (d, J$_{P-C}$ = 10.4 Hz, PPh$_3$), 131.10 (d, J$_{P-C}$ = 19.7 Hz, PPh$_3$), 129.26 (d, J$_{P-C}$ = 22.5 Hz, PPh$_3$), 128.77 (d, J$_{P-C}$ = 10.5 Hz, PPh$_3$), 36.41 (d, J$_{P-C}$ = 2.0 Hz, CH$_2$-S), 36.10 (CH$_2$), 34.30 (d, J$_{P-C}$ = 11.8 Hz, CH$_2$-S), 19.27 (d, J$_{P-C}$ = 3.9 Hz, Re-CH$_3$). ^{31}P NMR (C$_6$D$_6$) δ 28.05.

(edt)Re(O)(Me)(PPh$_3$): A mixture of 35 mg (80 μmol Re) of (PhS)$_4$Re$_2$(O)$_2$(Me)$_2$ and 27 mg (80 μmol) of PPh$_3$ were dissolved in 1.5 ml benzene. After stirring for 10 min at room temperature, 8.0 μl (90 μmol) of edt was added to the green solution. After 8 h, solvent was removed under vacuum; the red solid was washed with hexanes and recrystalized by layering

hexane over toluene. ^{1}H and ^{13}C NMR (C$_6$D$_6$) matched those already reported [17], ^{13}C

NMR J_{P-C} (Hz) are a factor of 4 smaller than earlier reported due to a miscalculation of Hz in

the original paper. ^{31}P NMR (C$_6$D$_6$) δ 31.69.

(RTA)Re(O)(Me)(PPh$_3$): A mixture of 85 mg (0.20 mmol Re) of (PhS)$_4$Re$_2$(O)$_2$(Me)$_2$ and 51

mg (0.20 mmol) of PPh$_3$ were dissolved in 4.0 ml of benzene. After stirring for 10 min at

room temperature, 82 mg (0.20 mmol) of RTAH$_2$was added to the green solution. After 8 h,

solvent was removed under vacuum, and the green oil was treated with hexanes and filtered.

Removal of hexanes under vacuum provided a green oil in 60% yield. Four isomers were

observed by ^{31}P NMR and ^{1}H NMR in approximately equimolar amounts. The isomers were

identified by ^{1}H NMR, four ReMe doublets near 2.87, and ^{31}P NMR, four distinct signals

near 27 ppm. ^{1}H NMR (C$_6$D$_6$) δ 4.04 (t, J = 6.8 Hz, 2H, CO$_2$CH$_2$), 3.73 (q, J = 7.0 Hz, 6H,

OCH$_2$CH$_3$), 3.25 (m, 2H, CH$_2$), 2.89 (d, J = 8.4 Hz, 3H, ReMe), 2.87 (d, J = 8.8 Hz, 3H,

ReMe) 2.85 (d, J = 8.0 Hz, 3H, ReMe) 2.85 (d, J = 8.4 Hz, 3H, ReMe), 2.42 (m, 1H, 7-CH$_2$),

2.07 (m, 2H, CH$_2$), 1.81 (m, 2H, SiCH$_2$-CH$_2$-CH$_2$O$_2$C-), 1.3-1.7 (m, 8H, CH$_2$), 1.19 (t, J =

7.0 Hz, 9H, OCH$_2$CH$_3$), 0.63 (m, 2H, SiCH$_2$). ^{31}P NMR (C$_6$D$_6$) δ 27.74, 27.69, 27.49, 27.19.

2.2.3. Preparation of silica-tethered complexes

(SiO$_2$-RTA)Re(O)(Me)(PPh$_3$): **Method (A)** (see Fig 2, path a). A solution of 143 mg (0.161

mmol Re) of (RTA)Re(O)(Me)(PPh$_3$) dissolved in 5.0 ml of toluene was added to 0.20 g of

SiO$_2$. The resulting slurry was refluxed for 12 h and then stirred overnight at room

temperature. Filtration, followed by washing with 3 x 5.0 ml of CH$_2$Cl$_2$, and drying under

vacuum gave a catalytically inactive red solid (see section 3.2.2) [26]. **Method (B)** (see Fig

2, path b). A mixture of 70 mg (0.16 mmol Re) of (PhS)$_4$Re$_2$(O)$_2$(Me)$_2$ and 45 mg (0.17

mmol) of PPh$_3$ were dissolved in 8.0 ml of benzene. After stirring for 10 min at room

temperature, the green solution was added to 0.6 g (0.4 mmol ligand) of SiO_2-$RTAH_2$ and stirred together at room temperature for 18 h. The resulting green solid support was filtered and washed with 3x10 ml of toluene and 3x10 ml of CH_2Cl_2. The resulting solid catalyst was dried under vacuum.

$(PhS)_2Re_2(O)(Me)(PPh_3)/(SiO_2)$: A mixture of 70 mg (0.16 mmol Re) of $(PhS)_4Re_2(O)_2(Me)_2$ and 45 mg (0.17 mmol) of PPh_3 were dissolved in 8.0 ml of benzene. After stirring for 10 min at room temperature, the green solution was added to 0.6 g of SiO_2 and the mixture was stirred at room temperature overnight for 18 h. The resulting solid was filtered, washed with 3x10 ml of toluene and 3x10 ml of CH_2Cl_2, and dried under vacuum.

2.3. Oxidation reactions

The rhenium catalyst was placed in a round bottom flask; solvent (typically 1 ml) and substrate (0.60 M or 9.45 mM) were added and allowed to briefly stand at room temperature; and then, TBHP was added via syringe. The reaction flask was immediately immersed in a constant temperature bath of appropriate temperature. The reaction was followed by GC analysis of samples removed from the reaction solution during and after the reaction. For MTS oxidation, the disappearance of MTS and appearance of methyltolylsulfoxide $(MTS(O))$ and methyltolylsulfone $(MTS(O)_2)$ was followed. For DBT and 4,6-Me_2DBT, disappearance of substrate was monitored with the aid of an internal standard of diphenylmethane. Product identity and extent of reaction could be confirmed by ^1H NMR.

3. Results and Discussion

3.1. Homogeneous catalytic oxidation of MTS

The selective oxidation of methyltolylsulfide (MTS) to methyltolylsulfoxide $(MTS(O))$ utilizing tert-butylhydroperoxide (TBHP) as the oxidant at room temperature in a

variety of solvents, Eq. (2), was used to examine catalyst activity and facilitate comparison to

previous work [3].

(2)
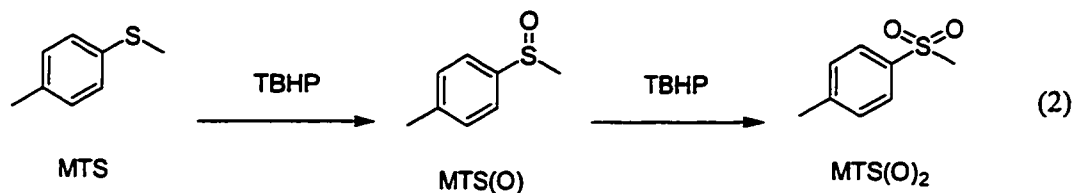
The results of a number of key experiments are compiled in Tables 1-4 and Graph 1. The

homogeneous $(RTA)Re(O)(Me)(PPh_3)$ catalyst (Table 1, entry 3, $t_{1/2} = 1.49$ h) has

comparable activity to the parent $(pdt)Re(O)(Me)(PPh_3)$ catalyst (Table 1, entry 2, $t_{1/2} = 1.06$

h). Thus, the tetherable chain only slightly decreases the catalytic activity. The catalytic

activity confirms that the four ^{31}P NMR signals arising from $(RTA)Re(O)(Me)(PPh_3)$

correspond to geometrical isomers of the complex as the overall activity is so similar to the

pdt analog. Comparison of $(pdt)Re(O)(Me)(PPh_3)$ (Table 1, entry 2, $t_{1/2} = 1.06$ h) to

$(edt)Re(O)(Me)(PPh_3)$ (Table 1, entry 1, $t_{1/2} = 2.65$ h) shows that both are strong catalysts.

This comparison (Table 1, entries 1 and 2) allows for easy extrapolation to other substrates

and conditions as the $(edt)Re(O)(Me)(PPh_3)$ catalyst has already been thoroughly

investigated [3].

The $(pdt)Re(O)(Me)(PPh_3)$ system was used to determine the effect of solvent on the

rate of reaction, collected in Table 2. Of the solvents examined, benzene provided the best

catalytic activity (Table 2, entry 1, $t_{1/2} = 0.94$ h). Deuterated chloroform (Table 2, entry 2,

$t_{1/2} = 1.06$ h) was comparable and only a slightly less favorable solvent. Both chloroform

(Table 2, entry 3, $t_{1/2} = 1.54$ h) and methylene chloride (Table 2, entry 4, $t_{1/2} = 2.13$ h)

showed reduced activity compared to $CDCl_3$. The cause of the reduced activity in chloroform

was identified as an effect of ethanol added as inhibitor, the commercial chloroform

contained 1% ethanol. A CDCl₃ solution with 10% ethanol (Table 2, entry 5, $t_{1/2}$ = 6.52 h) severely inhibited the reaction compared to pure CDCl₃, providing catalytic activity six and a half times slower.

3.2. Heterogeneous catalytic oxidation of MTS

Two strategies were used for the immobilization of (RTA)Re(O)(Me)(PPh₃) to a silica surface, Fig. 1. The tethered complex (SiO₂-RTA)Re(O)(Me)(PPh₃) prepared by **Method (B)** (Fig 2, path b; Table 1, entry 4, $t_{1/2}$ = 1.42 h) had activity comparable to the homogeneous (RTA)Re(O)(Me)(PPh₃) catalyst (Table 1, entry 3, $t_{1/2}$ = 1.49 h). However, (SiO₂-RTA)Re(O)(Me)(PPh₃) prepared by **Method (A)** (Fig. 2, path a; Table 1, entry 5, $t_{1/2}$ = 16.74 h) was over an order of magnitude slower than the homogeneous catalyst and only slightly more active than silica (Table 1, entry 7, $t_{1/2}$ = 24.62 h) without rhenium. The depressed activity of the catalyst, from **Method (A)**, is most likely due to partial decomposition of the rhenium catalyst at the elevated temperatures, refluxing toluene, used in the tethering process. As the sequentially prepared, **Method (B)**, (SiO₂-RTA)Re(O)(Me)(PPh₃) catalyst provided substantially better activity, it was used in subsequent experiments and future references to (SiO₂-RTA)Re(O)(Me)(PPh₃) refer to the sequentially prepared version.

While the homogeneous catalyst (Table 1, entry 3, $t_{1/2}$ = 1.49 h) showed slightly greater rates of reaction for methyltolylsulfide oxidation under our standard conditions, the supported immobilized catalyst (Table 1, entry 4, $t_{1/2}$ = 1.42 h) was completely recyclable. Five consecutive oxidation reactions, where the catalyst was filtered and washed between reactions, were performed with no loss of catalyst activity (Table 3). No activity was seen in the mother liquors after reaction (representative example: Table 1, entry 8, $t_{1/2}$ = 31.51 h)

above the level associated with that seen in blank solutions (Table 1, entry 9, $t_{1/2}$ = 38.82 h) indicating that leaching is not prevalent.

It should be noted that the oxidation of sulfides to sulfoxides and sulfones has been shown to be catalyzed by silica [27]. However under the reaction conditions used in this paper, methyltolylsulfide oxidation by TBHP catalyzed by silica (Table 1, entry 7, $t_{1/2}$ = 24.62 h) is only slightly faster than the oxidation that occurs with TBHP (Table 1, entry 9, $t_{1/2}$ = 38.82 h) in the presence of only solvent and substrate, and both are an order of magnitude slower than the rhenium catalyzed reactions (Table 1, entries 1-4). Furthermore, other sulfide substrates are more resistant to silica catalyzed oxidation yet fully amenable to oxorhenium(V) dithiolate catalyzed oxidation, see section 3.3.

The high activity of (SiO$_2$-RTA)Re(O)(Me)(PPh$_3$) (Table 1, entry 4, $t_{1/2}$ = 1.42 h) compared to the low activities of SiO$_2$ (Table 1, entry 7, $t_{1/2}$ = 24.62 h) and mother liquors (Table 1, entry 8, $t_{1/2}$ = 31.51 h) clearly shows the presence of an immobilized catalyst on the silica. The possibility that other catalytically active surface rhenium species contribute significantly to this activity was discounted by examination of the rhodium complex precursor adsorbed on silica (PhS)$_2$Re$_2$(O)(Me)(PPh$_3$)/(SiO$_2$) (Table 1, entry 6, $t_{1/2}$ = 10.76 h) which was more active than SiO$_2$ yet much less active than (SiO$_2$-RTA)Re(O)(Me)(PPh$_3$). These observations and the retention of activity of (SiO$_2$-RTA)Re(O)(Me)(PPh$_3$) when reused all indicate that the dithiolate rhenium complex is the active catalysts in these systems.

3.3. Catalytic oxidation of DBT and 4,6-Me$_2$DBT

Having established that the immobilized (SiO$_2$-RTA)Re(O)(Me)(PPh$_3$) catalyst has similar reactivity as its homogeneous oxorhenium(V) dithiolate analog, oxidation of the HDS

relevant sulfides, dibenzothiophene (DBT) and 4,6 dimethyldibenzothiophene (4,6-Me$_2$DBT), were examined. These substrates were not oxidized by TBHP (Table 5, entry 1) in solution or by TBHP in the presence of silica (Table 5, entry 2) when rhenium was not present. DBT was oxidized in toluene at 50 °C with TBHP using 0.1 mol% of (pdt)Re(O)(Me)(PPh$_3$) as a catalyst (Table 5, entry 3, t$_{1/2}$ = 0.832 h). However, the homogeneous (pdt)Re(O)(Me)(PPh$_3$) catalyst was incapable of oxidizing 10,000 equivalents of DBT, losing activity after approximately 1,000 turnovers (Table 5, entry 5). In contrast, the immobilized (SiO$_2$-RTA)Re(O)(Me)(PPh$_3$) catalyst was more efficient for DBT oxidation, oxidizing 1,000 equivalents of DBT (Table 5, entry 4, t$_{1/2}$ = 0.478 h) in almost half the time needed by the homogeneous analog. Furthermore, (SiO$_2$-RTA)Re(O)(Me)(PPh$_3$) was capable of oxidizing 10,000 equivalents of DBT (Table 5, entry 6, t$_{1/2}$ = 2.52 h).

When (SiO$_2$-RTA)Re(O)(Me)(PPh$_3$) was used as catalyst for the oxidation of a mixture of 1,000 eq. of MTS and 1,000 eq. of DBT in toluene at 50 °C with 2,000 equivalents of TBHP, graph 1, the catalyst reacted exclusively with MTS until it had been converted into the sulfoxide, 1 h. After the initial oxidation, MTS(O) effectively competed with DBT for further oxidation by the catalyst. The ratio of rates was approximately 2:3 with DBT oxidation being only slightly faster than MTS(O) overoxidation to the sulfone. The reaction proceeded for 6 h before all of the TBHP had been consumed. Complete oxidation of all of the sulfur could be achieved by addition of excess TBHP (not shown).

3.4. HDS conditions

To model HDS relevant conditions, the solvent system of toluene:hexanes (45:55%) and substrate concentration of 9.45 mM (DBT or 4,6-Me$_2$DBT; corresponding to 400 ppm sulfur) was used to simulate conditions found in gasoline. For DBT oxidation at these

concentrations (Table 6), using 0.625 mol% of (SiO$_2$-RTA)Re(O)(Me)(PPh$_3$) at 50°C with 3

equivalents of TBHP, half-lives of 0.275 h were observed for DBT (Table 6, entry 1, t$_{1/2}$ =

0.275 h). By lowering the catalyst amount to 0.156 mol%, a four-fold reduction in catalyst,

reaction times and half-lives were extended just over four-fold (Table 6, entry 2, t$_{1/2}$ = 1.304

h, t$_{95}$ = 5.216 h). Under these conditions, 4,6-Me$_2$DBT was also oxidized by (SiO$_2$-

RTA)Re(O)(Me)(PPh$_3$) (Table 6, entries 3-6). A series of reuse experiments showed the

catalyst as capable of 4,6-Me$_2$DBT oxidation (Table 6, entries 3-6, t$_{1/2}$ = 0.329, 0.241, 0.241,

and 0.309 h) as DBT oxidation (Table 6, entry 1, t$_{1/2}$ = 0.275 h). Thus, this catalyst system is

applicable for refractory oil sulfur content. The bulky DBT derivatives, such as 4,6-

Me$_2$DBT, which bedevil traditional HDS catalysts do not present a problem for our catalyst.

Presumably, this is because the oxidation step is a nucleophilic attack of the sulfur on the

coordinated oxo group and thus is an outer coordination sphere process occurring far enough

from the rhenium center to be sterically less demanding. Thus, 395-398 ppm of the initial

400 ppm of sulfur could be oxidized within 4 h, with less than 1 mol% of catalyst at 50 °C.

3.5. Effect of temperature on catalytic sulfide oxidation

For MTS oxidation by TBHP catalyzed by both (pdt)Re(O)(Me)(PPh$_3$) and (SiO$_2$-

RTA)Re(O)(Me)(PPh$_3$), a substantial rate increase was observed on heating the reaction from

20 °C to 50 °C in toluene. At 20 °C, 100 catalytic turnovers could be achieved in 6 h (Table

1, entries 2 and 4), but 1,000 turnovers were obtained after 40 min at 50 °C (Table 4, entries

4 and 5). Furthermore, at 50 °C, 10,000 equivalents of MTS could be cleanly oxidized in 18

h with (SiO$_2$-RTA)Re(O)(Me)(PPh$_3$) (Table 4, entry 7). It should be noted, however, at 50

°C the oxidation of MTS by TBHP with SiO$_2$ was also greatly increased (Table 4, entries 2

and 3), for example 1 ml of 0.6 M MTS in toluene could be oxidized by TBHP with 10.0 mg of SiO_2 within 10 h.

DBT oxidation also showed a temperature dependence. For the oxidation of DBT (0.6 M) with TBHP in toluene by 0.01 mol% $(SiO_2\text{-}RTA)Re(O)(Me)(PPh_3)$ at 20 °C no reaction was observed even after 3 d (not shown). However, at 50 °C, as mentioned in section 3.2.3., DBT oxidation was facile (Table 5, entry 6, $t_{1/2} = 2.52$ h, $t_{95} = 10.08$ h). The reaction was even faster at 100 °C (Table 5, entry 7, $t_{1/2} = 0.595$ h, $t_{95} = 2.38$ h), proceeding almost five times faster.

3.6. Catalyst lifetime and reuse

To determine the catalyst lifetime of $(SiO_2\text{-}RTA)Re(O)(Me)(PPh_3)$, series of 0.6 M DBT oxidations at 100 °C in toluene were performed. It was determined that $(SiO_2\text{-}RTA)Re(O)(Me)(PPh_3)$ could be recycled and used numerous times in 100 or 1,000 TON reactions without noticeable decrease in activity, but could only be used once with a 10,000 TON DBT reaction at peak efficiency. A second use at 10,000 TON was very sluggish and normally provided less than 1,000 TO over a day of reaction. Thus, $(SiO_2\text{-}RTA)Re(O)(Me)(PPh_3)$ has a lifetime of just over 10,000 TON.

The stability of the catalyst to the oxidant TBHP was probed by a series of catalyst pretreatments where the catalyst was exposed to TBHP in toluene at 50 °C prior to 4,6-Me_2DBT oxidation, Table 7. Thus, catalyst, solvent, and TBHP were incubated at 50 °C before 4,6-Me_2DBT was added. The baseline activity of the catalyst corresponds to no pretreatments (Table 7, entry 1, $t_{1/2} = 0.329$, h $t_{95} = 1.32$ h). After 3 h of pretreatment, there was no reduction in catalyst activity and the reaction was actually significantly faster (Table

7, entry 2, $t_{1/2}$ = 0.121 h, t_{95} = 0.484 h). With 5 h of pretreatment, the catalyst showed normal activity (Table 7, entry 3, $t_{1/2}$ = 0.331 h, t_{95} = 1.32 h). Pretreatment for 30 h reduced the catalyst activity (Table 7, entry 4, $t_{1/2}$ = 1.27 h, t_{95} = 5.08 h) to approximately ¼ of that exhibited by the untreated catalyst. Exposure to TBHP for 46 h at 50 °C, left the system inactive (Table 7, entry 5), but deactivation was due to TBHP decomposition. When fresh TBHP was added to the pretreated catalyst, oxidation of 4,6-Me$_2$DBT preceded smoothly (Table 7, entry 6, $t_{1/2}$ = 0.290 h, t_{95} = 1.16 h) and as rapidly as a non-pretreated sample (Table 7, entry 1, $t_{1/2}$ = 0.329 h, t_{95} = 1.32 h). Unfortunately, upon filtration of the 46 h pretreated sample, it was discovered that the silica retained no activity for 4,6-Me$_2$DBT oxidation even with fresh TBHP (Table 7, entry 7). Instead, the mother liquor was responsible for all of the observed activity with rates of the mother liquor (Table 7, entry 8, $t_{1/2}$ = 0.315 h, t_{95} = 1.26 h) being nearly identical to those observed for the sample that had not been filtered (Table 7, entry 6, $t_{1/2}$ = 0.290 h, t_{95} = 1.16 h). Thus, prolonged exposure to TBHP at 50 °C removes the rhenium catalyst from the surface. This most likely occurs at the ester linkage, perhaps by hydrolysis of the ester bond. Since the liberated rhenium species in solution are still highly active for sulfide oxidation, an intact oxorhenium(V) dithiolate unit is implied. Thus, the immobilized catalyst system is susceptible to TBHP, but the rhenium catalyst itself is not. Furthermore, recycling experiments indicate that any TBHP cleavage from the surface when substrate is present is negligible.

3.7. Epoxidation reactions

Both (SiO$_2$-RTA)Re(O)(Me)(PPh$_3$) and (pdt)Re(O)(Me)(PPh$_3$) were tested for their activity towards the epoxidation of 1-hexene and cyclooctene. Both TBHP and 4-picoline-N-oxide were examined as oxidants at 25, 50, or 100 °C in CDCl$_3$ or toluene. Under none of

these conditions was 1-hexene or cyclooctene oxidized to epoxides or other products after several days

4. Conclusion

An immobilized oxorhenium(V) dithiolate selective sulfide oxidation catalyst, $(SiO_2$-RTA$)Re(O)(Me)(PPh_3)$, has been synthesized and characterized. The catalyst activity and selectivity closely mirrors those exhibited by its solution analog. In addition, the supported catalyst is recyclable and displays impressive robustness (TON > 10,000). Furthermore, the catalyst easily converts refractory sulfur compounds, such as 4,6 dimethyldibenzothiophene, to easily removable and more HDS amendable monoxide and dioxide sulfur compounds. This process occurs within reasonable timescales for the sulfur concentrations relevant to HDS processes, i.e. ppm concentrations that model gas feedstocks.

References

[1] M. Borushko, Fed. Regist. 66 (2001) 5001.

[2] a) D.D. Whitehurst, T. Isoda, I. Mochida, Adv. Catal. 42 (1998) 345.

b) B.C. Gates, H. Topsøe, Polyhedron 16 (1997) 3213.

c) H. Topsøe; B.S. Clausen, F.E. Massoth, Hydrotreating Catalysis Science and Technology, Springer, Berlin, (1996) p. 7.

[3] Y. Wang, G. Lente, J.H. Espenson, Inorg. Chem. 41 (2002) 1272.

[4] F.M. Collins, A.R. Lucy, C. Sharp, J. Mol. Catal. A: Chem. 117 (1997) 397.

[5] K. Yatsu, H. Miki, K. Ukegaw, N. Yamamoto, (Ministry of Economy, Trade and Industry; National Industrial Research Institute, Japan). Jpn. Kokai Tokkyo Koho 2001; Patent No. JP2001/29376, p 12.

[6] S. Otsuki, T. Nonaka, W. Qian, A. Ishihara, T. Kabe, Sekiyu Gakkaishi 42 (1999) 315.

[7] K. Yazu, Y. Yamamoto, T. Furuya, K. Miki, K. Ukegawa, Energy & Fuels 15 (2001) 1535.

[8] a) R. Hille, Chem. Rev. 96 (1996) 2757.

b) R.H. Holm, J.M. Berg, Acc. Chem. Res. 19 (1986) 363.

c) R.H. Holm, Chem. Rev. 87 (1987) 1401.

d) S.J. Lippard, J.M. Berg, Principles of Bioinorganic Chemistry; University Science Books: Mill Valley, CA, 1994.

[9] a) G. N. George, J. Hilton, C. Temple, R.C. Prince, K.V. Rajagopalan, J. Am. Chem. Soc. 121 (1999) 1256.

b) K.-M Sung, R.H. Holm, J. Am. Chem. Soc. 123 (2001) 1931.

c) L.J. Laughlin, C.G. Young, Inorg. Chem. 35 (1996) 1050.

d) P.D. Smith, A.J. Millar, C.G. Young, A. Ghosh, P.J. Basu, J. Am. Chem. Soc. 122 (2000) 9298.

e) P.D. Smith, D.A. Slizys, G.N. George, C.G. Young, J. Am. Chem. Soc. 122 (2000) 2946.

[10] D.E. DeVos, B.F. Sels, P.A. Jacobs, Advances in Catalysis 46 (2001) 1.

[11] a) J.D. Morrison (Ed.), Asymmetric Synthesis, Vol. 5, Chiral Catalysis, Academic Press, Orlando, 1985.

b) D.E. Vos, I.F.J. Vankelecom, P.A. Jacobs (Eds.), Chiral Catalyst Immobilization and Recycling, Wiley-VCH, New York, 2000.

c) E.N. Jacobsen, A. Pfaltz, H. Yamamoto (Eds.), Comprehensive Asymmetric Catalysis, Vols. I-III, Springer, New York, 1999.

[12] J. Jacob, J.H. Espenson, Chem. Commun. (1999) 1003.

[13] J. Jacob, I.A. Guzei, J.H. Espenson, Inorg. Chem. 38 (1999) 1040.

[14] J. Jacob, G. Lente, I.A. Guzei, J.H. Espenson, Inorg. Chem. 38 (1999) 3762.

[15] G. Lente, J. Jacob, I.A. Guzei, J.H. Espenson, Inorg. React. Mech. (Amsterdam) 2 (2000) 169.

[16] G. Lente, I.A. Guzei, J.H. Espenson, Inorg. Chem. 39 (2000) 1311.

[17] G. Lente, X. Shan, I.A. Guzei, J.H. Espenson, Inorg. Chem. 39 (2000) 3572.

[18] G. Lente, J.H. Espenson, Inorg. Chem. 39 (2000) 4809.

[19] D.W. Lahti, J.H. Espenson, J. Am. Chem. Soc. 123 (2001) 6014.

[20] J.H. Espenson, X. Shan, Y. Wang, R. Huang, D.W. Lahti, J. Dixon, G. Lente, A. Ellern, I.A. Guzei, Inorg. Chem. 41 (2002) 2583.

[21] J. Dixon, J.H. Espenson, Inorg. Chem. 41 (2002) 4727.

[22] A.B. Pangborn, M.A. Giardello, R.H. Grubbs, R.K. Rosen, F. J. Timmers, Oganometallics 15 (1996) 1518.

[23] D.D. Perrin, W.L.F. Armarego, D.R. Perrin, Purification of Laboratory Chemicals, 2nd ed., Pergamon, New York, 1980.

[24] a) B.L Booth, G.C Ofunne, C. Stacey, P.J.T. Tait, Journal of Organometallic Chemistry 315 (1986) 143.

b) G. Dupas, P. Tintillier, T. Trefouel, J. Cazin, D. Losset, J. Bourguignon, G. Queguiner, New Journal of Chemistry 13 (1989), 255.

[25] J. Takacs, M.R. Cook, P. Kiprof, J.G. Kuchler, W.A. Herrmann, Organometallics 10 (1991), 316.

[26] Utilizing the same procedure for 1 week at room temperature yielded a light green solid that had a very low rhenium content and low activity consistent with the reduced rhenium content, ~1/50th of that obtained by method B.

[27] a) P.J. Kropp, G.W. Brenton, J.D. Fields, J.C. Tung, B.R. Loomis, J. Am. Chem. Soc. 122 (2000), 4280.

b) E.N. Kadnikova, N.M. Kostic, Journal of Non-Crystalline Solids 283 (2001) 63.

Table 1. Catalyst Activities for MTS oxidation by TBHP[a]

Entry	Catalyst	$t_{1/2}$ (h)	$t_{95\%}$ (h)
1	(edt)Re(O)(Me)(PPh₃)[b]	2.65	10.6
2	(pdt)Re(O)(Me)(PPh₃)[b]	1.06	4.24
3	(RTA)Re(O)(Me)(PPh₃)[b]	1.49	5.96
4	(SiO₂-RTA)Re(O)(Me)(PPh₃)[b, c]	1.42	5.68
5	(SiO₂-RTA)Re(O)(Me)(PPh₃)[b, c, d]	16.7	67.0
6	(PhS)₂Re₂(O)(Me)(PPh₃)/(SiO₂)[c]	10.8	43.0
7	SiO₂[c]	24.6	98.5
8	Mother Liquor[e,f]	31.5	126
9	Blank[e]	38.8	155

a) Reaction Conditions: 0.1 ml of CDCl₃ solvent, 0.60 M MTS, 0.66 M TBHP, 20 °C
b) 1.0 mol% rhenium catalyst
c) 10.0 mg of solid catalyst
d) (SiO₂-RTA)Re(O)(Me)(PPh₃) prepared by **Method (A)**
e) no catalyst
f) from entry 4

Table 2. Solvent Effects on MTS oxidation by TBHP[a]

Entry	Solvent System	$t_{1/2}$ (h)	$t_{95\%}$ (h)
1	C_6H_6	0.94	3.76
2	$CDCl_3$	1.06	4.24
3	$CHCl_3$[b]	1.54	6.16
4	CH_2Cl_2	2.13	8.52
5	$CDCl_3$ with 10% EtOH	6.52	26.1

a) Reaction Conditions: 0.1 ml of solvent, MTS 0.60 M, 0.66 M TBHP, 20 °C, 1.0 mol% (pdt)Re(O)(Me)(PPh₃) catalyst
b) Commercial $CHCl_3$ contains 1% EtOH as inhibiter.

Table 3. Supported Catalyst Reuse for MTS oxidation by TBHP[a]

Use #	Solvent	$t_{1/2}$ (h)	$t_{95\%}$ (h)
1	CDCl$_3$	1.42	5.68
2	CDCl$_3$	1.34	5.36
3	CDCl$_3$	1.38	5.52
4	CDCl$_3$	1.32	5.28
5	CDCl$_3$	1.37	5.48

a) Reaction Conditions: 0.1 ml of solvent, MTS 0.60 M, 0.66 M TBHP, 20 °C, 1.0 mol% (SiO$_2$-RTA)Re(O)(Me)(PPh$_3$) catalyst (10.0 mg of solid catalyst)

Table 4. Catalyst Activities for MTS oxidation by TBHP at 50 °C[a]

Entry	Catalyst	Re Mol %	$t_{1/2}$ (h)	$t_{95\%}$ (h)
1	Blank[b]	0	14.8	59.0
2	SiO_2[c]	0	2.29	9.16
3	SiO_2[d]	0	20.6	82.6
4	(pdt)Re(O)(Me)(PPh$_3$)[e]	0.1	0.0670	0.268
5	(SiO$_2$-RTA)Re (O)(Me)(PPh$_3$)[c, e]	0.1	0.156	0.624
6	(pdt)Re(O)(Me)(PPh$_3$)[f]	0.01	14.4	57.8
7	(SiO$_2$-RTA)Re(O)(Me)(PPh$_3$)[d, f]	0.01	4.50	18.0

a) Reaction Conditions: 1.0 ml of toluene solvent, 0.60 M MTS, 0.66 M TBHP, 50 °C
b) no catalyst
c) 10 mg of solid catalyst
d) 1.0 mg of solid catalyst
e) 0.1 mol% rhenium catalyst
f) 0.01 mol% rhenium catalyst

Table 5. Catalyst Activities for DBT oxidation by TBHP at 50 °C[a]

Entry	Catalyst	Re Mol %	T	$t_{1/2}$ (h)	$t_{95\%}$
1	Blank[b]	0	50	NR[c]	
2	SiO$_2$[d]	0	50	NR[c]	
3	(pdt)Re(O)(Me)(PPh$_3$)[f]	0.1	50	0.832	3.33
4	(SiO$_2$-RTA)Re (O)(Me)(PPh$_3$)[d, f]	0.1	50	0.478	1.91
5	(pdt)Re(O)(Me)(PPh$_3$)[g]	0.01	50	NA[h]	NA[h]
6	(SiO$_2$-RTA)Re (O)(Me)(PPh$_3$)[e, g]	0.01	50	2.52	10.1
7	(SiO$_2$-RTA)Re (O)(Me)(PPh$_3$)[e, g, i]	0.01	100	0.595	2.38

a) Reaction Conditions: 1.0 ml of toluene solvent, 0.60 M MTS, 0.66 M TBHP, 50 °C
b) no catalyst
c) no reaction observed over 12 h
d) 10 mg of solid catalyst
e) 1.0 mg of solid catalyst
f) 0.1 mol% rhenium catalyst
g) 0.01 mol% rhenium catalyst
h) catalyst losses activity after 1,000 TO (10% reaction)
i) 100 °C

Table 6. (SiO$_2$-RTA)Re (O)(Me)(PPh$_3$) catalyzed oxidation of DBT and 4,6-Me$_2$DBT by TBHP at 50 °C[a]

Entry	Substrate	Re Mol %	$t_{1/2}$ (h)	$t_{95\%}$
1	DBT	0.625	0.275	1.10
2	DBT[b]	0.156	1.30	5.22
3	4,6-Me$_2$DBT[c]	0.625	0.329	1.57
4	4,6-Me$_2$DBT[d]	0.625	0.241	0.964
5	4,6-Me$_2$DBT[e]	0.625	0.241	0.964
6	4,6-Me$_2$DBT[f]	0.625	0.309	1.24

a) Reaction Conditions: 1.0 ml of solvent mixture of toluene:hexanes (45:55), 9.45 mM DBT or 4,6-Me$_2$DBT, 28.4 mM TBHP, 50 °C, 1.0 mg of solid catalyst

b) [DBT] = 4.75 mM

c) first use

d) second use

e) third use

f) fourth use

Table 7. Effect of 50°C TBHP pretreatments on $(SiO_2\text{-}RTA)Re\ (O)(Me)(PPh_3)$ catalyzed oxidation of $4,6\text{-}Me_2DBT$ by TBHP at 50 °C[a]

Entry	Pretreatment (h)	$t_{1/2}$ (h)	$t_{95\%}$ (h)
1	0	0.329	1.32
2	3	0.121	0.484
3	5	0.331	1.32
4	30	1.27	5.08
5	46	NR[b]	NA
6	46[c]	0.290	1.16
7	46[d,c]	slow[e]	NA
8	46[f,c]	0.315	1.26

a) Reaction Conditions: 1.0 ml of solvent mixture of toluene:hexanes (45:55), 9.45 mM DBT or $4,6\text{-}Me_2DBT$, 28.4 mM TBHP, 50 °C, 1.0 mg of solid catalyst, 0.625 mol% rhenium

b) no reaction observed over 1 day

c) fresh TBHP added

d) immobilized catalyst washed after pretreatment prior to use

e) less than 1% reaction in 1 day

f) mother liquor from washed catalyst

Graph 1. (SiO₂-RTA)Re (O)(Me)(PPh₃) catalyzed oxidation of mixed sulfur compounds, MTS and DBT, with TBHP at 50 °Cᵃ
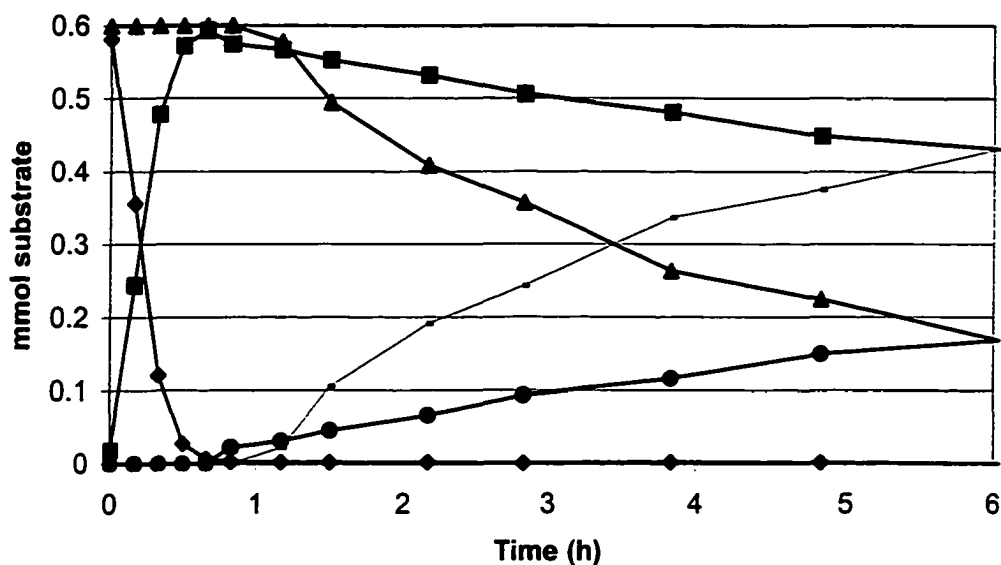
a) Reaction conditions: 0.60 M DBT and 0.60 M MTS in toluene, 50 °C, 1.2 M TBHP, 10.0

mg (SiO₂-RTA)Re (O)(Me)(PPh₃), 0.10 mol% Re. Reaction stopped after 6 h due to total

consumption of TBHP; addition of excess TBHP led to complete oxidation of both MTS and

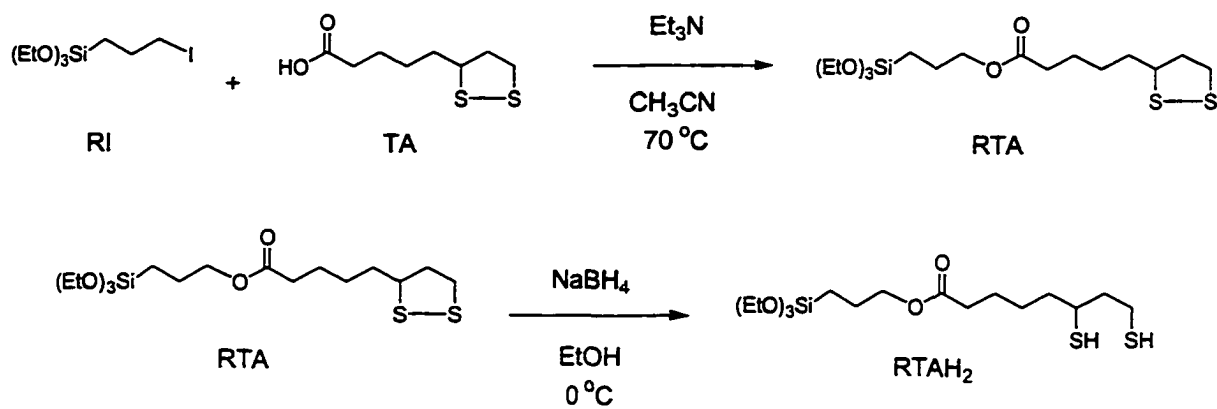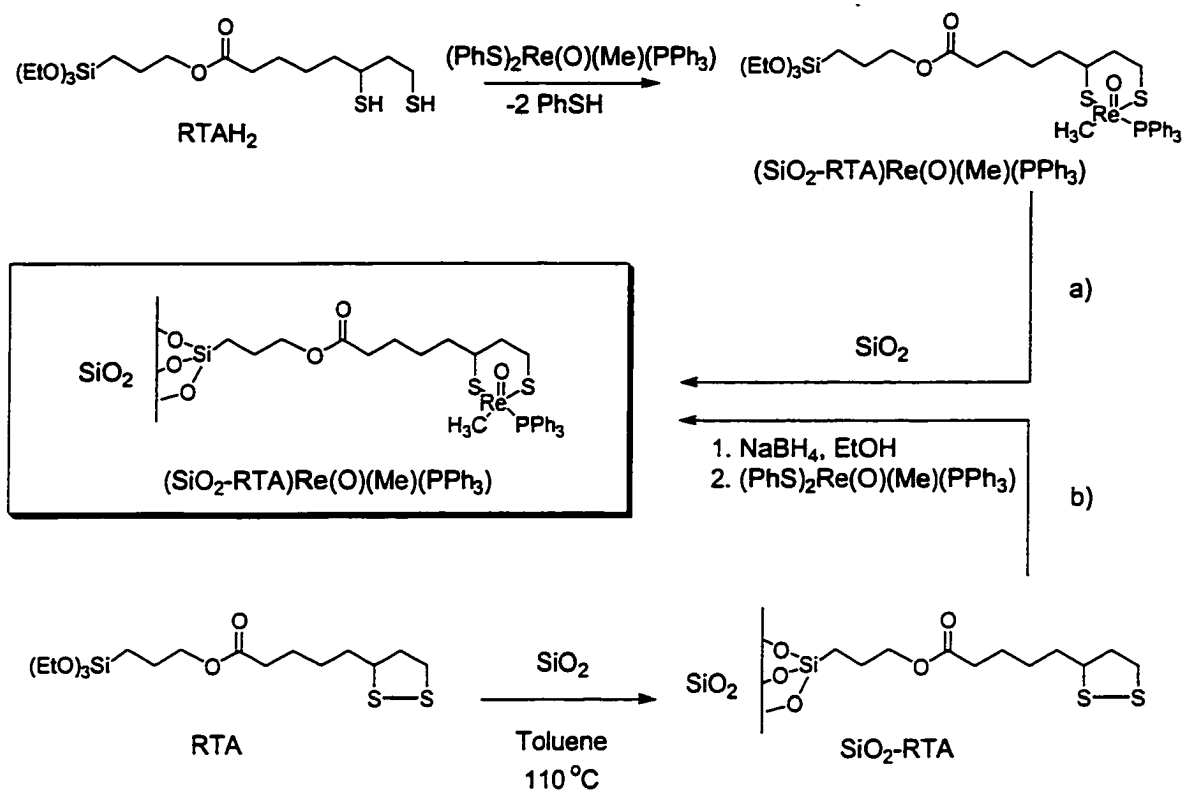DBT. (▲) DBT, (♦)MTS , (■) MTS(O), (●) MTS(O)₂, (-) DBTO

Figure 1. Synthesis of RTA and RTAH₂.

Figure 2. Synthesis of (SiO$_2$-RTA)Re(O)(Me)(PPh$_3$) catalyst.

General Conclusions

The desire to recover and reuse catalysts after reactions is a powerful driving force for the development of new methodologies and the refinement of existing techniques. The projects described in this dissertation outline some of the successes that can be obtained by the immobilization of homogeneous catalysts via tethering to silica. In addition, they illustrate the need for thorough characterization and control experimentation. The first project, in Chapter 2, expanded the realm of tethered enantioselective rhodium hydrogenation catalysts to silica supports containing palladium metal. A comprehensive picture of the tethered surface catalyst was obtained that showed it to have the same structure, reactivity, and reaction pathway as its solution analog. It was shown that the intact PPM-Rh unit was required for enantioselective hydrogenation of MAC, but was inactive for arene hydrogenation. New insights were gained about tethered rhodium complexes with palladium metal on inert supports. The presence of palladium failed to accelerate the rate of hydrogenation by the tethered rhodium catalyst. However, trace decomposition of the tethered rhodium catalyst resulted in surface bound rhodium species not attached to the tethered PPM ligand that were activated by palladium on the silica surface to a highly active racemic hydrogenation species, presumably rhodium metal. This rhodium metal on the silica surface was responsible for arene hydrogenation activity.

The activation of rhodium species, generated from the decomposition of tethered rhodium complexes, on silica surfaces by palladium metal prompted further examination of this phenomenon with model systems consisting of absorbed rhodium(I) complexes on silica and silica containing palladium metal (Chapter 3). These experiments clearly showed that palladium on the silica surface accelerated the reduction of adsorbed rhodium(I) species to

rhodium metal under reaction conditions. Also, the palladium metal assisted reduction of rhodium avoids high temperature reduction conditions that decrease the activity of rhodium metal in mixed rhodium-palladium systems. This rhodium metal is responsible for the arene hydrogenation activity in the tethered and adsorbed systems.

The possibility that the activity of tethered rhodium complexes, especially on silica with supported palladium metal, may actually be due to reduced rhodium metal prompted a re-evaluation of the hydrodefluorination reaction over rhodium catalysts in Chapter 4 and resulted in the elucidation of several interesting solvent and base effects. The rhodium metal catalyzed reaction of fluorobenzene (PhF) with H_2 was shown to exhibit selectivities dependent on the solvent used. Non-polar, aprotic solvents (heptane and DCE) favor arene hydrogenation to fluorocyclohexane (CyF), while polar, protic solvents (heptane/methanol and heptane/water) exclusively favor hydrodefluorination to cyclohexane (CyH). A benzene (PhH) intermediate, on the way to CyH, was detected in the heptane/methanol and heptane/water reactions and was found to inhibit the hydrodefluorination of PhF to PhH. Because of this, complete hydrodefluorination of PhF to CyH proceeds best in heptane/water under acidic conditions, where the hydrogenation of PhH to CyH is fastest. Since the supported rhodium catalysts most active for toluene hydrogenation are also the most active hydrodefluorination catalysts and benzene is observed to inhibit the hydrodefluorination reaction, the same catalytic sites on rhodium metal are probably used for both arene hydrogenation and fluorobenzene hydrodefluorination. A side reaction between CyF and HF, not catalyzed by rhodium, was also revealed that resulted in the production of cyclohexene. Thus, reaction conditions can be chosen to selectively yield fluorocyclohexane, cyclohexene, benzene, or cyclohexane.

Not only was the preparation of a tethered hydrogenation catalyst successful, but also the first tethered oxorhenium(V) dithiolate oxygen transfer catalyst was conceived, synthesized, and characterized (Chapter 5). Again, the rational for this work was the same as those in the previous chapters. Immobilized catalysts were produced that are selective and recyclable. The resulting catalysts were characterized and experiments performed to help understand the catalyst form, mode of activity, and limitations. For the tethered oxorhenium(V) dithiolate catalysts in Chapter 5, the catalyst activity and selectivity closely mirrors that exhibited by its solution analog. In addition, the supported catalyst is recyclable and displays impressive robustness (TON > 50,000). Furthermore, the catalyst easily converts refractory sulfur compounds, such as 4,6 dimethyldibenzothiophene, to the easily separated and more HDS-amendable monoxide and dioxide sulfur compounds. This process occurs within reasonable timescales for sulfur concentrations relevant to HDS processes, i.e. ppm concentrations that model gas feedstocks.

Acknowledgements